Theory of pulsed dye lasers including dye-molecule rotational relaxation

Roger A. Haas and Mark D. Rotter
Department of Applied Science, University of California, Davis–Livermore, L-794, P.O. Box 808, Livermore, California 94550
and Lawrence Livermore National Laboratory, P.O. Box 808, Livermore, California 94550
(Received 12 February 1990; revised manuscript received 29 October 1990)

In this paper a phenomenological semiclassical theory of pulsed-laser-pumped dye-laser light amplifiers is presented. The theory accounts for the broadband radiation absorption and emission characteristics of dye molecules in liquid solvents. Dye-molecule fluorescence, vibrational, rotational, and electric polarization relaxation processes are represented by phenomenological relaxation rates. In general, it is found that due to dye-molecule rotational relaxation the laser-pumped dye medium is optically anisotropic. The pump- and dye-laser beams propagate through the dye medium as essentially transverse electromagnetic waves whose amplitude and polarization state changes. The theory is applicable to pulse durations $\tau \lesssim 10-100$ ns including the ultrashort pulse regime. The regime $\tau \gtrsim 1$ ps in which the pump- and dye-laser pulse lengths are long compared to the dye-molecule vibrational and electric polarization relaxation times is considered in detail. Amplification of partially polarized quasimonochromatic light is described by a self-consistent set of equations for the components of the pump- and dye-laser light coherency matrices and the orientation populations of the lowest vibronic levels of the dye molecule's S_0 and S_1 electronic states. The interaction of the pump- and dye-laser beams with the dye molecules is characterized by complex electric susceptibility tensors. Kramers-Kronig or Hilbert transform relations are found that permit dye-molecule absorption and emission cross sections to be used to calculate the pump- and dye-laser susceptibility tensors. All the physical parameters in the theory may be determined by conventional experimental techniques. When the dye-molecule rotational relaxation rate γ_R is much larger than the fluorescence rate γ_F, τ^{-1}, and the pump-laser absorption and dye-laser stimulated emission rates, then the dye-molecule electric susceptibility tensors are diagonal. The laser-pumped dye-laser medium is optically isotropic. When these conditions do not hold the medium is optically anisotropic and coherency matrices may be used to describe the propagation of the pump- and dye-laser beams. This procedure is illustrated for the case of transversely pumped dye lasers. In the small-signal regime analytic solutions for the dye-laser-light coherency matrix components are developed for arbitrary initial polarization state, pulse duration, and γ_F/γ_R. In the large-signal regime numerical solutions are obtained for the amplification of short, $(\tau\gamma_F, \tau\gamma_R) \ll 1$, and quasi-steady-state $(\tau\gamma_F, \tau\gamma_R) \gg 1$, pulses for arbitrary values of γ_F/γ_R when the pump- and dye-laser polarizations are parallel. In general, it is found that for a wide range of physical conditions of interest dye-molecule rotational relaxation is important, and significant changes in the amplification characteristics of the medium, i.e., the rate of amplification, amplification efficiency, and polarization state of the light, will occur.

I. INTRODUCTION

For several years there has been considerable interest in the use of pulsed dye-laser media to generate and amplify light pulses.[1–3] Specific studies[4–11] have addressed a wide range of laser-pumped, dye-laser radiation and medium physical conditions. The characteristics of amplified spontaneous emission and mirrorless dye lasers have been explored.[4–9] Laser-pumped dye media have been used to generate and amplify high-power subpicosecond pulses.[10,11] In all of these studies a radiation-transport, rate-equation formulation was used to theoretically describe the coupled radiation-field, dye-medium dynamics. Rotational relaxation of the dye molecules was not included. However, dye-molecule rotational relaxation can be important because it makes the dye-laser medium optically anisotropic. This can significantly alter the amplification characteristics of the dye medium. Previous theoretical investigations of this behavior have been restricted to either the small-signal regime[12,13] or the limit of frozen or fixed dye-molecule orientation.[14–18] Building on these earlier investigations, a phenomenological semiclassical model of pulsed-dye-laser amplifiers has evolved. The model provides a self-consistent electromagnetic field treatment that accounts for the broadband emission and absorption of the dye medium,[1,2,19] the polarization state of the pump and laser radiation;[20–22] collisional relaxation of the induced dye-molecule electric polarization; and the fluorescence, vibrational, and rotational relaxation of the dye molecules. It is valid for both small- and large-signal amplification regimes. This paper presents the essential elements of this theoretical model of pulsed dye lasers. The regime in which the pump- and dye-laser-light pulse lengths are

long compared to the dye-molecule vibrational and electric polarization relaxation times is considered in some detail. Application of the theory is illustrated by treating the amplification of partially polarized, quasimonochromatic light pulses in transversely laser-pumped dye media. Both small- and large-signal regimes of amplification of short and quasi-steady-state light pulses are considered in detail. The methodology described here may be readily extended to treat tunable solid-state lasers.[23–27] The principal limitations of the present semiclassical approach are that spontaneous emission and nonradiative dye-molecule relaxation processes are described phenomenologically. However, in the applications considered all of the physical parameters in the theory may be determined by conventional measurement techniques. The inclusion of amplified spontaneous emission requires a complete quantum theory approach.[28,29]

This paper is divided into several sections. In Sec. II the characteristics of laser-pumped pulsed-dye-laser media are described. A phenomenological semiclassical theory of laser-pumped dye-laser amplifiers, including dye-molecule rotational relaxation, is presented. In Sec. III the amplification of pulsed, quasimonochromatic partially polarized radiation is considered in both the large- and small-signal regimes. The regime in which the pump- and dye-laser-light pulse lengths are long compared to the dye-molecule vibrational and electric polarization relaxation times is considered in some detail. Application of the theory is illustrated by treating transversely laser-pumped dye lasers. The polarization states of the pump- and dye-laser radiation are described by the coherency matrices of Wiener[20] and Wolf.[21,22] In Sec. IV the relationship between the theoretically calculated dye-laser radiation coherency matrix and its experimentally measured values is established by generalizing the concept of the time-dependent physical spectrum of light introduced by Eberly and Wodkiewicz.[30] Section V includes a summary and conclusions.

II. SEMICLASSICAL THEORY OF PULSED DYE LASERS

A. Physical characteristics of dye-laser media

The dye-laser medium consists of dye molecules such as DCM (Ref. 31) or rhodamine 6G (Refs. 32–34) dilutely dissolved in a liquid solvent. Table I summarizes the important physical characteristics of several organic dyes along with the solvents methyl alcohol (MeOH) and ethanol (EtOH). The broad emission and absorption properties of a dye molecule such as DCM or rhodamine 6G may be explained[1,2] by the electronic band-structure model sketched in Fig. 1. The dye molecule is typically a large, complex molecule with an electronic structure that is richly broadened by an almost continuous distribution of vibration-rotation substates. As shown in Fig. 1, the electronic structure consists of a ladder of singlet states S_i ($i=0,1,2,3,\ldots$) containing the ground state S_0 and a ladder of triplet states T_i ($i=1,2,3,\ldots$), which are displaced toward lower energy. Each electronic state has a number of vibrational levels superimposed on it, with an average separation[1,2] between vibrational levels of 1200–1600 cm^{-1}. In large dye molecules, many vibrational modes of differing frequencies are coupled to the electronic transition. Collisional and electrostatic perturbations due to the solvent molecules broaden these vibrational states.[1,2] Interaction with solvent molecules and intramolecular coupling leads to vibrational relaxation on a subpicosecond time scale.[38,39] The relative importance of intramolecular and intermolecular vibrational relaxation processes is not presently well understood. Each vibronic level has closely spaced rotational levels superimposed on it. These rotational levels are broadened by frequent collisions with solvent molecules and thus form a near continuum between each vibrational level. Rotational relaxation of the dye molecules takes much longer than vibrational relaxation. It occurs on a time scale[35] of 100–500 ps for the solvents methyl alcohol and ethanol. However, for highly viscous solvents, it can exceed a nanosecond.[35]

The longest-wavelength light absorption is from S_0 to S_1. The absorption from S_0 to T_i is spin forbidden. Nonradiative coupling of the singlet and triplet manifolds is also weak with a time scale typically greater than 100 ns. Since the laser-pulse lengths and stimulated emission times of interest in the applications[1–11] are much less than this time, excitation of triplet states may be neglected. Consequently, when the dye molecule is optically excited to the S_1 state it then decays rapidly by vibrational relaxation to the lowest vibronic sublevel of the S_1 state. Spontaneous (fluorescence) and stimulated emission occur between this level and a vibronic sublevel of S_0. These

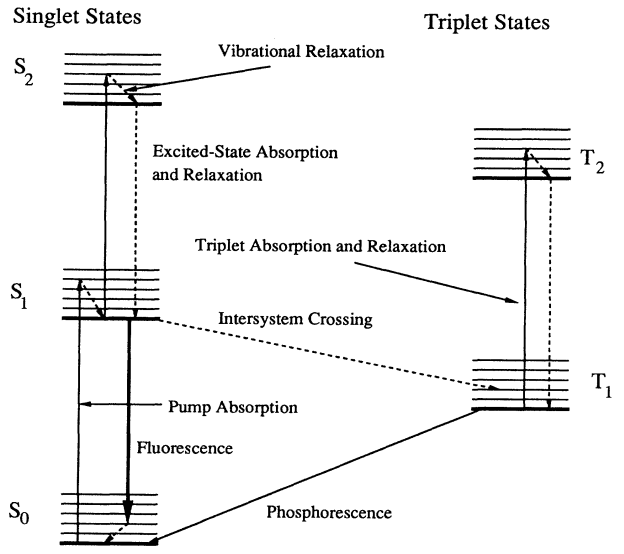

FIG. 1. Energy level diagram (Ref. 1) of a typical dye molecule with radiative (——) and nonradiative (— — —) transitions indicated.

vibronic sublevels then rapidly relax by another nonradiative decay to the lowest vibronic sublevel of S_0. The wide distribution of available vibronic sublevels of S_0 gives the observed broadband fluorescence and gain. The strength of the interaction of light with a dye molecule depends on the orientation of the dye molecule relative to the polarization direction of the electric field of the light. Consequently, the orientation distribution of the dye molecule's S_0 and S_1 states during the lasing process is determined by the relative magnitudes of the laser-pulse length, absorption, stimulated emission, fluorescence, and rotational relaxation time scales. When the orientation distribution of the dye molecules is not completely random or isotropic the dye-laser medium becomes optically anisotropic.[12–18] In this paper, the effect of dye-molecule rotational relaxation on pulsed-dye-laser dynamics is treated in some detail. The orientation of the radiation-induced dipole moments of the dye molecule's $S_1 \rightarrow S_0$ transition is denoted by spherical polar angles θ and ϕ. Euler angles[35] may also be used to specify the orientation of the dye molecule. The energy-level structure and the vibrational and rotational relaxation behavior of the dye molecule described here depends on the solvent. In addition, many solvents are available with a wide range of optical and fluid properties (Table I). In general, the dye-laser medium is a nonmagnetic dielectric.

The excited-state absorption process $S_1 \rightarrow S_2$ followed by rapid internal conversion $S_2 \rightarrow S_1$ is a potentially serious loss process. However, experimental data have shown that the absorption cross section for this process is small compared to the stimulated emission cross section for the dyes considered.[32–34] In general, in addition to fluorescence as shown in Fig. 1, the S_1 band may also relax by internal conversion and intersystem crossing.

TABLE I. Typical physical parameters of organic dyes and solvents; dye-molecule photochemical properties refer to rhodamine 6G except where noted otherwise.

Quantity	Numerical value	Reference
	Dye-molecule properties	
Fluorescence lifetime[a]	1–5 nsec	35,33
Intersystem crossing lifetime	290 nsec	36
$S_2 \rightarrow S_1$ lifetime[b]	30–50 psec	37
Vibrational relaxation lifetime[b,c] within S_1	190–500 fsec	38,39
Rotational relaxation time[d]	100–500 psec	35
Dephasing time[b]	75 fsec	40
Excited-state-absorption cross section	4×10^{-17} cm^2	34
Peak emission cross section	$1.8–4\times10^{-16}$ cm^2	1,32–34
Peak absorption cross section	$2.7–4.2\times10^{-16}$ cm^2	1,32–34
Quantum yield	0.8–0.86 (MeOH)	41
	0.982 (MeOH)	42
	0.93 (EtOH)	34
	0.88 (EtOH)	41
	0.95 (EtOH)	43
	0.96±0.02 (H_2O)	44
	0.76–0.81 (H_2O)	41
	0.45±0.05 Q_{EtOH} (H_2O)	45
	Methanol (M) and ethanol (E) properties	
Refractive index	1.3288 (M); 1.3611 (E) at Na D line	46
Loss coefficient	0.0031 cm^{-1} (M); 0.01 cm^{-1} (E) at 570 nm	
Nonlinear index n_2	2.2×10^{-13} esu (M); 2.5×10^{-13} esu (E) at 10 ps	47,48
Raman gain	5.5×10^{-10} cm/W (M)	49
	5.1×10^{-10} cm/W (E)	49
Raman Stokes shift	2831 cm^{-1} (M); 2921 cm^{-1} (E)	49
Density	0.7914 g/cm^3 (M); 0.7893 g/cm^3 (E)	46
Viscosity	0.547 cP (M); 1.2 cP (E) at 25 °C	46
Boiling point	65 °C (M); 78.5 °C (E)	46
Thermal conductivity	2.02×10^{-3} W/cm °K (M)	46
	1.67×10^{-3} W/cm °K (E)	46
Specific heat	0.609 cal/g °K (M); 0.586 cal/g °K (E)	46

[a]Typical range.
[b]Cresyl violet.
[c]Rhodamine 640.
[d]Typical range in the solvents methanol and ethanol.

Thus the observed lifetime of the S_1 state is less than the radiative lifetime. The ratio of the observed lifetime to the radiative lifetime is known as the quantum yield (Table I). For good laser dyes, such a rhodamine 6G, the quantum yield approaches unity.

B. Propagation of electromagnetic radiation

Consider a dye-laser medium that is optically pumped with a separate laser. The propagation of pump laser ($j=p$) light and dye-laser ($j=l$) light through a dye-laser medium is described by the field equations[50–53]

$$\nabla\times[\nabla\times\mathbf{E}_j(\mathbf{x},t)]+c^{-2}\partial_t^2\mathbf{E}_j(\mathbf{x},t)=-\mu_0\partial_t^2\mathbf{P}_j(\mathbf{x},t) \quad (2.1)$$

and

$$\nabla\cdot[\epsilon_0\mathbf{E}_j(\mathbf{x},t)+\mathbf{P}_j(\mathbf{x},t)]=0\ , \quad (2.2)$$

where $\mathbf{E}_j$ is the electric-field intensity and

$$\mathbf{P}_j(\mathbf{x},t)=\epsilon_0\int_{-\infty}^{t}dt'\chi_s(t-t')\mathbf{E}_j(\mathbf{x},t') + \int_{4\pi}d\Omega\,\mathbf{P}_j(\mathbf{x},t,\Omega) \quad (2.3)$$

is the medium electric polarization associated with the light at location $\mathbf{x}$ and time t. The quantities c, ϵ_0, and μ_0 are the speed of light, permittivity, and permeability of free space, respectively. Unless otherwise specified, throughout this paper the subscript $j=(l,p)$. The first term on the right-hand side of Eq. (2.3) is the electric polarization due to the interaction of the light with the solvent molecules. The quantity χ_s is the electric susceptibility response function of the solvent. The solvent electric susceptibility $\hat{\chi}_s$ is given by the Fourier transform

$$\hat{\chi}_s(\omega)=\int_{-\infty}^{\infty}dt\,\chi_s(t)e^{i\omega t}\ . \quad (2.4)$$

In general, $\hat{\chi}_s$ is complex and may be written as $\hat{\chi}_s=\chi_s'+i\chi_s''$. Since the solvent is generally nearly transparent in the dye-molecule absorption and fluorescence wavelength bands, $\chi_s'\gg\chi_s''$ there. In this region, the solvent refractive index and absorption coefficient are given by $n_s^2=1+\chi_s'$ and $\alpha_s=\omega\chi_s''/cn_s$, respectively.

The second term on the right-hand side of Eq. (2.3) is the electric polarization due to the interaction of the pump laser ($j=p$) light and dye laser ($j=l$) light with the dye molecules of all orientations. The quantity $\mathbf{P}_j(\mathbf{x},t,\Omega)$ is the induced electric polarization per unit solid angle due to dye molecules whose orientation $\Omega=(\theta,\phi)$ is in the solid angle range Ω to $\Omega+d\Omega$ where $d\Omega=\sin\theta\,d\theta\,d\phi$. Equations (2.1) and (2.2) are coupled by the electric polarization produced by the dye- and solvent-molecule response to the pump and laser electric fields. In each case this polarization $\mathbf{P}_j(\mathbf{x},t,\Omega)$ due to the dye molecules depends on the details of the pump and laser light fields and the dye-molecule dynamics discussed in Sec. II A. The determination of the $\mathbf{P}_j(\mathbf{x},t,\Omega)$ for the pump and laser radiations is taken up in Sec. II C by considering only the dye-molecule–radiation interaction. Relaxation processes are included in Sec. II D, using a phenomenological methodology.[19,50–53]

C. Macroscopic dye-molecule–radiation interaction

Consider a group of dye molecules whose orientation is the same. At a given location $\mathbf{x}$ in the dye-laser medium, in the semiclassical and electric dipole approximations, the interaction of a dye molecule with electromagnetic radiation is described by the Schrödinger equation

$$i\hbar\partial_t|\Psi\rangle=[H_d+e\mathbf{x}_e\cdot\mathcal{E}(t)]|\Psi\rangle\ , \quad (2.5)$$

where $|\Psi\rangle$ is the state vector of the optically active electron in the dye molecule. The time-independent quantity H_d is the Hamiltonian operator associated with the dynamics of this electron in the coupled dye-molecule–solvent environment. The time-dependent relaxation dynamics due to the dye-molecule–solvent interaction are treated phenomenologically in Sec. II D. The vector $\mathbf{x}_e$ in Eq. (2.5) denotes the electron position with respect to the dye-molecule center in a coordinate system fixed relative to the dye molecule. The local macroscopic electric-field intensity at the dye molecule, uniform over the molecule, is $\mathcal{E}(t)=\mathcal{E}_p(t)+\mathcal{E}_l(t)$. The local pump laser and dye-laser electric-field intensities are $\mathcal{E}_p(t)$ and $\mathcal{E}_l(t)$, respectively. In this section, for notational simplicity, the parametric dependence of physical quantities, such as $\mathcal{E}_j$, on location of $\mathbf{x}$ of the dye molecule is suppressed, i.e., $\mathcal{E}_j(t)=\mathcal{E}_j(\mathbf{x},t)$. The physical constants e and $\hbar$ are the charge on an electron and Planck's constant divided by 2π, respectively.

It should be noted that in a dielectric medium, the local macroscopic electric field $\mathcal{E}$ and corresponding induced polarization $\mathcal{P}$ are not equal to the total macroscopic electric field $\mathbf{E}$ and polarization $\mathbf{P}$ in the medium that appears in the field equations, Eqs. (2.1)–(2.3). In the dye-laser medium, these differences are due to the influence of the polarizable solvent molecules on the local electric field seen by each dye molecule. The prescription for relating the total and local fields depends on the symmetry properties of the medium and the characteristics of the field and is known as the Lorentz local-field correction.[52,53] For an isotropic medium, such as the dye-laser medium, and a monochromatic high frequency ν, field $\mathcal{E}=L\mathbf{E}$ and $\mathbf{P}=L\mathcal{P}$, where $L(\nu)=[n_s^2(\nu)+2]/3$ is the Lorentz correction factor. If the fields are nonmonochromatic, these relations may be applied to each high-frequency component. Generally, the solvent refractive index is essentially constant over the dye-molecule absorption and emission bands and the frequency dependence of the Lorentz correction factor can be neglected. In the following the Lorentz correction factor will be used to express equations in terms of the total macroscopic fields used in Eqs. (2.1)–(2.3).

Based on the discussion of Sec. II A, the dye-molecule energy-level structure may be represented by the simplified model shown in Fig. 2. The time-independent eigenvectors $|\psi_0^0\rangle$ and $|\psi_0^1\rangle$ represent the lowest vibronic states of S_0 and S_1, respectively, and satisfy $H_d|\psi_0^\mu\rangle=W_0^\mu|\psi_0^\mu\rangle$, where $\mu=(0,1)$ and W_0^μ is the energy of the corresponding state. In the following the superscript 0 or 1 relates to the electronic state S_0 or S_1, respectively. The band of substates of energy W_α^μ, other than the lowest, composing S_μ are described by the time-

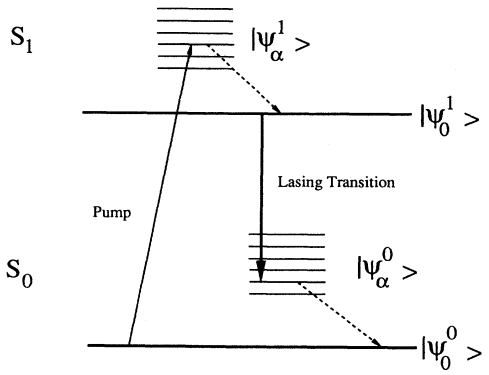

FIG. 2. Simplified dye-molecule energy-level model for a pulsed dye laser. Radiative (——) and nonradiative (— — —) transitions are indicated. The quantities $|\psi_0^0\rangle$, $\{|\psi_\alpha^0\rangle\}$, $|\psi_0^1\rangle$, and $\{|\psi_\alpha^1\rangle\}$ are the time-independent state vectors of the vibronic sublevels of the singlet S_0 and S_1 electronic states of the dye molecule.

independent eigenvector sets $\{|\psi_\alpha^\mu\rangle\}$, which satisfy $H_d|\psi_\alpha^\mu\rangle = W_\alpha^\mu|\psi_\alpha^\mu\rangle$. Each band of substates is taken to be a continuum[19] and denoted by the quantum-number parameter α. Physically the 0 and α subscripts represent the set of quantum numbers required to specify the electronic substate of the dye molecule in the solvent environment. Since the surrounding solvent is uniform and isotropic, the time-independent state vectors $\{|\psi_k^\mu\rangle\}$ are taken to form a complete, orthogonal basis independent of Ω, namely, $\langle\psi_0^\mu|\psi_0^\nu\rangle = \delta_{\mu\nu}$, $\langle\psi_0^\mu|\psi_\alpha^\nu\rangle = 0$, all μ, ν, and $\langle\psi_\beta^\mu|\psi_\alpha^\nu\rangle = \delta_{\mu\nu}\delta(\alpha-\beta)/\rho_\alpha^\mu$, where $\mu=(0,1)$ and $\nu=(0,1)$. The identity operator is

$$I=\sum_{\mu=0}^{1}\left[|\psi_0^\mu\rangle\langle\psi_0^\mu| + \int_{S_\mu} d\alpha\,\rho_\alpha^\mu|\psi_\alpha^\mu\rangle\langle\psi_\alpha^\mu|\right] . \tag{2.6}$$

The quantity ρ_α^μ is the density of states of the S_μ electronic band. The sign $\int_{S_\mu}$ denotes summation over band S_μ, but not including the lowest state. Consequently, the state vector of the dye molecule may be written

$$|\Psi_\Omega\rangle=\sum_{\mu=0}^{1}\left[a_0^\mu(t,\Omega)e^{-iW_0^\mu t/\hbar}|\psi_0^\mu\rangle + \int_{S_\mu} d\alpha\,\rho_\alpha^\mu a_\alpha^\mu(t,\Omega)e^{-iW_\alpha^\mu t/\hbar}|\psi_\alpha^\mu\rangle\right] . \tag{2.7}$$

The normalization condition $\langle\Psi_\Omega|\Psi_\Omega\rangle = 1$ yields

$$\sum_{\mu=0}^{1}\left[|a_0^\mu(t,\Omega)|^2 + \int_{S_\mu} d\alpha\,\rho_\alpha^\mu|a_\alpha^\mu(t,\Omega)|^2\right]=1 . \tag{2.8}$$

The quantity $|a_k^\mu(t,\Omega)|^2$ is the probability that a dye molecule with orientation Ω is in the kth vibrational sublevel of the S_μ electronic state.

Suppose the electronic states of the dye molecule in the solvent do not possess permanent dipole moments. Furthermore, from the discussion of Sec. II A, the pump electric field $\mathbf{E}_p(t)$ induces transitions between the lowest vibronic level of S_0 and the α vibronic sublevels of S_1. Likewise, the laser field $\mathbf{E}_l(t)$ induces transitions between the lowest vibronic level of S_1 and the α vibronic sublevels of S_0. For ultrashort pulses this assumption may not be entirely satisfactory. Radiative coupling between the lowest vibronic levels of S_0 and S_1 is not considered here although it occurs in some dyes. Radiation-induced intraband transitions are generally unimportant. Under these circumstances, in terms of the probability amplitudes $\{a_k^\mu(t,\Omega)\}$, the Schrödinger equation takes the form

$$i\hbar\partial_t a_0^0(t,\Omega)=\int_{S_1} d\alpha\,\rho_\alpha^1 a_\alpha^1(t,\Omega)e^{-i\omega_{\alpha p}t}\boldsymbol{L}\boldsymbol{\mu}_{\alpha p}^*(\Omega)\cdot\mathbf{E}_p(t) , \tag{2.9}$$

$$i\hbar\partial_t a_\alpha^0(t,\Omega)=a_0^1(t,\Omega)e^{-i\omega_{\alpha l}t}\boldsymbol{L}\boldsymbol{\mu}_{\alpha l}^*(\Omega)\cdot\mathbf{E}_l(t) , \tag{2.10}$$

$$i\hbar\partial_t a_0^1(t,\Omega)=\int_{S_0} d\alpha\,\rho_\alpha^0 a_\alpha^0(t,\Omega)e^{+i\omega_{\alpha l}t}\boldsymbol{L}\boldsymbol{\mu}_{\alpha l}(\Omega)\cdot\mathbf{E}_l(t) , \tag{2.11}$$

and

$$i\hbar\partial_t a_\alpha^1(t,\Omega)=a_0^0(t,\Omega)e^{+i\omega_{\alpha p}t}\boldsymbol{L}\boldsymbol{\mu}_{\alpha p}(\Omega)\cdot\mathbf{E}_p(t) . \tag{2.12}$$

Here and in the following the superscript $*$ denotes complex conjugate. The induced dipole moments $\boldsymbol{\mu}_{\alpha j}(\Omega)$ and coupling frequencies $\omega_{\alpha j}$ are $\boldsymbol{\mu}_{\alpha p}(\Omega)=\langle\psi_\alpha^1|e\mathbf{x}_e|\psi_0^0\rangle$, $\boldsymbol{\mu}_{\alpha l}(\Omega)=\langle\psi_0^1|e\mathbf{x}_e|\psi_\alpha^0\rangle$, $\omega_{\alpha p}=(W_\alpha^1-W_0^0)/\hbar$, and $\omega_{\alpha l}=(W_0^1-W_\alpha^0)/\hbar$. In the following the orientation Ω of the dye molecule is specified by the direction of the induced dipole moments $\boldsymbol{\mu}_{\alpha j}(\Omega)$ as shown in Fig. 3. It is assumed that all the pump-laser and dye-laser-induced dipole moments are parallel[17,18,54] and therefore the direction of all $\boldsymbol{\mu}_{\alpha j}(\Omega)$ are specified by the same spherical polar angles θ and ϕ.

The local macroscopic equations governing the dye-molecule–radiation coupling can be obtained in the following way. Since Eqs. (2.9)–(2.12) do not include rotational relaxation, the local number density $n(\Omega)$ of dye molecules per unit solid angle whose orientation is in the solid angle range Ω to $\Omega+d\Omega$ must be time independent. Furthermore,

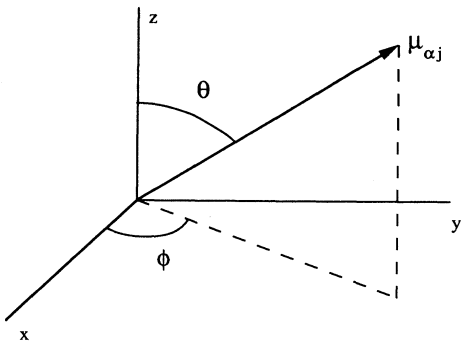

FIG. 3. Orientation of the induced dye-molecule dipole moments $\boldsymbol{\mu}_{\alpha j}(\Omega)$.

$$N=\int_{4\pi} d\Omega\, n(\Omega) \tag{2.13}$$

is the total number density of dye molecules in the solvent. In general, N is a constant determined by the dye-molecule concentration in the solvent. It is typically $\lesssim 10^{-4}$ times the solvent molecule number density. In addition, if $n_k^\mu(t,\Omega)$ is the local number density per unit solid angle of dye molecules with orientation Ω in the kth vibrational sublevel of the S_μ electronic state, then

$$n_k^\mu(t,\Omega)=n(\Omega)\overline{|a_k^\mu(t,\Omega)|^2}\ , \tag{2.14}$$

where the overbar denotes ensemble average. Taking the ensemble average of Eq. (2.8) and then multiplying the result by $n(\Omega)$ yields the conservation relation

$$\sum_{\mu=0}^{1}\left[n_0^\mu(t,\Omega)+\int_{S_\mu} d\alpha\,\rho_\alpha^\mu n_\alpha^\mu(t,\Omega)\right]=n(\Omega)\ . \tag{2.15}$$

The macroscopic electric polarization per unit solid angle generated by the dye molecules with orientation Ω due to their interaction with the combined pump- and dye-laser electromagnetic field is

$$\mathbf{P}_d(t,\Omega)=n(\Omega)L\overline{\langle\Psi_\Omega|(-e\mathbf{x}_e)|\Psi_\Omega\rangle}\ . \tag{2.16}$$

Substituting Eq. (2.7) into Eq. (2.16) it can be shown that

$$\mathbf{P}_d(t,\Omega)=\mathbf{P}_p(t,\Omega)+\mathbf{P}_l(t,\Omega)\ , \tag{2.17}$$

where

$$\mathbf{P}_p(t,\Omega)=\int_{S_1} d\alpha\,\rho_\alpha^1[\mathbf{P}_{\alpha p}(t,\Omega)+\mathbf{P}_{\alpha p}^*(t,\Omega)] \tag{2.18}$$

and

$$\mathbf{P}_l(t,\Omega)=\int_{S_0} d\alpha\,\rho_\alpha^0[\mathbf{P}_{\alpha l}(t,\Omega)+\mathbf{P}_{\alpha l}^*(t,\Omega)] \tag{2.19}$$

are the dye-molecule macroscopic electric polarizations per unit solid angle generated by the pump-laser and dye-laser fields, respectively. The induced macroscopic polarization per unit solid angle depends on the level probability amplitudes, induced dipole moments, and coupling frequencies through the complex quantities

$$\mathbf{P}_{\alpha p}(t,\Omega)=-n(\Omega)\overline{a_0^{0*}(t,\Omega)a_\alpha^1(t,\Omega)}e^{-i\omega_{\alpha p}t}L\boldsymbol{\mu}_{\alpha p}^*(\Omega) \tag{2.20}$$

and

$$\mathbf{P}_{\alpha l}(t,\Omega)=-n(\Omega)\overline{a_\alpha^{0*}(t,\Omega)a_0^1(t,\Omega)}e^{-i\omega_{\alpha l}t}L\boldsymbol{\mu}_{\alpha l}^*(\Omega)\ . \tag{2.21}$$

Equations for the kth vibrational sublevel populations $n_k^\mu(t,\Omega)$ of the S_μ electronic state may be obtained by first using Eqs. (2.9)–(2.12) to derive equations for the ensemble-average sublevel occupation probabilities $\{|a_k^\mu(t,\Omega)|^2\}$. These equations may then be multiplied by $n(\Omega)$ to obtain, after using Eqs. (2.20) and (2.21) the continuity equations,

$$\partial_t n_0^1(t,\Omega)=\int_{S_0} d\alpha\,\rho_\alpha^0[\mathbf{P}_{\alpha l}(t,\Omega)-\mathbf{P}_{\alpha l}^*(t,\Omega)]\cdot\mathbf{E}_l(t)/i\hbar\ , \tag{2.22}$$

$$\partial_t n_\alpha^1(t,\Omega)=[\mathbf{P}_{\alpha p}(t,\Omega)-\mathbf{P}_{\alpha p}^*(t,\Omega)]\cdot\mathbf{E}_p(t)/i\hbar\ , \tag{2.23}$$

$$\partial_t n_\alpha^0(t,\Omega)=[\mathbf{P}_{\alpha l}^*(t,\Omega)-\mathbf{P}_{\alpha l}(t,\Omega)]\cdot\mathbf{E}_l(t)/i\hbar\ , \tag{2.24}$$

and

$$\partial_t n_0^0(t,\Omega)=\int_{S_1} d\alpha\,\rho_\alpha^1[\mathbf{P}_{\alpha p}^*(t,\Omega)-\mathbf{P}_{\alpha p}(t,\Omega)]\cdot\mathbf{E}_p(t)/i\hbar\ . \tag{2.25}$$

Differentiating Eqs. (2.20) and (2.21) with respect to time and using Eqs. (2.9)–(2.12), it follows that

$$\begin{aligned}\partial_t\mathbf{P}_{\alpha p}(t,\Omega)=&-i\omega_{\alpha p}\mathbf{P}_{\alpha p}(t,\Omega)\\&-[n_0^0(t,\Omega)-n_\alpha^1(t,\Omega)]\\&\times L^2\boldsymbol{\mu}_{\alpha p}^*(\Omega)[\boldsymbol{\mu}_{\alpha p}(\Omega)\cdot\mathbf{E}_p(t)]/i\hbar\\&+\int_{S_1} d\beta\,\rho_\beta^1\overleftrightarrow{\mathbf{B}}_{\alpha\beta}(t,\Omega)\cdot\mathbf{E}_p(t)/i\hbar\end{aligned} \tag{2.26}$$

and

$$\begin{aligned}\partial_t\mathbf{P}_{\alpha l}(t,\Omega)=&-i\omega_{\alpha l}\mathbf{P}_{\alpha l}(t,\Omega)\\&+[n_0^1(t,\Omega)-n_\alpha^0(t,\Omega)]\\&\times L^2\boldsymbol{\mu}_{\alpha l}^*(\Omega)[\boldsymbol{\mu}_{\alpha l}(\Omega)\cdot\mathbf{E}_l(t)]/i\hbar\\&-\int_{S_0} d\beta\,\rho_\beta^0\overleftrightarrow{\mathbf{A}}_{\alpha\beta}(t,\Omega)\cdot\mathbf{E}_l(t)/i\hbar\ .\end{aligned} \tag{2.27}$$

The dyadic tensor quantities $\overleftrightarrow{\mathbf{A}}_{\alpha\beta}(t,\Omega)$ and $\overleftrightarrow{\mathbf{B}}_{\alpha\beta}(t,\Omega)$ are defined by

$$\begin{aligned}\overleftrightarrow{\mathbf{A}}_{\alpha\beta}(t,\Omega)=&n(\Omega)\overline{a_\alpha^{0*}(t,\Omega)a_\beta^0(t,\Omega)}\\&\times e^{+i\Omega_{\alpha\beta}^0 t}L^2\boldsymbol{\mu}_{\alpha l}^*(\Omega)\boldsymbol{\mu}_{\beta l}(\Omega)\end{aligned} \tag{2.28}$$

and

$$\begin{aligned}\overleftrightarrow{\mathbf{B}}_{\alpha\beta}(t,\Omega)=&n(\Omega)\overline{a_\alpha^1(t,\Omega)a_\beta^{1*}(t,\Omega)}\\&\times e^{-i\Omega_{\alpha\beta}^1 t}L^2\boldsymbol{\mu}_{\alpha p}^*(\Omega)\boldsymbol{\mu}_{\beta p}(\Omega)\ ,\end{aligned} \tag{2.29}$$

with $\overleftrightarrow{\mathbf{A}}_{\alpha\alpha}(t,\Omega)=\overleftrightarrow{\mathbf{B}}_{\alpha\alpha}(t,\Omega)=0$ for all α and $\Omega_{\alpha\beta}^\mu=(W_\alpha^\mu-W_\beta^\mu)/\hbar$.

The set of equations, Eq. (2.22)–(2.27), can be closed by differentiating Eqs. (2.28) and (2.29) with respect to time and using Eqs. (2.9)–(2.21) to obtain

$$\partial_t\overleftrightarrow{\mathbf{A}}_{\alpha\beta}(t,\Omega)=i\Omega_{\alpha\beta}^0\overleftrightarrow{\mathbf{A}}_{\alpha\beta}(t,\Omega)+L^2\{\boldsymbol{\mu}_{\alpha l}^*(\Omega)[\boldsymbol{\mu}_{\alpha l}(\Omega)\cdot\mathbf{E}_l(t)]\mathbf{P}_{\beta l}^*(t,\Omega)-\mathbf{P}_{\alpha l}(t,\Omega)\boldsymbol{\mu}_{\beta l}(\Omega)[\boldsymbol{\mu}_{\beta l}^*(\Omega)\cdot\mathbf{E}_l(t)]\}/i\hbar \tag{2.30}$$

and

$$\partial_t\overleftrightarrow{\mathbf{B}}_{\alpha\beta}(t,\Omega)=-i\Omega_{\alpha\beta}^1\overleftrightarrow{\mathbf{B}}_{\alpha\beta}(t,\Omega)+L^2\{\mathbf{P}_{\alpha p}(t,\Omega)\boldsymbol{\mu}_{\beta p}(\Omega)[\boldsymbol{\mu}_{\beta p}^*(\Omega)\cdot\mathbf{E}_p(t)]-\boldsymbol{\mu}_{\alpha p}^*(\Omega)[\boldsymbol{\mu}_{\alpha p}(\Omega)\cdot\mathbf{E}_p(t)]\mathbf{P}_{\beta p}^*(t,\Omega)\}/i\hbar\ . \tag{2.31}$$

The above equations, a generalization of those derived by Fu and Haken,[19] include only radiative processes and to this level of approximation form a complete set of equations that describe the response of a dye molecule of fixed orientation Ω to the macroscopic radiation field.

Due to collisions with the solvent molecules the dye-molecule sublevel amplitudes a_α^0 and a_α^1 are randomly phased relative to each other and, in general,

$$n_\alpha^0(t,\Omega)L^2\boldsymbol{\mu}_{\alpha l}^*(\Omega)[\boldsymbol{\mu}_{\alpha l}(\Omega)\cdot\mathbf{E}_l(t)] \gg \int_{S_0} d\beta\,\rho_\beta^0 \overleftrightarrow{\mathbf{A}}_{\alpha\beta}(t,\Omega)\cdot\mathbf{E}_l(t) \quad (2.32)$$

and

$$n_\alpha^1(t,\Omega)L^2\boldsymbol{\mu}_{\alpha p}^*(\Omega)[\boldsymbol{\mu}_{\alpha p}(\Omega)\cdot\mathbf{E}_p(t)] \gg \int_{S_1} d\beta\,\rho_\beta^1 \overleftrightarrow{\mathbf{B}}_{\alpha\beta}(t,\Omega)\cdot\mathbf{E}_p(t)\ . \quad (2.33)$$

Under these circumstances Eqs. (2.30) and (2.31) may be neglected and Eqs. (2.26) and (2.27) become

$$\partial_t\mathbf{P}_{\alpha p}(t,\Omega) = -i\omega_{\alpha p}\mathbf{P}_{\alpha p}(t,\Omega) - [n_0^0(t,\Omega)-n_\alpha^1(t,\Omega)]L^2\boldsymbol{\mu}_{\alpha p}^*(\Omega) \times[\boldsymbol{\mu}_{\alpha p}(\Omega)\cdot\mathbf{E}_p(t)]/i\hbar \quad (2.34)$$

and

$$\partial_t\mathbf{P}_{\alpha l}(t,\Omega) = -i\omega_{\alpha l}\mathbf{P}_{\alpha l}(t,\Omega) + [n_0^1(t,\Omega)-n_\alpha^0(t,\Omega)]L^2\boldsymbol{\mu}_{\alpha l}^*(\Omega) \times[\boldsymbol{\mu}_{\alpha l}(\Omega)\cdot\mathbf{E}_l(t)]/i\hbar\ . \quad (2.35)$$

Equations (2.22)–(2.25), (2.34) and (2.35) describe the light–dye-molecule dynamics for dye molecules of specific orientation.

D. Macroscopic dye-medium–radiation interaction with phenomenological relaxation

From Eqs (2.22)–(2.25), (2.34) and (2.35) it can be seen that the strength of the dye-molecule interaction with the electromagnetic field depends on the orientation of its induced dipole moment $\boldsymbol{\mu}_{\alpha p}(\Omega)$ or $\boldsymbol{\mu}_{\alpha l}(\Omega)$ relative to the direction or polarization of the exciting electric field $\mathbf{E}_p(\mathbf{x},t)$ or $\mathbf{E}_l(\mathbf{x},t)$, respectively. Therefore the orientational or rotational dynamics of the dye molecule is important as regards its coupling to the light field.[12–18,35] It should be noted that orientational effects are also expected and observed in amorphous solid-state laser media such as Nd:Glass.[55]

The macroscopic response of the dye molecules, including relaxation processes, to the macroscopic electric field $\mathbf{E}$ at location $\mathbf{x}$ and time t may be obtained as follows. Since the dye molecules are distributed dilutely throughout the solvent, they have collisions predominantly with solvent molecules. These elastic and inelastic collision events cause various relaxation processes (Table I) to occur. In addition, spontaneous emission of radiation may occur on the laser transition. These processes may be treated phenomenologically by introducing relaxation rate constants into Eqs. (2.22)–(2.25), and (2.34), and (2.35) at location $\mathbf{x}$, hereafter indicated explicitly for macroscopic physical quantities. When dye-molecule rotation occurs the local number density n of dye molecules with orientation Ω is no longer time independent as in Sec. II C, i.e., $n(\mathbf{x},\Omega)\rightarrow n(\mathbf{x},t,\Omega)$. Under these circumstances the conservation condition Eq. (2.15) becomes

$$\sum_{\mu=0}^{1}\left[n_0^\mu(\mathbf{x},t,\Omega)+\int_{S_\mu} d\alpha\,\rho_\alpha^\mu n_\alpha^\mu(\mathbf{x},t,\Omega)\right]=n(\mathbf{x},t,\Omega)\ . \quad (2.36)$$

However, for a uniform dye-molecule doping density or concentration, the total number density of dye molecules remains a constant, i.e., Eq. (2.13) becomes

$$N=\int_{4\pi} d\Omega\, n(\mathbf{x},t,\Omega)\ . \quad (2.37)$$

The total vibrational level populations of the S_μ electronic states are

$$N_k^\mu(\mathbf{x},t)=\int_{4\pi} d\Omega\, n_k^\mu(\mathbf{x},t,\Omega)\ , \quad (2.38)$$

where the quantities $n_k^\mu(\mathbf{x},t,\Omega)$ are the dye-molecule vibronic sublevel number densities per unit solid angle with orientation Ω. In addition, in Eq. (2.3), the total macroscopic polarization per unit solid angle, $\mathbf{P}_j(\mathbf{x},t,\Omega)$, due to dye molecules of orientation Ω that is induced by the pump laser and dye-laser electric fields is given by Eqs. (2.18) and (2.19), namely,

$$\mathbf{P}_p(\mathbf{x},t,\Omega)=\int_{S_1} d\alpha\,\rho_\alpha^1[\mathbf{P}_{\alpha p}(\mathbf{x},t,\Omega)+\mathbf{P}_{\alpha p}^*(\mathbf{x},t,\Omega)] \quad (2.39)$$

and

$$\mathbf{P}_l(\mathbf{x},t,\Omega)=\int_{S_0} d\alpha\,\rho_\alpha^0[\mathbf{P}_{\alpha l}(\mathbf{x},t,\Omega)+P_{\alpha l}^*(\mathbf{x},t,\Omega)]\ . \quad (2.40)$$

The complex polarization components $\mathbf{P}_{\alpha j}$ are determined by Eqs. (2.34) and (2.35) modified to include relaxation, i.e.,

$$\partial_t\mathbf{P}_{\alpha p}(\mathbf{x},t,\Omega) = -(\gamma_{\alpha p}+i\omega_{\alpha p})\mathbf{P}_{\alpha p}(\mathbf{x},t,\Omega) - [n_0^0(\mathbf{x},t,\Omega)-n_\alpha^1(\mathbf{x},t,\Omega)] \times L^2\boldsymbol{\mu}_{\alpha p}^*(\Omega)[\boldsymbol{\mu}_{\alpha p}(\Omega)\cdot\mathbf{E}_p(\mathbf{x},t)]/i\hbar \quad (2.41)$$

and

$$\partial_t\mathbf{P}_{\alpha l}(\mathbf{x},t,\Omega) = -(\gamma_{\alpha l}+i\omega_{\alpha l})\mathbf{P}_{\alpha l}(\mathbf{x},t,\Omega) + [n_0^1(\mathbf{x},t,\Omega)-n_\alpha^0(\mathbf{x},t,\Omega)] \times L^2\boldsymbol{\mu}_{\alpha l}^*(\Omega)[\boldsymbol{\mu}_{\alpha l}(\Omega)\cdot\mathbf{E}_l(\mathbf{x},t)]/i\hbar\ , \quad (2.42)$$

where $\gamma_{\alpha p}$ and $\gamma_{\alpha l}$ are dye-molecule phenomenological relaxation rates for the pump-laser and dye-laser-field-induced polarizations, respectively. They are due primarily to elastic dye-molecule collisions with solvent molecules. The induced polarizations $\mathbf{P}_j(\mathbf{x},t,\Omega)$ are parallel to the dye-molecule-induced dipole moments $\boldsymbol{\mu}_{\alpha j}(\Omega)$, which specify the orientation of the dye molecule as

shown in Fig. 3. As noted earlier the pump-laser and dye-laser-induced dipole moments are assumed to be parallel.[17,18,54]

When dye-molecule relaxation processes are included, Eq. (2.22) then becomes the continuity rate equation for the number density per unit solid angle $n_0^1(\mathbf{x},t,\Omega)$ of the dye molecules with orientation Ω in the lowest vibronic level of the S_1 electronic band, namely,

$$\partial_t n_0^1(\mathbf{x},t,\Omega)=\int_{S_1} d\alpha\,\rho_\alpha^1\gamma_V^1(\alpha,0)n_\alpha^1(\mathbf{x},t,\Omega)+\int_{4\pi} d\Omega'\gamma_0^1(\Omega',\Omega)n_0^1(\mathbf{x},t,\Omega') -\gamma_{R0}^1(\Omega)n_0^1(\mathbf{x},t,\Omega)-\gamma_F n_0^1(\mathbf{x},t,\Omega)+\int_{S_0} d\alpha\,\rho_\alpha^0[\mathbf{P}_{\alpha l}(\mathbf{x},t,\Omega)-\mathbf{P}_{\alpha l}^*(\mathbf{x},t,\Omega)]\cdot\mathbf{E}_l(\mathbf{x},t)/i\hbar\ , \tag{2.43}$$

where for the S_1 band of states $\gamma_V^1(\alpha,0)$ is the vibrational relaxation rate from the vibrational sublevel α to sublevel 0, $\gamma_0^1(\Omega',\Omega)$ is the rotational relaxation rate from orientation $\Omega'\rightarrow\Omega$ for the lowest vibrational sublevel,

$$\gamma_{R0}^1(\Omega)=\int_{4\pi} d\Omega'\gamma_0^1(\Omega',\Omega) \tag{2.44}$$

is the corresponding total rotational relaxation rate, and γ_F is the total fluorescence rate for the S_1 to S_0 transition.

The first term in Eq. (2.43) represents the vibrational relaxation of all α sublevels of S_1 into the lowest sublevel of S_1. Since the solvent is an isotropic amorphous medium, it is reasonable to expect the vibrational relaxation rates $\gamma_V^1(\alpha,0)$ to be independent of dye-molecule orientation. It is assumed that vibrational relaxation is a one-step process $S_1(\alpha)\rightarrow S_1(0)$ and does not involve intermediate sublevels.[38,39] The second term represents the rotational relaxation of all orientations Ω' into orientation Ω. The third term represents rotational relaxation from orientation Ω to all other orientations. The fourth term is due to spontaneous emission and internal conversion. The fifth term in Eq. (2.43) is due to radiative coupling of all laser transitions $S_1(0)\leftrightarrow S_0(\alpha)$.

If $\gamma_{F\alpha}$ is the fluorescence relaxation rate for the $S_1(0)\rightarrow S_0(\alpha)$ transition, then

$$\gamma_F=\int_{S_0} d\alpha\,\rho_\alpha^0\gamma_{F\alpha}\ . \tag{2.45}$$

Since it is assumed that the relaxation rate $\gamma_{F\alpha}$ is due to spontaneous emission and internal conversion, $\gamma_{F\alpha}$ is essentially independent of dye-molecule orientation. Consequently, γ_F is also independent of dye-molecule orientation.

The dye-molecule orientation or rotational relaxation is essentially a random-walk process involving many small rotational increments.[35] Since the solvent is an isotropic, amorphous medium, the total dye-molecule rotational relaxation rate must be independent of the initial orientation of the dye molecule. Therefore $\gamma_{R0}^1(\Omega)$ is equal to γ_{R0}^1 and, consequently, $\gamma_0^1(\Omega',\Omega)=\gamma_0^1(\Omega')$. Furthermore, the rate of rotational relaxation must be essentially the same for each orientation. Therefore $\gamma_0^1(\Omega')$ is equal to γ_0^1. Consequently, from Eq. (2.44), $\gamma_0^1=\gamma_{R0}^1/4\pi$. Therefore the phenomenological rotational relaxation terms in Eq. (2.43) may be approximated by

$$\int_{4\pi} d\Omega'\gamma_0^1(\Omega',\Omega)n_0^1(\mathbf{x},t,\Omega')-\gamma_{R0}^1(\Omega)n_0^1(\mathbf{x},t,\Omega) \approx\gamma_{R0}^1\left[\int_{4\pi} d\Omega' n_0^1(\mathbf{x},t,\Omega')/4\pi-n_0^1(\mathbf{x},t,\Omega)\right]\ . \tag{2.46}$$

Furthermore, if the orientational distribution gradients are not too large, then the local diffusion approximation[35] yields

$$\gamma_{R0}^1\left[\int_{4\pi} d\Omega' n_0^1(\mathbf{x},t,\Omega')/4\pi-n_0^1(\mathbf{x},t,\Omega)\right] \approx D_{R0}^1\nabla_\Omega^2 n_0^1(\mathbf{x},t,\Omega)\ , \tag{2.47}$$

where D_{R0}^1 is the isotropic rotational diffusion coefficient[35] for the lowest vibrational sublevel. The quantity ∇_Ω^2 is the Laplacian operator in spherical coordinates:

$$\nabla_\Omega^2=(1/\sin\theta)[\partial_\theta(\sin\theta\partial_\theta)+(1/\sin\theta)\partial_\phi^2]\ . \tag{2.48}$$

The diffusion coefficient D_{R0}^1 and the total rotational relaxation rate γ_{R0}^1 are related by[35] $\gamma_{R0}^1=6D_{R0}^1$. The magnitude of the rotational relaxation rate and diffusion coefficient depends strongly on the solvent.[35]

The assumption of isotropic rotational relaxation is a good approximation for many dye molecules, but is not essential to the semiclassical methodology developed here. More sophisticated models[35] that exhibit the anisotropic nature of dye-molecule rotational relaxation can be readily incorporated into the level population equations, e.g., Eq. (2.43). In this case, Ω may be interpreted as specifying the Euler angles for the dye-molecule orientation. For the isotropic rotational relaxation diffusion model,[12,35] in the following assumed to hold for all vibronic substates of S_0 and S_1, Eq. (2.43) becomes

$$\partial_t n_0^1(\mathbf{x},t,\Omega)=\int_{S_1} d\alpha\,\rho_\alpha^1\gamma_V^1(\alpha,0)n_\alpha^1(\mathbf{x},t,\Omega)+\gamma_{R0}^1[\langle n_0^1(\mathbf{x},t)\rangle-n_0^1(\mathbf{x},t,\Omega)]-\gamma_F n_0^1(\mathbf{x},t,\Omega) +\int_{S_0} d\alpha\,\rho_\alpha^0[\mathbf{P}_{\alpha l}(\mathbf{x},t,\Omega)-\mathbf{P}_{\alpha l}^*(\mathbf{x},t,\Omega)]\cdot\mathbf{E}_l(\mathbf{x},t)/i\hbar\ , \tag{2.49}$$

where

$$\langle n_0^1(\mathbf{x},t)\rangle=\int_{4\pi} d\Omega\, n_0^1(\mathbf{x},t,\Omega)/4\pi \tag{2.50}$$

is the orientation-averaged density per unit solid angle of dye molecules in $S_1(0)$.

From Table I, for typical dye-laser media the dye-molecule vibrational relaxation rates are much larger than the corresponding rotational relaxation rates, i.e.,

$\gamma_V^\mu(\alpha,0) \gg \gamma_{R0}^\mu$. Consequently, Eqs. (2.23) and (2.24) become the continuity equations for the number densities $n_\alpha^1(\mathbf{x},t,\Omega)$ and $n_\alpha^0(\mathbf{x},t,\Omega)$ of dye molecules with orientation Ω in the α vibronic sublevels of S_1 and S_0, respectively,

$$\partial_t n_\alpha^1(\mathbf{x},t,\Omega) = -\gamma_V^1(\alpha,0) n_\alpha^1(\mathbf{x},t,\Omega) + [\mathbf{P}_{\alpha p}(\mathbf{x},t,\Omega) - \mathbf{P}_{\alpha p}^*(\mathbf{x},t,\Omega)]\cdot\mathbf{E}_p(\mathbf{x},t)/i\hbar \quad (2.51)$$

and

$$\partial_t n_\alpha^0(\mathbf{x},t,\Omega) = -\gamma_V^0(\alpha,0) n_\alpha^0(\mathbf{x},t,\Omega) + \gamma_{F\alpha} n_0^1(\mathbf{x},t,\Omega) + [\mathbf{P}_{\alpha l}^*(\mathbf{x},t,\Omega) - \mathbf{P}_{\alpha l}(\mathbf{x},t,\Omega)]\cdot\mathbf{E}_l(\mathbf{x},t)/i\hbar \, . \quad (2.52)$$

In Eqs. (2.51) and (2.52) for the S_μ band of states, $\gamma_V^\mu(\alpha,0)$ is the vibrational relaxation rate from vibronic sublevel α to sublevel 0. The last term in Eq. (2.51) represents coupling of pump-laser radiation to the transitions $S_0(0) \leftrightarrow S_1(\alpha)$. Likewise, the last term in Eq. (2.52) accounts for radiative coupling of the dye-laser transitions $S_1(0) \leftrightarrow S_0(\alpha)$.

The equations for the level populations are completed by the relaxation form of Eq. (2.25), namely,

$$\partial_t n_0^0(\mathbf{x},t,\Omega) = \int_{S_0} d\alpha\, \rho_\alpha^0 \gamma_V^0(\alpha,0) n_\alpha^0(\mathbf{x},t,\Omega) + \gamma_{R0}^0[\langle n_0^0(\mathbf{x},t)\rangle - n_0^0(\mathbf{x},t,\Omega)] + \int_{S_1} d\alpha\, \rho_\alpha^1[\mathbf{P}_{\alpha p}^*(\mathbf{x},t,\Omega) - \mathbf{P}_{\alpha p}(\mathbf{x},t,\Omega)]\cdot\mathbf{E}_p(\mathbf{x},t)/i\hbar \, , \quad (2.53)$$

where $\langle n_0^0(\mathbf{x},t)\rangle$ is the orientation-averaged density per unit solid angle of dye molecules in the $S_0(0)$ level. Equation (2.53) is the continuity rate equation for the number density per unit solid angle $n_0^0(\mathbf{x},t,\Omega)$ of the dye molecules with orientation Ω in the lowest vibronic level of the S_0 electronic band. The quantity γ_{R0}^0 is the rotational relaxation rate for this level. It is related to the isotropic rotational diffusion coefficient D_{R0}^0 of this level by[35] $D_{R0}^0 = \gamma_{R0}^0/6$. The first term in Eq. (2.53) represents vibrational relaxation of all α sublevels of S_0 into the lowest level of S_0. The second term represents the rotational relaxation of the lowest vibrational level of S_0. The third term is due to laser-pump radiation coupling of all the transitions $S_0(0) \leftrightarrow S_1(\alpha)$.

In constructing the continuity equations, Eqs. (2.49), (2.51), and (2.52), for the dye-molecule excited-state level populations it is assumed that, due to the nonequilibrium laser dynamics and $(W_0^1, W_\alpha^\mu) \gg kT$ the level population densities are much larger than their thermal equilibrium values. In addition, the phenomenological vibration relaxation rates γ_V^μ represent the one-step vibrational relaxation $S_\mu(\alpha) \rightarrow S_\mu(0)$. This approximation is motivated by the limited current understanding of the vibronic mode structure and relaxation dynamics of dye molecules in liquid solvents. It could be tested by comparisons between the theory presented here and the results from ultrashort-pulse dye-laser experiments.

The self-consistent Eqs. (2.1)–(2.3) and (2.36)–(2.53) developed in Sec. II, together with suitable boundary and initial conditions for the electromagnetic field and dye-medium properties, describe the macroscopic dynamics of pulsed-dye-laser media including rotational relaxation of the dye molecules. These equations are applicable to radiation pulse lengths much less than the nonradiative coupling time of the singlet-triplet manifolds of the dye molecule. They also form a foundation for inclusion of nonlinear processes such as self-focusing[53] and Raman scattering[49,53] that are known to be important at high light intensities, i.e., $\gtrsim 100$ MW/cm^2. In the following, the utility of this theoretical formalism is illustrated by application to several situations of practical interest.

III. AMPLIFICATION OF QUASIMONOCHROMATIC LIGHT PULSES

Consider a laser-pumped dye-laser medium in which the pump laser and dye-laser-light beams are quasimonochromatic plane waves:

$$\mathbf{E}_j(\mathbf{x},t) = \mathrm{Re}\{\hat{\mathbf{E}}_j(\mathbf{x},t)\exp[i(\mathbf{k}_j\cdot\mathbf{x} - \omega_j t)]\} \, , \quad (3.1)$$

where Re denotes the real part. The complex electric-field amplitudes $\hat{\mathbf{E}}_j(\mathbf{x},t)$ are slowly varying in space and time compared to the field wavelength $\lambda_j = 2\pi/k_j$ and period $2\pi/\omega_j$, respectively. The pump-laser frequency $\nu_p = \omega_p/2\pi$ ranges over the dye molecule $S_0 \rightarrow S_1$ absorption band. Similarly, the dye-laser frequency $\nu_l = \omega_l/2\pi$ ranges over the dye molecule $S_1 \rightarrow S_0$ emission band. The durations of the pump- and dye-laser pulses are much greater than an optical period.

A. General description

Due to the linearity of the field equations, Eqs. (2.1) and (2.2), the pump-laser and dye-laser-induced polarizations are of the form

$$\mathbf{P}_j(\mathbf{x},t) = \mathrm{Re}\{\hat{\mathbf{P}}_j(\mathbf{x},t)\exp[i(\mathbf{k}_j\cdot\mathbf{x} - \omega_j t)]\} \, , \quad (3.2)$$

where $\hat{\mathbf{P}}_j(\mathbf{x},t)$ is the slowly varying complex polarization amplitude. In general, the complex polarization amplitudes $\mathbf{P}_{\alpha j}(\mathbf{x},t,\Omega)$ produced by the interaction of the pump-laser and dye-laser electric fields with the dye molecules of the orientation Ω may be written

$$\mathbf{P}_{\alpha j}(\mathbf{x},t,\Omega) = \mathbf{A}_{\alpha j}(\mathbf{x},t,\Omega)\exp[i(\mathbf{k}_j\cdot\mathbf{x} - \omega_j t)] + \mathbf{B}_{\alpha j}(\mathbf{x},t,\Omega)\exp[-i(\mathbf{k}_j\cdot\mathbf{x} - \omega_j t)] \, , \quad (3.3)$$

where $\mathbf{A}_{\alpha j}(\mathbf{x},t,\Omega)$ and $\mathbf{B}_{\alpha j}(\mathbf{x},t,\Omega)$ are slowly varying complex amplitudes. Using Eqs. (2.3), (2.39), (2.40), (3.1),

and (3.3), it can be shown that the complex polarization amplitudes in Eq. (3.2) are given by

$$\hat{\mathbf{P}}_p(\mathbf{x},t)=2\int_{4\pi}d\Omega\int_{S_1}d\alpha\,\rho_\alpha^1[\,\mathbf{A}_{\alpha p}(\mathbf{x},t,\Omega)+\mathbf{B}_{\alpha p}^*(\mathbf{x},t,\Omega)] +\epsilon_0\hat{\chi}_s(\omega_p)\hat{\mathbf{E}}_p(\mathbf{x},t) \tag{3.4}$$

and

$$\hat{\mathbf{P}}_l(\mathbf{x},t)=2\int_{4\pi}d\Omega\int_{S_0}d\alpha\,\rho_\alpha^0[\,\mathbf{A}_{\alpha l}(\mathbf{x},t,\Omega)+\mathbf{B}_{\alpha l}^*(\mathbf{x},t,\Omega)] +\epsilon_0\hat{\chi}_s(\omega_l)\hat{\mathbf{E}}_l(\mathbf{x},t)\ . \tag{3.5}$$

In general, the dye concentration in the solvent is such that the dye-molecule number density N is much less than the solvent-molecule number density. Consequently, the induced electric polarization contribution from the dye molecules is much less than the contribution from the solvent molecules:

$$\epsilon_0\hat{\chi}_s(\omega_p)\hat{\mathbf{E}}_p(\mathbf{x},t) \gg 2\int_{4\pi}d\Omega\int_{S_1}d\alpha\,\rho_\alpha^1[\,\mathbf{A}_{\alpha p}(\mathbf{x},t,\Omega)+\mathbf{B}_{\alpha p}^*(\mathbf{x},t,\Omega)] \tag{3.6}$$

and

$$\epsilon_0\hat{\chi}_s(\omega_l)\hat{\mathbf{E}}_l(\mathbf{x},t) \gg 2\int_{4\pi}d\Omega\int_{S_0}d\alpha\,\rho_\alpha^0[\,\mathbf{A}_{\alpha l}(\mathbf{x},t,\Omega)+\mathbf{B}_{\alpha l}^*(\mathbf{x},t,\Omega)]\ . \tag{3.7}$$

In the field equations the induced electric polarization due to the dye molecules may be treated as a perturbation. If Eqs. (3.1), (3.2), (3.4), and (3.5) are substituted into the field equations, Eqs. (2.1) and (2.2), and the slowly varying plane-wave approximation is employed, it can be shown that the complex electric-field amplitudes of the pump-laser and dye-laser beams must satisfy the following: for the pump-laser beam

$$\mathbf{k}_p\cdot\hat{\mathbf{E}}_p(\mathbf{x},t)=0 \tag{3.8}$$

and

$$(n_s/c)\partial_t\hat{\mathbf{E}}_p(\mathbf{x},t)+(\mathbf{k}_p/k_p)\cdot\nabla\hat{\mathbf{E}}_p(\mathbf{x},t)=i(\mu_0\omega_p^2/k_p)\int_{4\pi}d\Omega\int_{S_1}d\alpha\,\rho_\alpha^1[\,\mathbf{A}_{\alpha p}(\mathbf{x},t,\Omega)+\mathbf{B}_{\alpha p}^*(\mathbf{x},t,\Omega)]-\alpha_s\hat{\mathbf{E}}_p(\mathbf{x},t)\ , \tag{3.9}$$

and for the dye-laser beam

$$\mathbf{k}_l\cdot\hat{\mathbf{E}}_l(\mathbf{x},t)=0 \tag{3.10}$$

and

$$(n_s/c)\partial_t\hat{\mathbf{E}}_l(\mathbf{x},t)+(\mathbf{k}_l/k_l)\cdot\nabla\hat{\mathbf{E}}_l(\mathbf{x},t)=i(\mu_0\omega_l^2/k_l)\int_{4\pi}d\Omega\int_{S_0}d\alpha\,\rho_\alpha^0[\,\mathbf{A}_{\alpha l}(\mathbf{x},t,\Omega)+\mathbf{B}_{\alpha l}^*(\mathbf{x},t,\Omega)]-\alpha_s\hat{\mathbf{E}}_l(\mathbf{x},t)\ . \tag{3.11}$$

Equations (3.8) and (3.10) indicate that to first order the pump-laser and dye-laser beams propagate through the dye medium as transverse electromagnetic waves. However, Eqs. (3.9) and (3.11) suggest that the polarization states of the pump-laser and dye-laser beams may change as they propagate through the dye medium.

Equations governing the complex polarization components $\mathbf{A}_{\alpha j}$ and $\mathbf{B}_{\alpha j}$ may be obtained by substituting Eqs. (3.1) and (3.3) into Eqs. (2.41) and (2.42):

$$\partial_t\,\mathbf{A}_{\alpha p}(\mathbf{x},t,\Omega)=-[\gamma_{\alpha p}-i(\omega_p-\omega_{\alpha p})]\,\mathbf{A}_{\alpha p}(\mathbf{x},t,\Omega) -[n_0^0(\mathbf{x},t,\Omega)-n_\alpha^1(\mathbf{x},t,\Omega)] \times L^2\boldsymbol{\mu}_{\alpha p}^*(\Omega)[\boldsymbol{\mu}_{\alpha p}(\Omega)\cdot\hat{\mathbf{E}}_p(\mathbf{x},t)]/2i\hbar\ , \tag{3.12}$$

$$\partial_t\mathbf{B}_{\alpha p}(\mathbf{x},t,\Omega)=-[\gamma_{\alpha p}+i(\omega_p+\omega_{\alpha p})]\mathbf{B}_{\alpha p}(\mathbf{x},t,\Omega) -[n_0^0(\mathbf{x},t,\Omega)-n_\alpha^1(\mathbf{x},t,\Omega)] \times L^2\boldsymbol{\mu}_{\alpha p}^*(\Omega)[\boldsymbol{\mu}_{\alpha p}(\Omega)\cdot\hat{\mathbf{E}}_p^*(\mathbf{x},t)]/2i\hbar\ , \tag{3.13}$$

$$\partial_t\,\mathbf{A}_{\alpha l}(\mathbf{x},t,\Omega)=-[\gamma_{\alpha l}-i(\omega_l-\omega_{\alpha l})]\,\mathbf{A}_{\alpha l}(\mathbf{x},t,\Omega) +[n_0^1(\mathbf{x},t,\Omega)-n_\alpha^0(\mathbf{x},t,\Omega)] \times L^2\boldsymbol{\mu}_{\alpha l}^*(\Omega)[\boldsymbol{\mu}_{\alpha l}(\Omega)\cdot\hat{\mathbf{E}}_l(\mathbf{x},t)]/2i\hbar\ , \tag{3.14}$$

and

$$\partial_t\mathbf{B}_{\alpha l}(\mathbf{x},t,\Omega)=-[\gamma_{\alpha l}+i(\omega_l+\omega_{\alpha l})]\mathbf{B}_{\alpha l}(\mathbf{x},t,\Omega) +[n_0^1(\mathbf{x},t,\Omega)-n_\alpha^0(\mathbf{x},t,\Omega)] \times L^2\boldsymbol{\mu}_{\alpha l}^*(\Omega)[\boldsymbol{\mu}_{\alpha l}(\Omega)\cdot\hat{\mathbf{E}}_l^*(\mathbf{x},t)]/2i\hbar\ . \tag{3.15}$$

In experiments[1-11] reported to date, measurements are typically made with a time resolution that is much longer than an optical period. If Eqs. (3.1) and (3.3) are substituted into the medium response Eqs. (2.49)–(2.53) and the resulting equations are time-averaged over an optical period, then

$$\partial_t n_0^1(\mathbf{x},t,\Omega)=\int_{S_1} d\alpha\,\rho_\alpha^1\gamma_V^1(\alpha,0)n_\alpha^1(\mathbf{x},t,\Omega)+\gamma_{R0}^1[\langle n_0^1(\mathbf{x},t)\rangle-n_0^1(\mathbf{x},t,\Omega)]-\gamma_F n_0^1(\mathbf{x},t,\Omega)$$
$$+\int_{S_0} d\alpha\,\rho_\alpha^0\{[\mathbf{A}_{\alpha l}(\mathbf{x},t,\Omega)-\mathbf{B}_{\alpha l}^*(\mathbf{x},t,\Omega)]\cdot\hat{\mathbf{E}}_l^*(\mathbf{x},t)-[\mathbf{A}_{\alpha l}^*(\mathbf{x},t,\Omega)-\mathbf{B}_{\alpha l}(\mathbf{x},t,\Omega)]\cdot\hat{\mathbf{E}}_l(\mathbf{x},t)\}/2i\hbar\ . \tag{3.16}$$

$$\partial_t n_0^0(\mathbf{x},t,\Omega)=\int_{S_0} d\alpha\,\rho_\alpha^0\gamma_V^0(\alpha,0)n_\alpha^0(\mathbf{x},t,\Omega)+\gamma_{R0}^0[\langle n_0^0(\mathbf{x},t)\rangle-n_0^0(\mathbf{x},t,\Omega)]$$
$$+\int_{S_1} d\alpha\,\rho_\alpha^1\{[A_{\alpha p}^*(\mathbf{x},t,\Omega)-\mathbf{B}_{\alpha p}(\mathbf{x},t,\Omega)]\cdot\hat{\mathbf{E}}_p(\mathbf{x},t)-[\mathbf{A}_{\alpha p}(\mathbf{x},t,\Omega)-\mathbf{B}_{\alpha p}^*(\mathbf{x},t,\Omega)]\cdot\hat{\mathbf{E}}_p^*(\mathbf{x},t)\}/2i\hbar\ , \tag{3.17}$$

$$\partial_t n_\alpha^1(\mathbf{x},t,\Omega)=-\gamma_V^1(\alpha,0)n_\alpha^1(\mathbf{x},t,\Omega)$$
$$+\{[\mathbf{A}_{\alpha p}(\mathbf{x},t,\Omega)-\mathbf{B}_{\alpha p}^*(\mathbf{x},t,\Omega)]\cdot\hat{\mathbf{E}}_p^*(\mathbf{x},t,\Omega)-[\mathbf{A}_{\alpha p}^*(\mathbf{x},t,\Omega)-\mathbf{B}_{\alpha p}(\mathbf{x},t,\Omega)]\cdot\hat{\mathbf{E}}_p(\mathbf{x},t)\}/2i\hbar\ , \tag{3.18}$$

and

$$\partial_t n_\alpha^0(\mathbf{x},t,\Omega)=-\gamma_V^0(\alpha,0)n_\alpha^0(\mathbf{x},t,\Omega)+\gamma_{F\alpha}n_0^1(\mathbf{x},t,\Omega)$$
$$+\{[\mathbf{A}_{\alpha l}^*(\mathbf{x},t,\Omega)-\mathbf{B}_{\alpha l}(\mathbf{x},t,\Omega)]\cdot\hat{\mathbf{E}}_l(\mathbf{x},t)-[\mathbf{A}_{\alpha l}(\mathbf{x},t,\Omega)-\mathbf{B}_{\alpha l}^*(\mathbf{x},t,\Omega)]\cdot\hat{\mathbf{E}}_l^*(\mathbf{x},t)\}/2i\hbar\ . \tag{3.19}$$

Equations (2.36) and (2.37) are unchanged by the time averaging because the level populations change significantly on a time scale that is long compared to an optical period. It is interesting to note that Eqs. (3.16)–(3.19) are compatible with Eqs. (2.36) and (2.37). Taking the partial time derivative of Eq. (2.36) and substituting Eqs. (3.16)–(3.19) into the result produces

$$\partial_t n(\mathbf{x},t,\Omega)=\gamma_{R0}^0[\langle n_0^0(\mathbf{x},t)\rangle-n_0^0(\mathbf{x},t,\Omega)]$$
$$+\gamma_{R0}^1[\langle n_0^1(\mathbf{x},t)\rangle-n_0^1(\mathbf{x},t,\Omega)]\ . \tag{3.20}$$

Averaging this equation over all solid angles Ω, all dye-molecule orientations, yields $\partial_t\langle n(\mathbf{x},t)\rangle=\partial_t N/4\pi=0$. The coupled equations, Eqs. (3.8)–(3.19), (2.36) and (2.37) together with suitable boundary and initial conditions provide a complete self-consistent description of laser-pumped, dye-laser dynamics when the pump-laser and dye-laser beams are partially polarized, quasimonochromatic plane waves. They are applicable to a wide range of physically interesting situations; including coherent and partially coherent light pulses and ultrashort pulses. In the following the utility and some of the novel physical features of this model are illustrated by considering the amplification of pulses that for typical dye media (Table I) would be in the 10^{-3}–10 ns regime.

B. Fast dye-molecule vibrational and induced-polarization relaxation

For many situations of practical interest[1–11] the pump- and dye-laser-pulse lengths are long compared to the dye-molecule vibrational relaxation and induced polarization dephasing times yet greater than or comparable to the dye-molecule fluorescence and rotational relaxation times, Table I, i.e.,

$$\partial_t\hat{\mathbf{P}}_{\alpha j}(\mathbf{x},t,\Omega)\ll\gamma_{\alpha j}\hat{\mathbf{P}}_{\alpha j}(\mathbf{x},t,\Omega) \tag{3.21}$$

and

$$\partial_t n_\alpha^\mu(\mathbf{x},t,\Omega)\ll\gamma_V^\mu n_\alpha^\mu(\mathbf{x},t,\Omega)\ . \tag{3.22}$$

These conditions easily hold for pulse lengths in excess of a few picoseconds. Furthermore, in general, the dye-molecule vibrational relaxation rates $\gamma_V^0(\alpha,0)$ for the $S_0(\alpha)\rightarrow S_0(0)$ vibrational sublevel relaxation are much faster than the $S_1(0)\rightarrow S_0(\alpha)$ laser light stimulated emission rate, i.e., $\gamma_V^0(\alpha,0)\gg\sigma_s(\nu_l)I_l/h\nu_l$, where σ_s is the stimulated emission cross section for the $S_1\rightarrow S_0$ transition and I_l is the dye-laser radiation intensity. For typical dye-laser medium conditions, Table I, this requires $I_l\ll h\nu_l\gamma_V^0/\sigma_s\sim 10$ GW/cm^2, which is easily satisfied in applications.[1–11] Similarly, the dye-molecule vibrational relaxation rate $\gamma_V^1(\alpha,0)$ for the $S_1(\alpha)\rightarrow S_1(0)$ vibrational relaxation is much faster than the $S_0(0)\rightarrow S_1(\alpha)$ pump light absorption rate, i.e., $\gamma_V^1(\alpha,0)\gg\sigma_a(\nu_p)I_p/h\nu_p$, where σ_a is the absorption cross section for the $S_0\rightarrow S_1$ transition and I_p is the pump radiation intensity. For typical dye-laser-medium conditions, Table I, this requires $I_p\ll h\nu_p\gamma_V^1/\sigma_a\sim 10$ GW/cm^2, which is easily satisfied in applications.[1–11] Under these circumstances it follows that

$$n_0^\mu\gg\int_{S_\mu} d\alpha\,\rho_\alpha^\mu n_\alpha^\mu\ . \tag{3.23}$$

Essentially all of the dye molecules are in either of two vibronic levels; the lowest vibronic levels of the S_0 or S_1 electronic states. Consequently, for a wide range of interesting conditions, Eqs. (3.12)–(3.15) may be solved for the complex polarization amplitudes:

$$\mathbf{A}_{\alpha p}(\mathbf{x},t,\Omega)=-n_0^0(\mathbf{x},t,\Omega)L^2\boldsymbol{\mu}_{\alpha p}^*(\Omega)$$
$$\times[\boldsymbol{\mu}_{\alpha p}(\Omega)\cdot\hat{\mathbf{E}}_p(\mathbf{x},t)]/2\hbar$$
$$\times[(\omega_p-\omega_{\alpha p})+i\gamma_{\alpha p}]\ , \tag{3.24}$$

$$\mathbf{B}_{\alpha p}(\mathbf{x},t,\Omega)=n_0^0(\mathbf{x},t,\Omega)L^2\boldsymbol{\mu}_{\alpha p}^*(\Omega)[\boldsymbol{\mu}_{\alpha p}(\Omega)\cdot\hat{\mathbf{E}}_p^*(\mathbf{x},t)]/2\hbar$$
$$\times[(\omega_p+\omega_{\alpha p})-i\gamma_{\alpha p}]\ , \tag{3.25}$$

$$\mathbf{A}_{\alpha l}(\mathbf{x},t,\Omega)=n_0^1(\mathbf{x},t,\Omega)L^2\boldsymbol{\mu}_{\alpha l}^*(\Omega)[\boldsymbol{\mu}_{\alpha l}(\Omega)\cdot\hat{\mathbf{E}}_l(\mathbf{x},t)]/2\hbar$$
$$\times[(\omega_l-\omega_{\alpha l})+i\gamma_{\alpha l}]\ , \tag{3.26}$$

and

$$\mathbf{B}_{\alpha l}(\mathbf{x},t,\Omega)=-n_0^1(\mathbf{x},t,\Omega)L^2\boldsymbol{\mu}_{\alpha l}^*(\Omega)[\boldsymbol{\mu}_{\alpha l}(\Omega)\cdot\hat{\mathbf{E}}_l^*(\mathbf{x},t)]/2\hbar$$
$$\times[(\omega_l+\omega_{\alpha l})-i\gamma_{\alpha l}]\ . \tag{3.27}$$

It is clear from Eqs. (3.24)–(3.27) that $\mathbf{A}_{\alpha j}(\mathbf{x},t,\Omega)$ represents the resonant and $\mathbf{B}_{\alpha j}(\mathbf{x},t,\Omega)$ represents the nonresonant part of the light–dye-molecule coupling since, typically, $\omega_j \sim \omega_{\alpha j} \gg \gamma_{\alpha j}$. Thus $\mathbf{A}_{\alpha j}(\mathbf{x},t,\Omega)$ is generally much greater than $\mathbf{B}_{\alpha j}(\mathbf{x},t,\Omega)$.

1. *Dye-molecule population dynamics*

Retaining only the resonant parts of the light–dye-molecule coupling, Eqs. (3.24) and (3.26), and using the fast vibrational relaxation approximation, Eq. (3.22), the vibrational sublevels populations, Eqs. (3.18) and (3.19), are determined by

$$\gamma_V^1(\alpha,0)n_\alpha^1(\mathbf{x},t,\Omega)=[\,\mathbf{A}_{\alpha p}(\mathbf{x},t,\Omega)\cdot\hat{\mathbf{E}}_p^*(\mathbf{x},t) - \mathbf{A}_{\alpha p}^*(\mathbf{x},t,\Omega)\cdot\hat{\mathbf{E}}_p(\mathbf{x},t)\,]/2i\hbar \tag{3.28}$$

and

$$\gamma_V^0(\alpha,0)n_\alpha^0(\mathbf{x},t,\Omega)=\gamma_{F\alpha}n_0^1(\mathbf{x},t,\Omega) +[\,\mathbf{A}_{\alpha l}^*(\mathbf{x},t,\Omega)\cdot\hat{\mathbf{E}}_l(\mathbf{x},t) - \mathbf{A}_{\alpha l}(\mathbf{x},t,\Omega)\cdot\hat{\mathbf{E}}_l^*(\mathbf{x},t)\,]/2i\hbar\ . \tag{3.29}$$

Retaining only the resonant parts of the dye-molecule radiation interaction in Eqs. (3.16) and (3.17) results in an error, for typical dye-laser media (Table I), of less than 1%. Using Eqs. (3.28) and (3.29), then Eqs. (3.16) and (3.17) may be written

$$\partial_t n_0^1(\mathbf{x},t,\Omega)=n_0^0(\mathbf{x},t,\Omega)\gamma_p(\mathbf{x},t,\Omega) +\gamma_{R0}^1[\langle n_0^1(\mathbf{x},t)\rangle - n_0^1(\mathbf{x},t,\Omega)] -\gamma_F n_0^1(\mathbf{x},t,\Omega)-n_0^1(\mathbf{x},t,\Omega)\gamma_e(\mathbf{x},t,\Omega) \tag{3.30}$$

and

$$\partial_t n_0^0(\mathbf{x},t,\Omega)=-n_0^0(\mathbf{x},t,\Omega)\gamma_p(\mathbf{x},t,\Omega) +\gamma_{R0}^0[\langle n_0^0(\mathbf{x},t)\rangle - n_0^0(\mathbf{x},t,\Omega)] +\gamma_F n_0^1(\mathbf{x},t,\Omega)+n_0^1(\mathbf{x},t,\Omega)\gamma_e(\mathbf{x},t,\Omega)\ , \tag{3.31}$$

where the pump-laser absorption and dye-laser simulated emission rates are

$$\gamma_p(\mathbf{x},t,\Omega)=\int_{S_1} d\alpha\,\rho_\alpha^1 L^2|\boldsymbol{\mu}_{\alpha p}(\Omega)\cdot\hat{\mathbf{E}}_p(\mathbf{x},t)|^2\gamma_{\alpha p}/2\hbar^2[(\omega_p-\omega_{\alpha p})^2+\gamma_{\alpha p}^2] \tag{3.32}$$

and

$$\gamma_e(\mathbf{x},t,\Omega)=\int_{S_0} d\alpha\,\rho_\alpha^0 L^2|\boldsymbol{\mu}_{\alpha l}(\Omega)\cdot\hat{\mathbf{E}}_l(\mathbf{x},t)|^2\gamma_{\alpha l}/2\hbar^2[(\omega_l-\omega_{\alpha l})^2+\gamma_{\alpha l}^2]\ , \tag{3.33}$$

respectively. From Eq. (3.23) it follows that Eq. (2.36) becomes

$$n_0^0(\mathbf{x},t,\Omega)+n_0^1(\mathbf{x},t,\Omega)=n(\mathbf{x},t,\Omega)\ . \tag{3.34}$$

The dye-molecule population continuity Eqs. (3.30) and (3.31) may be shown to be compatible with Eqs. (2.37) and (3.34) in the following way. If Eqs. (3.30) and (3.31) are added together and the result is averaged over solid angle, then

$$\partial_t[\langle n_0^0(\mathbf{x},t)\rangle+\langle n_0^1(\mathbf{x},t)\rangle]=0\ . \tag{3.35}$$

Substituting Eq. (3.34) into Eq. (3.35) yields N is a constant as required by Eq. (2.37).

When the rate of dye-molecule rotational relaxation exceeds the fluorescence, pump-laser absorption and dye-laser stimulated emission rates, namely, $\gamma_{R0}^\mu \gg (\gamma_F,\gamma_p,\gamma_e)$, where $\gamma_p \sim \sigma_a(\nu_p)I_p/h\nu_p$ and $\gamma_e \sim \sigma_s(\nu_l)I_l/h\nu_l$, then, from Eqs. (3.30) and (3.31), the level populations will be approximately equal to their average values

$$n_0^\mu(\mathbf{x},t,\Omega)=\langle n_0^\mu(\mathbf{x},t)\rangle=N_0^\mu(\mathbf{x},t)/4\pi\ , \tag{3.36}$$

where $N_0^\mu(\mathbf{x},t)$ is the total number density of dye molecules in the lowest vibrational level of electronic state S_μ, $\mu=(0,1)$. Therefore the level populations $n_0^\mu(\mathbf{x},t,\Omega)$ are isotropically distributed over all orientations. This condition depends strongly on the solvent.[35] Under these circumstances Eqs. (3.30), (3.31), and (3.34) may be integrated over solid angle, all dye-molecule orientations, to obtain equations for the total dye-molecule population densities $N_0^\mu(\mathbf{x},t)$:

$$\partial_t N_0^1(\mathbf{x},t)=\sigma_a(\nu_p)N_0^0(\mathbf{x},t)I_p(\mathbf{x},t)/h\nu_p-\gamma_F N_0^1(\mathbf{x},t) -\sigma_s(\nu_l)N_0^1(\mathbf{x},t)I_l(\mathbf{x},t)/h\nu_l \tag{3.37}$$

and

$$N_0^0(\mathbf{x},t)+N_0^1(\mathbf{x},t)=N\ , \tag{3.38}$$

where

$$\sigma_a(\nu_p)=\int_{S_1} d\alpha\,\rho_\alpha^1 L^2|\boldsymbol{\mu}_{\alpha p}|^2\omega_p\gamma_{\alpha p}/\{3cn_s\epsilon_0\hbar[\gamma_{\alpha p}^2+(\omega_p-\omega_{\alpha p})^2]\} \tag{3.39}$$

is the total absorption cross section for the transition $S_0 \rightarrow S_1$ evaluated at the pump-laser frequency ν_p and

$$\sigma_s(\nu_l)=\int_{S_0} d\alpha\,\rho_\alpha^0 L^2|\boldsymbol{\mu}_{\alpha l}|^2\omega_l\gamma_{\alpha l}/\{3cn_s\epsilon_0\hbar[\gamma_{\alpha l}^2+(\omega_l-\omega_{\alpha l})^2]\} \tag{3.40}$$

is the total stimulated emission cross section for the broadband laser transition $S_1 \rightarrow S_0$ evaluated at the dye-laser frequency ν_l. Equations (3.37) and (3.38) are the rate equation description used previously.[1-11] For pulsed-dye lasers, this description is typically restricted to dye-laser media with fluorescence lifetimes much longer than the dye-molecule rotational relaxation time, i.e., $\gamma_{R0}^{\mu} \gg \gamma_F$.

2. Dye-molecule absorption and stimulated emission cross sections

The total absorption cross section, Eq. (3.39) can be expressed in terms of the Einstein A coefficient $A(S_1(\alpha),S_0(0))$ for a given vibronic sublevel electronic transition $S_0(0) \rightarrow S_1(\alpha)$

$$\sigma_a(\nu_p)=(\lambda_p^2/8\pi n_s^2)\int_{S_1} d\alpha \rho_\alpha^1 A(S_1(\alpha),S_0(0))g_{\alpha p}(\nu_p) \tag{3.41}$$

where

$$A(S_1(\alpha),S_0(0))=\omega_p^3 n_s L^2|\mu_{\alpha p}|^2/3\pi\epsilon_0\hbar c^3 , \tag{3.42}$$

and

$$g_{\alpha p}(\nu_p)=2\gamma_{\alpha p}/[\gamma_{\alpha p}^2+(\omega_p-\omega_{\alpha p})^2] \tag{3.43}$$

is the normalized line-shape function for the transition. Similarly, the total stimulated emission cross section, Eq. (3.40), may be written

$$\sigma_s(\nu_l)=(\lambda_l^2/8\pi n_s^2)\int_{S_0} d\alpha \rho_\alpha^0 A(S_1(0),S_0(\alpha))g_{\alpha l}(\nu_l) , \tag{3.44}$$

where

$$A(S_1(0),S_0(\alpha))=\omega_l^3 n_s L^2|\mu_{\alpha l}|^2/3\pi\epsilon_0\hbar c^3 \tag{3.45}$$

is the Einstein A coefficient for a given vibronic-sublevel electronic transition $S_1(0) \rightarrow S_0(\alpha)$ and

$$g_{\alpha l}(\nu_l)=2\gamma_{\alpha l}/[\gamma_{\alpha l}^2+(\omega_l-\omega_{\alpha l})^2] \tag{3.46}$$

is the corresponding normalized line-shape function for the transition.

Equations (3.41)–(3.46) show that the absorption and stimulated emission cross sections depend on the radiative transition probabilities and collisional dephasing rates for each vibronic sublevel that participates in the process. This result, Eq. (3.44), for the stimulated emission cross section can be cast in the conventional form[56]

$$\sigma_s(\nu_l)=\lambda_l^2 g(\nu_l)/8\pi n_s^2\tau_r , \tag{3.47}$$

where τ_r is the radiative lifetime, given by

$$\tau_r=\left[\int_{S_0} d\alpha \rho_\alpha^0 A(S_1(0),S_0(\alpha))\right]^{-1} , \tag{3.48}$$

and the normalized fluorescence line-shape function is

$$g(\nu_l)=\int_{S_0} d\alpha \rho_\alpha^0 A(S_1(0),S_0(\alpha))g_{\alpha l}(\nu_l) \Big/ \int_{S_0} d\alpha \rho_\alpha^0 A(S_1(0),S_0(\alpha)) . \tag{3.49}$$

Furthermore, if Q is the fluorescence quantum yield, Table I, then $\gamma_F=1/Q\tau_r$ and $\gamma_{F\alpha}=A(S_1(0),S_0(\alpha))/Q$, provided intersystem crossing is unimportant as assumed in the present formulation.

In Fig. 4 the measured[31-34] absorption $\sigma_a(\lambda_p)$ and stimulated emission $\sigma_s(\lambda_l)$ cross sections for the dye-laser media rhodamine 6G fluoroborate in 95% ethanol and DCM in dimethyl sulfoxide (DMSO) are presented. In the following, for simplicity rhodamine 6G in ethanol stands for rhodamine 6G fluoroborate in 95% ethanol.

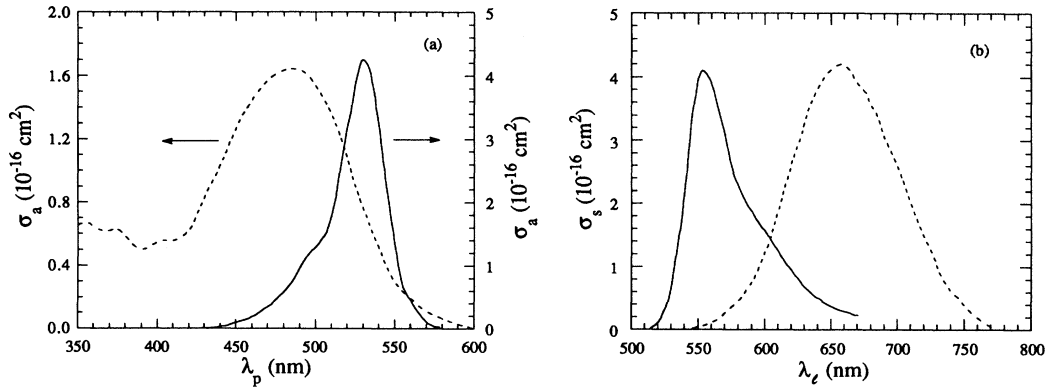

FIG. 4. Wavelength dependence of the (a) absorption cross section $\sigma_a(\lambda_p)$ and (b) stimulated emission cross section $\sigma_s(\lambda_l)$ for the dye-laser media rhodamine 6G fluoroborate (Refs. 32–34) dissolved in 95% ethanol (——) and DCM (Ref. 31) dissolved in DMSO (— — —).

The absorption spectrum is typically measured by determining the decadic molar extinction coefficient ε with a spectrophotometer.[56] If ε is expressed in liter/mol cm and C is the dye concentration in mol/liter then

$$N\sigma_a(\nu_p)=\varepsilon(\nu_p)C\ln 10 . \tag{3.50}$$

From Eq. (3.47) the stimulated emission cross section may be determined by measuring the fluorescence lineshape function $g(\nu_l)$ and the radiative lifetime τ_r. Since $\tau_r\gamma_F Q=1$, the determination of τ_r requires measurement of the fluorescence lifetime γ_F^{-1} and the quantum yield Q. Lifetimes may be determined by phase shift[57,58] or flash (e.g., short-pulse pump-laser[33]) techniques. Quantum yields have been measured using both photometric[58] and calorimetric[59] techniques. Measured values of these quantities for rhodamine 6G in ethanol and DCM in DMSO are listed in Table II.

In general, since measurement of the quantum yield requires special equipment, it is useful to have approximate methods for estimating the radiative lifetime. If the $S_1\rightarrow S_0$ emission is strong and the nuclear configurations of the S_0 and S_1 electronic states are "sufficiently similar," then[56-58]

$$1/\tau_r=2.880\times 10^{-9}n_s^2c^3\langle\nu_l^{-3}\rangle_{\rm av}^{-1}\int d\nu_p\varepsilon(\nu_p)/\nu_p , \tag{3.51}$$

where

$$\langle\nu_l^{-3}\rangle_{\rm av}=\int d\nu_l g(\nu_l)/\nu_l^3 . \tag{3.52}$$

When Eq. (3.51) is a good approximation it has been found[56-58] that the fluorescence and absorption spectra of the dye molecule satisfy the mirror symmetry relation

$$\varepsilon(\nu_p)/\nu_p\propto g(2\nu_0-\nu_p)/(2\nu_0-\nu_p)^3 , \tag{3.53}$$

where ν_0 is the frequency that gives the best fit of $\varepsilon(\nu)/\nu$ to the fluorescence spectrum $g(\nu)/\nu^3$ mirror image. The theoretical grounds[56,58] for this relation have been established and it has been found empirically[56-58] to hold for many dyes. Using their measured[31-34] absorption cross sections and fluorescence spectra Eq. (3.51) was used to estimate the dye-molecule radiative lifetimes for the dye-laser-media rhodamine 6G in ethanol and DCM in DMSO. The results of these calculations are presented in Table II. The corresponding mirror symmetry plots for these dye laser media are presented in Fig. 5. It should be noted that in Eqs. (3.51) and (3.53) the frequency extends over only the $S_0\rightarrow S_1$ absorption band. Other absorption processes $S_0\rightarrow S_n$ must not be included. As shown in Fig. 5, in the case of DCM the $S_0\rightarrow S_1$ absorption band was approximately established by extrapolating $\sigma_a(\lambda_p)$ to zero with a dash-dotted (—·—·—·) line on the short-wavelength side of the absorption band. From Table II, Eq. (3.51) yields an excellent estimate of τ_r for rhodamine 6G in ethanol. This is supported by the mirror symmetry plot, Fig. 5, for this dye-laser medium. However, from Table II, Eq. (3.51) does not yield a very good estimate of τ_r for DCM in DMSO. This result is also supported by the mirror symmetry plot, Fig. 5, for this dye-laser medium. For DCM it appears that the configuration of the S_1 state differs significantly from that of the S_0 state. These results together with those in the literature[56-59] indicate that Eq. (3.51) can be useful in estimating τ_r. However, as evidenced by the mirror symmetry plot, for good results the configurations of the S_0 and S_1 states must be sufficiently similar.[56]

3. *Dye-molecule electric susceptibility tensors*

If Eqs. (3.24)–(3.27) for the complex polarization amplitudes $\mathbf{A}_{\alpha j}(\mathbf{x},t,\Omega)$ and $\mathbf{B}_{\alpha j}(\mathbf{x},t,\Omega)$ are substituted into Eqs. (3.4) and (3.5) it can be shown that

$$\hat{\mathbf{P}}_j(\mathbf{x},t)=\epsilon_0[\hat{\overleftrightarrow{\chi}}_j(\mathbf{x},t,\omega_j)+\hat{\chi}_s(\omega_j)\overleftrightarrow{1}]\cdot\hat{\mathbf{E}}_j(\mathbf{x},t) , \tag{3.54}$$

where $\overleftrightarrow{1}$ is the unit tensor. The quantity $\hat{\overleftrightarrow{\chi}}_j(\mathbf{x},t,\omega_j)$ is the complex dye-molecule electric susceptibility tensor that characterizes the interaction between the pump-laser ($j=p$) and dye-laser ($j=l$) radiation electric field with the dye molecules. The pump-laser susceptibility tensor

$$\hat{\overleftrightarrow{\chi}}_p(\mathbf{x},t,\omega_p)=\int_{4\pi}d\Omega\, n_0^0(\mathbf{x},t,\Omega)\int_{S_1}d\alpha\,\rho_\alpha^1(L^2/\epsilon_0\hbar)\{\boldsymbol{\mu}_{\alpha p}^*(\Omega)\boldsymbol{\mu}_{\alpha p}(\Omega)/[(\omega_{\alpha p}-\omega_p)-i\gamma_{\alpha p}]$$
$$+\boldsymbol{\mu}_{\alpha p}(\Omega)\boldsymbol{\mu}_{\alpha p}^*(\Omega)/[(\omega_{\alpha p}+\omega_p)+i\gamma_{\alpha p}]\} \tag{3.55}$$

describes the absorption of pump-laser radiation by the dye-molecule $S_0\rightarrow S_1$ electronic transition. The dye-laser susceptibility tensor that describes the stimulated emission of radiation produced by the dye-molecule $S_1\rightarrow S_0$ electronic transition is

TABLE II. Typical dye-laser media $S_1\rightarrow S_0$ radiative relaxation properties.

Dye laser medium	Q	γ_F^{-1} (ns)	τ_r (ns)	$(\tau_r)_{\rm est}$ (ns)
Rhodamine 6G in ethanol	0.93[a]	3.5[a]	3.8[a]	3.8[c]
DCM in DMSO	0.71[b]	1.9[b]	2.7[b]	4.8[c]

[a]Reference 34.
[b]Reference 31.
[c]Estimate based on Eq. (3.51) in text.

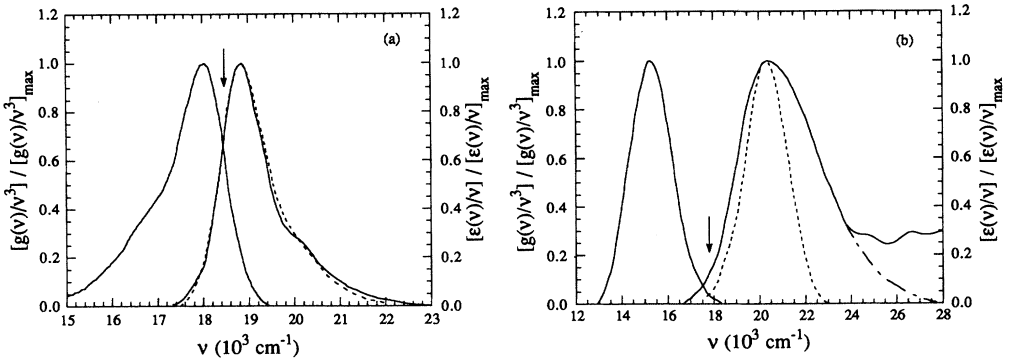

FIG. 5. Mirror symmetry plots (Refs. 56–58) for the dye-laser media (a) rhodamine 6G fluoroborate dissolved in 95% ethanol and (b) DCM dissolved in DMSO. In each case, the left-hand solid curve goes with the left-hand ordinate and the right-hand solid curve goes with the right-hand ordinate. The mirror image of the emission curve [Eq. (3.53) is given by the dashed line (— — —) with the arrow indicating the value of ν_0.

$$\hat{\vec{\chi}}_l(\mathbf{x},t,\omega_l)=-\int_{4\pi}d\Omega\, n_0^1(\mathbf{x},t,\Omega)\int_{S_0}d\alpha\,\rho_\alpha^0(L^2/\epsilon_0\hbar)\{\boldsymbol{\mu}_{\alpha l}^*(\Omega)\boldsymbol{\mu}_{\alpha l}(\Omega)/[(\omega_{\alpha l}-\omega_l)-i\gamma_{\alpha l}] +\boldsymbol{\mu}_{\alpha l}(\Omega)\boldsymbol{\mu}_{\alpha l}^*(\Omega)/[(\omega_{\alpha l}+\omega_l)+i\gamma_{\alpha l}]\}\ . \tag{3.56}$$

If the induced dipole moments $\boldsymbol{\mu}_{\alpha j}(\Omega)$ are expressed in spherical coordinates as shown in Fig. 3, then Eqs. (3.55) and (3.56) may be written in the form

$$\hat{\vec{\chi}}_p(\mathbf{x},t,\omega_p)=3\hat{\chi}_p(\omega_p)\int_0^{2\pi}d\phi\int_0^{\pi}d\theta\, n_0^0(\mathbf{x},t,\Omega)\vec{\mathrm{O}}(\Omega) \tag{3.57}$$

and

$$\hat{\vec{\chi}}_l(\mathbf{x},t,\omega_l)=3\hat{\chi}_l(\omega_l)\int_0^{2\pi}d\phi\int_0^{\pi}d\theta\, n_0^1(\mathbf{x},t,\Omega)\vec{\mathrm{O}}(\Omega)\ , \tag{3.58}$$

where $\vec{\mathrm{O}}(\Omega)$ is the symmetric real tensor whose elements are

$$O_{xx}(\Omega)=\sin^3\theta\cos^2\phi\ , \tag{3.59}$$

$$O_{xy}(\Omega)=O_{yx}(\Omega)=(\sin^3\theta\sin2\phi)/2\ , \tag{3.60}$$

$$O_{xz}(\Omega)=O_{zx}(\Omega)=\sin^2\theta\cos\theta\cos\phi\ , \tag{3.61}$$

$$O_{yy}(\Omega)=\sin^3\theta\sin^2\phi\ , \tag{3.62}$$

$$O_{yz}(\Omega)=O_{zy}(\Omega)=\sin^2\theta\cos\theta\sin\phi\ , \tag{3.63}$$

$$O_{zz}(\Omega)=\sin\theta\cos^2\theta\ , \tag{3.64}$$

with

$$\hat{\chi}_p(\omega_p)=\int_{S_1}d\alpha\,\rho_\alpha^1(L^2|\boldsymbol{\mu}_{\alpha p}|^2/3\epsilon_0\hbar)\times\{[(\omega_{\alpha p}-\omega_p)-i\gamma_{\alpha p}]^{-1}+[(\omega_{\alpha p}+\omega_p)+i\gamma_{\alpha p}]^{-1}\} \tag{3.65}$$

and

$$\hat{\chi}_l(\omega_l)=-\int_{S_0}d\alpha\,\rho_\alpha^0(L^2|\boldsymbol{\mu}_{\alpha l}|^2/3\epsilon_0\hbar)\times\{[(\omega_{\alpha l}-\omega_l)-i\gamma_{\alpha l}]^{-1}+[(\omega_{\alpha l}+\omega_l)+i\gamma_{\alpha l}]^{-1}\}\ . \tag{3.66}$$

When Eq. (3.36) holds, dye-molecule population densities n_0^μ are isotropic and the dye-molecule susceptibility tensors, Eqs. (3.57) and (3.58), are diagonal:

$$\hat{\vec{\chi}}_p(\mathbf{x},t,\omega_p)=\hat{\chi}_p(\omega_p)N_0^0(\mathbf{x},t)\vec{1} \tag{3.67}$$

and

$$\hat{\vec{\chi}}_l(\mathbf{x},t,\omega_l)=\hat{\chi}_l(\omega_l)N_0^1(\mathbf{x},t)\vec{1}\ . \tag{3.68}$$

Consequently, $\hat{\chi}_j$ is the dye-molecule electric susceptibility per dye molecule per unit volume or the specific dye-molecule electric susceptibility when dye-molecule rotational relaxation is very fast.

The previous results indicate that the dye-laser medium is optically isotropic in the limit that dye-molecule rotational relaxation is very fast. However, when dye-molecule rotational relaxation is slow the dye-laser medium will be optically anisotropic for propagation of both the pump- and dye-laser light. The amplitudes and polarization states of the pump laser and dye laser will change as they propagate. Since the dye-molecule susceptibility tensor $\hat{\vec{\chi}}_p(\mathbf{x},t,\omega_p)$ [$\hat{\vec{\chi}}_l(\mathbf{x},t,\omega_l)$] in the pump-laser absorption [dye-laser emission] band is complex, there are generally two distinct physical phenomena that alter the pump-laser [dye-laser] radiation state. In general, the pump-laser [dye-laser] amplitude and polarization state are altered because the absorption [amplification] and phase shift of the light will depend on the amplitude and

polarization state and relative direction of propagation of the pump- and dye-laser beams. However, it will be shown later that there are physical conditions of interest where the polarization states of the pump-laser and dye-laser beams are preserved during their propagation through the dye-laser medium. These conditions include circumstances where the dye-molecule rotational relaxation rate is slow.

When the dye-molecule electric susceptibilities $\hat{\vec{\chi}}_j(\mathbf{x},t,\omega_j)$ and $\hat{\chi}_j(\omega_j)$, $j=(l,p)$, are viewed as functions in the complex ω_j plane they are analytic in the upper half plane and possess simple poles in the lower half plane at $\omega_j=\pm\omega_{\alpha j}-i\gamma_{\alpha j}$. Consequently, their real and imaginary parts satisfy the well-known Kramers-Kronig or Hilbert transform relations. For example, if $\hat{\chi}(\omega_j)$ represents $\hat{\vec{\chi}}_j(\mathbf{x},t,\omega_j)$ or $\hat{\chi}_j(\omega_j)$, and $\hat{\chi}(\omega_j)=\chi'(\omega_j)+i\chi''(\omega_j)$, then

$$\chi'(\omega_j)=\mathrm{P}\int_{-\infty}^{\infty} d\omega\,\chi''(\omega)/\pi(\omega-\omega_j)\ , \tag{3.69}$$

and

$$\chi''(\omega_j)=-\mathrm{P}\int_{-\infty}^{\infty} d\omega\,\chi'(\omega)/\pi(\omega-\omega_j)\ , \tag{3.70}$$

where $\chi'(\omega_j)$ represents $\vec{\chi}'_j(\mathbf{x},t,\omega_j)$ or $\chi'_j(\omega_j)$, and $\chi''(\omega_j)$ represents $\vec{\chi}''_j(\mathbf{x},t,\omega_j)$ or $\chi''_j(\omega_j)$, respectively, and P denotes the Cauchy principal value. Furthermore, from Eqs. (3.55), (3.56), (3.65) and (3.66) it follows that $\chi'(\omega_j)=\chi'(-\omega_j)$ and $\chi''(\omega_j)=-\chi''(-\omega_j)$. Thus Eqs. (3.69) and (3.70) can be transformed to integrals over positive frequencies, namely,

$$\chi'(\omega_j)=2\mathrm{P}\int_0^{\infty} d\omega\,\omega\chi''(\omega)/\pi(\omega^2-\omega_j^2) \tag{3.71}$$

and

$$\chi''(\omega_j)=-2\mathrm{P}\int_0^{\infty} d\omega\,\omega_j\chi'(\omega)/\pi(\omega^2-\omega_j^2)\ . \tag{3.72}$$

The utility of these results will now be demonstrated.

In general, $\hat{\chi}_j(\omega_j)$ may be accurately approximated for positive real frequencies by keeping only the resonant parts of Eqs. (3.65) and (3.66), i.e.,

$$\hat{\chi}_p(\omega_p)=\int_{S_1} d\alpha\,\rho_\alpha^1 L^2|\boldsymbol{\mu}_{\alpha p}|^2/3\epsilon_0\hbar[(\omega_{\alpha p}-\omega_p)-i\gamma_{\alpha p}] \tag{3.73}$$

and

$$\hat{\chi}_l(\omega_l)=-\int_{S_0} d\alpha\,\rho_\alpha^0 L^2|\boldsymbol{\mu}_{\alpha l}|^2/3\epsilon_0\hbar[(\omega_{\alpha l}-\omega_l)-i\gamma_{\alpha l}]\ . \tag{3.74}$$

If Eqs. (3.73) and (3.74) are partitioned into their real and imaginary parts, it can be shown that the absorption, Eq. (3.39), and stimulated emission, Eq. (3.40), cross sections can be written as

$$\sigma_a(\omega_p)=\omega_p\chi_p''(\omega_p)/cn_s \tag{3.75}$$

and

$$\sigma_s(\omega_l)=-\omega_l\chi_l''(\omega_l)/cn_s\ . \tag{3.76}$$

Consequently, if the dye-molecule absorption and stimulated emission cross sections are known, say from experiment, then the imaginary parts of $\hat{\chi}_j(\omega_j)$ and $\hat{\vec{\chi}}_j(\mathbf{x},t,\omega_j)$ can be calculated from Eqs. (3.75) and (3.76). Furthermore, using Eqs. (3.75), (3.76), and (3.71) it follows that

$$\chi_p'(\omega_p)=2cn_s\mathrm{P}\int_0^{\infty} d\omega\,\sigma_a(\omega)/\pi(\omega^2-\omega_p^2) \tag{3.77}$$

and

$$\chi_l'(\omega_l)=-2cn_s\mathrm{P}\int_0^{\infty} d\omega\,\sigma_s(\omega)/\pi(\omega^2-\omega_l^2)\ , \tag{3.78}$$

where as before ω_p ranges over the dye molecule's $S_0\rightarrow S_1$ absorption band and ω_l ranges over the dye molecule's $S_1\rightarrow S_0$ emission band. Equations (3.77) and (3.78) permit the calculation of the real parts of $\hat{\chi}_j(\omega_j)$ and $\hat{\vec{\chi}}_j(\mathbf{x},t,\omega_j)$. Therefore, if through experiment the dye-molecule absorption and stimulated emission cross

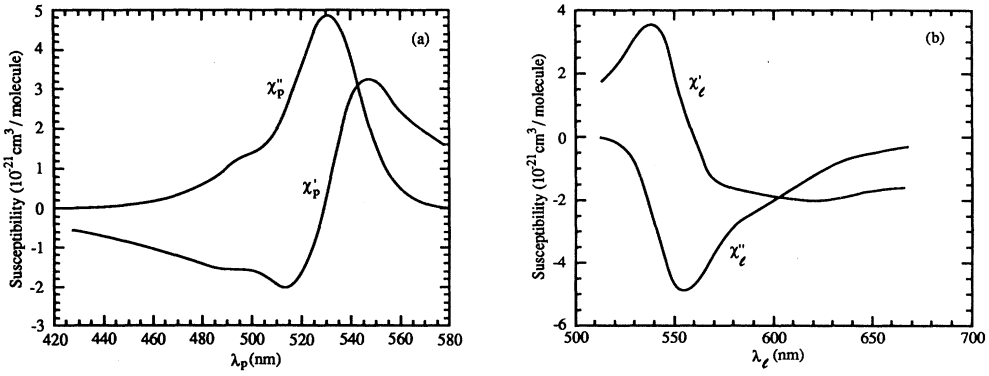

FIG. 6. Wavelength dependence of the real χ_j' and imaginary χ_j'' parts of the specific dye-molecule electric susceptibilities that characterize the (a) pump-laser ($j=p$) and (b) dye-laser ($j=l$) radiation interaction with the rhodamine 6G fluoroborate dye molecule dissolved in 95% ethanol.

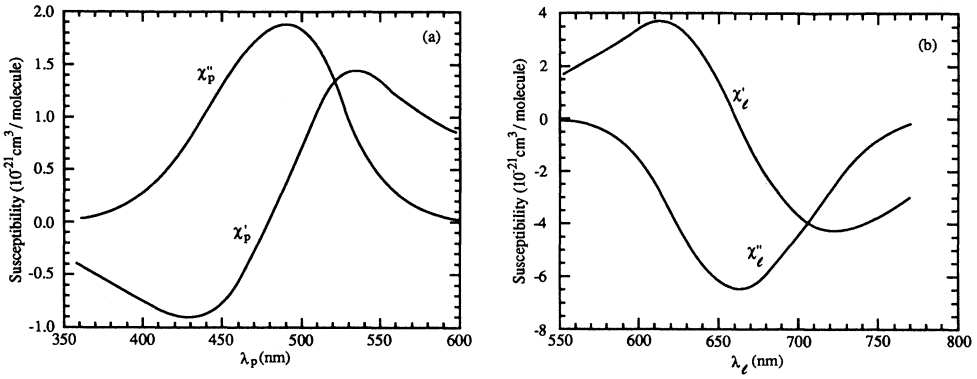

FIG. 7. Wavelength dependence of the real χ'_j and imaginary χ''_j parts of the specific dye-molecule electric susceptibilities that characterize the (a) pump-laser ($j=p$) and (b) dye-laser ($j=l$) radiation interaction with the DCM dye molecule dissolved in DMSO.

sections are known then the dye-molecule pump-laser and dye-laser electric susceptibility tensors $\hat{\vec{\chi}}_j(\mathbf{x},t,\omega_j)$ can be determined in their respective wavelength bands λ_j.

In Fig. 4 the measured[31–34] absorption $\sigma_a(\lambda_p)$ and stimulated emission $\sigma_s(\lambda_l)$ cross sections for the dye-laser-media rhodamine 6G in ethanol and DCM in DMSO are presented. Using the methodology described above the real and imaginary parts of the dye-molecule electric susceptibilities per dye molecule per unit volume $\hat{\chi}_j$ are calculated, in the Appendix, for the pump-laser absorption λ_p and dye-laser emission λ_l bands of these dyes. The refractive indices n_s of the solvents ethanol and DMSO were taken to be[46] 1.36 and 1.48, respectively. The results of these calculations for rhodamine 6G in ethanol and DCM in DMSO are presented in Figs. 6 and 7, respectively.

4. Pump- and dye-laser-light propagation

In general, the dye concentration is such that the dye-molecule density N is much less than the solvent-molecule density and

$$\hat{\chi}_s(\omega_j)\overleftrightarrow{1}\cdot\hat{\mathbf{E}}_j(\mathbf{x},t)\gg\hat{\vec{\chi}}_j(\mathbf{x},t,\omega_j)\cdot\hat{\mathbf{E}}_j(\mathbf{x},t)\ .$$

The optical anisotropy introduced by the dye molecules may be treated as a perturbation. If Eqs. (3.24)–(3.27) are substituted into the paraxial field wave equations, Eqs. (3.9) and (3.11), it can be shown that the complex electric field amplitudes of the pump- and dye-laser beams must satisfy

$$(n_s/c)\partial_t\hat{\mathbf{E}}_j(\mathbf{x},t)+(\mathbf{k}_j/k_j)\cdot\nabla\hat{\mathbf{E}}_j(\mathbf{x},t)=i(\omega_j/2cn_s)\hat{\vec{\chi}}_j(\mathbf{x},t,\omega_j)\cdot\hat{\mathbf{E}}_j(\mathbf{x},t)-\alpha_s\hat{\mathbf{E}}_j(\mathbf{x},t)\ . \tag{3.79}$$

To first order the pump- and dye-laser radiation beams propagate as transverse electromagnetic waves. However, Eqs. (3.79) show that, in general, as these beams propagate through the dye medium, their polarization state changes. The coupled Eqs. (3.30)–(3.34), (2.37), (3.57)–(3.66), (3.8), (3.10), and (3.79) together with suitable boundary and initial conditions provide a complete description of quasimonochromatic laser-pumped dye-laser dynamics when the physical circumstances required by Eqs. (3.21) and (3.22) hold. Further insight into the implications and utility of these results requires consideration of particular pump-laser and dye-laser geometries. In the following, the often-used transverse pump geometry is considered in detail.

5. Transversely laser-pumped pulsed dye lasers

(a) General description. The two most popular pumping arrangements[1,2] for laser-pumped dye lasers are called coaxial and transverse because of the relative orientation of the pump- and dye-laser beams. In the coaxial (transverse) approach the pump-laser and dye-laser-light beams are aligned (perpendicular) as they propagate through the dye-laser medium. Consider a transverse laser-pumped dye-laser amplifier. Suppose the dye-laser medium is oriented along the z axis and is thin in the x-y plane so that the pump light electric field is unaffected during propagation along the y axis through the dye medium. Thus from Eq. (3.8) the complex electric-field amplitude of the pump-laser beam is polarized in the x-z plane,

$$\hat{\mathbf{E}}_p(t)=\hat{E}_{px}(t)\mathbf{e}_x+\hat{E}_{pz}(t)\mathbf{e}_z\ , \tag{3.80}$$

is known and only time dependent. The quantity $\mathbf{e}_n$ is a unit vector in the n direction. Since arbitrary pump polarization states are of interest, it is useful to introduce the coherency matrix[20–22] of the pump

$$[\overleftrightarrow{J}_p(t)]_{rs}=(cn_s\epsilon_0/2)\hat{E}_{pr}(t)\hat{E}^*_{ps}(t)\ , \tag{3.81}$$

where $r=(x,z)$ and $s=(x,z)$. The pump coherency matrix is Hermitian and has the units of radiation intensity.

In addition, the intensity of the pump radiation is given by the trace of $\overleftrightarrow{J}_p(t)$, i.e.,

$$I_p(t)=\mathrm{Tr}[\overleftrightarrow{J}_p(t)] \ . \tag{3.82}$$

The dye-laser radiation propagates along the positive z axis and consequently from Eq. (3.10) its complex electric-field amplitude is polarized in the x-y plane:

$$\hat{\mathbf{E}}_l(z,t)=\hat{E}_x(z,t)\mathbf{e}_x+\hat{E}_y(z,t)\mathbf{e}_y \ . \tag{3.83}$$

If Eqs. (3.80) and (3.83) are substituted into Eq. (3.79), it can be shown that

$$\begin{aligned}(n_s/c)\partial_t\hat{E}_x+\partial_z\hat{E}_x&=[3\sigma_s(\nu_l)/2][1-i\chi_l'(\omega_l)/\chi_l''(\omega_l)]\\&\times(\hat{E}_x n_{xx}+\hat{E}_y n_{xy}/2)-\alpha_s\hat{E}_x/2\end{aligned} \tag{3.84}$$

and

$$\begin{aligned}(n_s/c)\partial_t\hat{E}_y+\partial_z\hat{E}_y&=[3\sigma_s(\nu_l)/2][1-i\chi_l'(\omega_l)/\chi_l''(\omega_l)]\\&\times(\hat{E}_x n_{xy}/2+\hat{E}_y n_{yy})-\alpha_s\hat{E}_y/2 \ ,\end{aligned} \tag{3.85}$$

where

$$n_{nn}=\int_0^{2\pi}d\phi\int_0^{\pi}d\theta\, n_0^1(z,t,\Omega)O_{nn}(\Omega) \ , \tag{3.86}$$

and

$$n_{xy}=2\int_0^{2\pi}d\phi\int_0^{\pi}d\theta\, n_0^1(z,t,\Omega)O_{xy}(\Omega) \ , \tag{3.87}$$

where the components of $\overleftrightarrow{O}(\Omega)$ are given by Eqs. (3.59)–(3.64) and the subscript $n=(x,y)$ here and in the following. The form of Eqs. (3.84) and (3.85) indicates that, in general, as the dye-laser light propagates through the dye-laser amplifier medium its polarization state will change. To describe this phenomenon it is useful to represent the polarization state of the dye-laser light by the coherency matrix[20–22]

$$[\overleftrightarrow{J}(z,t)]_{nm}=(cn_s\epsilon_0/2)\hat{E}_n(z,t)\hat{E}_m^*(z,t) \ , \tag{3.88}$$

where $m=(x,y)$. The coherency matrix $\overleftrightarrow{J}(z,t)$ is Hermitian and its trace is the dye-laser-light intensity, i.e.,

$$I_l(z,t)=\mathrm{Tr}[\overleftrightarrow{J}(z,t)] \ . \tag{3.89}$$

Equations (3.84) and (3.85) and their complex conjugates may be used to derive the following equations that govern the evolution of the components of $\overleftrightarrow{J}(z,t)$:

$$(n_s/c)\partial_t J_{xx}+\partial_z J_{xx}=3\sigma_s(\nu_l)J_{xx}n_{xx}-\alpha_s J_{xx}+[3\sigma_s(\nu_l)/2][\mathrm{Re}(J_{xy})-\chi_l'(\omega_l)\mathrm{Im}(J_{xy})/\chi_l''(\omega_l)]n_{xy} \ , \tag{3.90}$$

$$(n_s/c)\partial_t J_{yy}+\partial_z J_{yy}=3\sigma_s(\nu_l)J_{yy}n_{yy}-\alpha_s J_{yy}+[3\sigma_s(\nu_l)/2][\mathrm{Re}(J_{xy})+\chi_l'(\omega_l)\mathrm{Im}(J_{xy})/\chi_l''(\omega_l)]n_{xy} \ , \tag{3.91}$$

and

$$\begin{aligned}(n_s/c)\partial_t J_{xy}+\partial_z J_{xy}&=[3\sigma_s(\nu_l)/2]J_{xy}\{n_{xx}+n_{yy}-i[\chi_l'(\omega_l)/\chi_l''(\omega_l)](n_{xx}-n_{yy})\}\\&-\alpha_s J_{xy}+[3\sigma_s(\nu_l)/4][J_{xx}+J_{yy}+i\chi_l'(\omega_l)(J_{xx}-J_{yy})/\chi_l''(\omega_l)]n_{xy} \ .\end{aligned} \tag{3.92}$$

Furthermore, Eqs. (3.30)–(3.33) for the dye-molecule level populations n_0^μ may be rewritten in terms of the pump- and dye-laser coherency matrices by using Eqs. (3.81) and (3.88):

$$\partial_t n_0^1=n_0^0\gamma_p+\gamma_{R0}^1(\langle n_0^1\rangle-n_0^1)-\gamma_F n_0^1-n_0^1\gamma_e \tag{3.93}$$

and

$$\partial_t n_0^0=-n_0^0\gamma_p+\gamma_{R0}^0(\langle n_0^0\rangle-n_0^0)+\gamma_F n_0^1+n_0^1\gamma_e \ , \tag{3.94}$$

where

$$\gamma_p(t,\Omega)=[3\sigma_a(\nu_p)/h\nu_p]\{J_{pxx}(t)\sin^2\theta\cos^2\phi+J_{pzz}(t)\cos^2\theta+\mathrm{Re}[J_{pxz}(t)]\sin2\theta\cos\phi\} \ , \tag{3.95}$$

$$\gamma_e(z,t,\Omega)=[3\sigma_s(\nu_l)/h\nu_l]\{J_{xx}(z,t)\sin^2\theta\cos^2\phi+J_{yy}(z,t)\sin^2\theta\sin^2\phi+\mathrm{Re}[J_{xy}(z,t)]\sin^2\theta\sin2\phi\} \ , \tag{3.96}$$

$n_0^\mu=n_0^\mu(z,t,\Omega)$ and $\langle n_0^\mu\rangle=\langle n_0^\mu(z,t)\rangle$; $\mu=(0,1)$. The set of Eqs. (3.84)–(3.96) is completed by requiring

$$n_0^0(z,t,\Omega)+n_0^1(z,t,\Omega)=n(z,t,\Omega) \ , \tag{3.97}$$

where

$$N=\int_{4\pi}d\Omega\, n(z,t,\Omega) \tag{3.98}$$

is the constant total dye-molecule number density.

When dye-molecule rotational relaxation is very fast, i.e., Eqs. (3.36) hold, then Eqs. (3.84) and (3.85) for the dye-laser-light complex electric-field amplitudes and Eqs. (3.90)–(3.92) for the coherency matrix elements become

$$\begin{aligned}(n_s/c)\partial_t\hat{\mathbf{E}}_l(z,t)+\partial_z\hat{\mathbf{E}}_l(z,t)&=\{[1-i\chi_l'(\omega_l)/\chi_l''(\omega_l)]\\&\times\sigma_s(\nu_l)N_0^1(z,t)-\alpha_s\}\hat{\mathbf{E}}_l(z,t)/2\end{aligned} \tag{3.99}$$

and

$$(n_s/c)\partial_t \overleftrightarrow{J}(z,t)+\partial_z \overleftrightarrow{J}(z,t) = [\sigma_s(\nu_l)N_0^1(z,t)-\alpha_s]\overleftrightarrow{J}(z,t) . \quad (3.100)$$

The dye-laser radiation propagates through the laser-pumped dye-laser medium without change in its state of polarization. The trace of Eq. (3.100) yields the radiation transport equation[1-11] for the dye-laser-light intensity:

$$(n_s/c)\partial_t I_l(z,t)+\partial_z I_l(z,t) = [\sigma_s(\nu_l)N_0^1(z,t)-\alpha_s]I_l(z,t) , \quad (3.101)$$

which when combined with Eqs. (3.37)–(3.40) provides the conventional description[1-11] of quasimonochromatic light amplification by transversely pumped dye-laser media. The polarization state of the dye-laser radiation is unchanged during amplification. It is clear, however, that this description is valid only when the time scale of dye-molecule rotational relaxation is much shorter than the dye-molecule fluorescence, pump absorption, and dye-laser stimulated emission times.

(b) Small-signal amplification. The general description of transversely pumped dye lasers given above is valid for both small- and large-pump and dye-laser intensity levels. To study the role of dye-molecule rotational relaxation in dye-laser-light amplification, suppose the laser-pulse lengths are comparable to the fluorescence lifetime and the pump-laser intensity I_p is much less than the pump saturation intensity I_{ps}, namely, $I_p \ll I_{ps}=\gamma_F h\nu_p/\sigma_a(\nu_p)$. In this regime there is negligible dye-molecule ground-state or S_0-state population depletion, $n_0^1 \ll n_0^0 \approx N/4\pi$, and Eq. (3.93) becomes

$$\partial_t n_0^1 = N\gamma_p/4\pi+\gamma_{R0}^1(\langle n_0^1\rangle - n_0^1)-\gamma_F n_0^1 - n_0^1\gamma_e , \quad (3.102)$$

where the pump and stimulated emission rates are given by Eqs. (3.95) and (3.96), respectively. This equation together with Eqs. (3.90)–(3.92) for the coherency matrix $\overleftrightarrow{J}$ elements and suitable boundary and initial conditions provide a complete description of dye-laser-light propagation in this regime.

In the small-signal regime the stimulated emission term in Eq. (3.102) is relatively small and may be neglected, i.e., $I_l \ll I_s=\gamma_F h\nu_l/\sigma_s(\nu_l)$, where I_s is the dye-laser-light saturation intensity. In this regime Eq. (3.102) becomes

$$\partial_t n_0^1(t,\Omega)=[3\sigma_a(\nu_p)N/4\pi h\nu_p]\{J_{pxx}(t)\sin^2\theta\cos^2\phi+J_{pzz}(t)\cos^2\theta+\mathrm{Re}[J_{pxz}(t)]\sin 2\theta\cos\phi\} + \gamma_{R0}^1[\langle n_0^1(t)\rangle - n_0^1(t,\Omega)]-\gamma_F n_0^1(t,\Omega) . \quad (3.103)$$

Equations (3.90)–(3.92) and (3.103) can be solved for the pulse problem by first averaging Eq. (3.103) over orientation, solid angle, to obtain an equation for $\langle n_0^1(t)\rangle$, namely,

$$\partial_t\langle n_0^1(t)\rangle = [\sigma_a(\nu_p)N/4\pi h\nu_p]I_p(t)-\gamma_F\langle n_0^1(t)\rangle . \quad (3.104)$$

If before pumping is initiated, all dye molecules are in the lowest vibrational level of the S_0 electronic state, then the appropriate solutions to Eqs. (3.103) and (3.104) are

$$\langle n_0^1(t)\rangle = [\sigma_a(\nu_p)N/4\pi h\nu_p]\int_{-\infty}^{t} dt' I_p(t')e^{-\gamma_F(t-t')} \quad (3.105)$$

and

$$n_0^1(t,\Omega)=[\sigma_a(\nu_p)N/h\nu_p]\int_{-\infty}^{t} dt' \left[\gamma_{R0}^1 e^{-\gamma_{R0}^1(t-t')}\int_{-\infty}^{t'} dt'' I_p(t'')e^{-\gamma_F(t-t'')} + 3\{J_{pxx}(t')\sin^2\theta\cos^2\phi+J_{pzz}(t')\cos^2\theta+\mathrm{Re}[J_{pxz}(t')]\sin 2\theta\cos\phi\}e^{-(\gamma_F+\gamma_{R0}^1)(t-t')}\right] . \quad (3.106)$$

When Eq. (3.106) is substituted into Eqs. (3.86) and (3.87) it can be shown that $n_{xy}(t)=0$,

$$n_{xx}(t)=[\sigma_a(\nu_p)N/3h\nu_p]\int_{-\infty}^{t} dt' \left[\gamma_{R0}^1 e^{-\gamma_{R0}^1(t-t')}\int_{-\infty}^{t'} dt'' I_p(t'')e^{-\gamma_F(t-t'')}+\tfrac{9}{5}e^{-(\gamma_F+\gamma_{R0}^1)(t-t')}[J_{pxx}(t')+J_{pzz}(t')/3]\right] , \quad (3.107)$$

and

$$n_{yy}(t)=[\sigma_a(\nu_p)N/3h\nu_p]\int_{-\infty}^{t} dt' \left[\gamma_{R0}^1 e^{-\gamma_{R0}^1(t-t')}\int_{-\infty}^{t'} dt'' I_p(t'')e^{-\gamma_F(t-t'')}+\tfrac{3}{5}e^{-(\gamma_F+\gamma_{R0}^1)(t-t')}I_p(t')\right] . \quad (3.108)$$

Using these results, Eqs. (3.90)–(3.92) for the dye-laser-light coherency matrix may be integrated using the method of characteristics. The results are

$$J_{nn}(z,t)=J_{nn}(0,t-n_s z/c)\exp\left[[3\sigma_s(\nu_l)c/n_s]\int_{t-n_s z/c}^{t}dt' n_{nn}(t')-\alpha_s z\right], \tag{3.109}$$

and

$$J_{xy}(z,t)=J_{xy}(0,t-n_s z/c)\times\exp\left[[3\sigma_s(\nu_l)c/2n_s]\int_{t-n_s z/c}^{t}dt'\{n_{xx}(t')+n_{yy}(t')-i[\chi_l'(\omega_l)/\chi_l''(\omega_l)][n_{xx}(t')-n_{yy}(t')]\}-\alpha_s z\right], \tag{3.110}$$

where $\overleftrightarrow{J}(0,t)$ is the dye-laser-light coherency matrix at the input to the amplifier located at $z=0$. These results are applicable to general pulse shapes whose duration is much greater than the dye-molecule vibrational relaxation and polarization dephasing times. For example, suppose that the pump-laser and dye-laser-light pulses are turned on to a constant value in the distant past. Then $\overleftrightarrow{J}_p(t)\sim\overleftrightarrow{J}_p$, $\overleftrightarrow{J}(0,t)\sim\overleftrightarrow{J}(0)$, and $\overleftrightarrow{J}(z,t)\sim\overleftrightarrow{J}(z)$, and Eqs. (3.105)–(3.110) reduce to the steady-state solution of Eqs. (3.90)–(3.92), (3.103), and (3.104), namely,

$$J_{nm}(z)=J_{nm}(0)\exp\{[g_0(\nu_l)R_{nm}-\alpha_s]z\}, \tag{3.111}$$

where $g_0(\nu_l)=\sigma_s(\nu_l)N\eta$ is the small-signal gain coefficient when dye-molecule rotational relaxation is fast, $\eta=I_p/I_{ps}$ is the normalized pump-laser intensity, and $\gamma=\gamma_F/\gamma_{R0}^1$ is the ratio of the dye molecule's fluorescence rate to the rotational relaxation rate of the lowest vibronic level of its S_1 state. The quantities R_{nm} are given by

$$R_{xx}(\gamma,J_{pxx}/I_p)=[1+(3\gamma/5)(1+2J_{pxx}/I_p)]/(1+\gamma), \tag{3.112}$$

$$R_{yy}(\gamma)=(1+3\gamma/5)/(1+\gamma) \tag{3.113}$$

and

$$R_{xy}(\gamma,J_{pxx}/I_p,\omega_l)=\{1+(3\gamma/5)(1+J_{pxx}/I_p)-i[\chi_l'(\omega_l)/\chi_l''(\omega_l)](3\gamma J_{pxx}/5I_p)\}/(1+\gamma). \tag{3.114}$$

The functions R_{nm} register the effect of finite dye-molecule rotational relaxation on the coherency matrix elements J_{nm} of the dye-laser-light during quasi-steady-state light pulse amplification in the small signal regime. If dye-molecule rotational relaxation is fast, i.e., $\gamma_{R0}^1\gg\gamma_F$, then $\gamma\ll1$ and all $R_{nm}=1$. The polarization state of the dye-laser light is unchanged during amplification. This situation also holds if the pump radiation is linearly polarized along the z axis, i.e., if $J_{pzz}=I_p$ and $J_{pxx}=0$, for then

$$R_{xx}=R_{yy}=R_{xy}=(1+3\gamma/5)/(1+\gamma). \tag{3.115}$$

However, in this case, since $R_{nm}<1$ for finite γ, the spatial rate of amplification of the dye-laser light is reduced due to the finite dye-molecule rotational relaxation rate.

When the dye-molecule rotational relaxation rate is comparable to or slower than the $S_1\rightarrow S_0$ fluorescence rate, the excited dye-molecules fluoresce before they rotate significantly. Consequently, only excited dye molecules with induced dipole moments nearly aligned with the pump-laser-light electric field are present in the medium. In general, this situation leads to changes in polarization state and enhanced (reduced) gain for $x(y)$-polarized components of the dye-laser radiation. The exception to this occurs when the dye-laser light is linearly polarized along either the x or y axis. Since the pump-laser light is polarized in the x-z plane, the x and y axes are symmetry axes for the dye-laser radiation polarization. In this case the x or y polarization state of the dye-laser light does not change. However, x-polarized light will experience more gain than y-polarized light. For example, consider two amplifiers each pumped with linearly polarized laser light. Suppose the pump radiation electric field is aligned along the x axis, i.e., $J_{pxx}=I_p$ and $J_{pzz}=0$. If two dye-laser-light pulses of equal intensity, one x polarized and the other y polarized, are each injected into a different amplifier of normalized gain length g_0L, then, from Eqs. (3.111)–(3.113), the ratio of the intensities of the two amplified pulses will be

$$J_{xx}/J_{yy}=\exp[6\gamma g_0 L/5(\gamma+1)]. \tag{3.116}$$

The strong dependence of J_{xx}/J_{yy} on γ is clearly evident. The x-polarized radiation generally experiences much more gain in the regime where dye-molecule rotational relaxation is important, i.e., finite γ.

The magnitude of γ, i.e., the importance of dye-molecule rotational relaxation, depends strongly on the solvent. For example, for rhodamine 6G in ethanol the rotational relaxation time[35] $\tau_R\simeq310$ ps and consequently from Table II, $\gamma=\gamma_F/\gamma_{R0}^1\sim\gamma_F\tau_R\sim0.09$. However, for rhodamine 6G in ethylene glycol, a highly viscous solvent, the rotational relaxation time[35] $\tau_R\simeq3$ ns. Assuming that the fluorescence lifetime of rhodamine 6G depends weakly on the solvent then, in this case, $\gamma\sim0.9$.

(c) Large-signal amplification. The results derived in Sec. III B 5 (b) indicate that optimal performance (largest gain and no dye-laser-light depolarization) of a transversely laser-pumped dye-laser-light amplifier occurs when the pump- and dye-laser light electric fields are parallel. This regime of pulsed-dye-laser operation is considered in more detail in this section. Suppose that the pump-laser and dye-laser-light beams are both polarized along the x axis, i.e., $I_p=J_{pxx}$ and $I_l=J_{xx}$. Assuming, for simplicity, that $\gamma_R=\gamma_{R0}^0=\gamma_{R0}^1$ and the solvent is lossless ($\alpha_s=0$), then dye-laser-light amplification is governed by the appropriate form of Eqs. (3.90)–(3.96), namely,

$$(n_s/c)\partial_t I_l(z,t)+\partial_z I_l(z,t) = 3\sigma_s(\nu_l)I_l(z,t)\int_0^{2\pi}d\phi\int_0^{\pi}d\theta\, n_0^1(z,t,\Omega)\sin^3\theta\cos^2\phi \ , \tag{3.117}$$

$$\partial_t n_0^1 = n_0^0\gamma_p+\gamma_R(\langle n_0^1\rangle - n_0^1)-\gamma_F n_0^1 - n_0^1\gamma_e \ , \tag{3.118}$$

and

$$\partial_t n_0^0 = -n_0^0\gamma_p+\gamma_R(\langle n_0^0\rangle - n_0^0)+\gamma_F n_0^1 + n_0^1\gamma_e \ , \tag{3.119}$$

where

$$\gamma_p = [3\sigma_a(\nu_p)I_p(t)/h\nu_p]\sin^2\theta\cos^2\phi \ , \tag{3.120}$$

$$\gamma_e = [3\sigma_s(\nu_l)I_l(z,t)/h\nu_l]\sin^2\theta\cos^2\phi \ , \tag{3.121}$$

and

$$\langle n_0^\mu(z,t)\rangle = (1/4\pi)\int_0^{2\pi}d\phi\int_0^{\pi}d\theta\sin\theta n_0^\mu(z,t,\Omega) \tag{3.122}$$

together with Eqs. (3.97) and (3.98). These equations may be greatly simplified by noting that the x axis is an axis of symmetry. Transforming from spherical polar coordinates (θ,ϕ) about the z axis to spherical polar coordinates (α,β) about the x axis, integrating over the azimuthal angle β and transforming the polar angle α by letting $\xi=\cos\alpha$ yields

$$(n_s/c)\partial_t I_l(z,t)+\partial_z I_l(z,t) = 6\pi\sigma_s(\nu_l)I_l(z,t)\int_{-1}^{1}d\xi\,\xi^2 n_0^1(z,t,\xi) \tag{3.123}$$

together with Eqs. (3.118)–(3.119) where

$$\gamma_p = [3\sigma_a(\nu_p)I_p(t)/h\nu_p]\xi^2 \ , \tag{3.124}$$

$$\gamma_e = [3\sigma_s(\nu_l)I_l(z,t)/h\nu_l]\xi^2 \ , \tag{3.125}$$

and Eq. (3.122) becomes

$$\langle n_0^\mu(z,t)\rangle = \tfrac{1}{2}\int_{-1}^{1}d\xi\, n_0^\mu(z,t,\xi) \ . \tag{3.126}$$

These equations describe light amplification in pulsed-laser transversely pumped dye-laser media when the pump- and dye-laser-light electric fields are parallel. The appropriate boundary and initial conditions for an amplifier whose input is at $z=0$ are $I_l(0,t)$, $n_0^1(z,0,\xi)$, and $n_0^0(z,0,\xi)$. To examine the characteristics of the solutions to these equations consider two important regimes of operation: short-pulse and quasi-steady-state pulse amplification.

(i) Short-pulse amplification. Consider a dye-laser amplifier that is transversely pumped with a laser light pulse of constant intensity I_p and duration τ_p. The pump time is greater than or comparable to the dye-molecule fluorescence lifetime, i.e., $\tau_p\gamma_F \gtrsim 1$. During laser pumping the excited dye molecules fluoresce and rotationally relax. For simplicity, depumping of excited dye molecules by amplified spontaneous emission (ASE) is neglected, although under high-gain conditions[10,11] it is important. Immediately after the pump-laser pulse terminates a short dye-laser pulse is amplified by passing it through the excited dye-laser medium. This situation is analogous to the conventional short-pulse amplifier containing a homogeneously broadened medium, first treated by Frantz and Nodvik.[60] A treatment of the short-pulse dye laser, including ASE depumping but neglecting dye-molecule orientation and rotational relaxation effects, has been given by Migus *et al.*[10,11]

Suppose that prior to dye-laser-light pulse amplification the dye molecules are pumped separately by x-polarized laser light with initial conditions $n_0^1(z,0,\xi)=0$ and $n_0^0(z,0,\xi)=N_0^0/4\pi=N/4\pi$. All the dye molecules are initially in the ground state $S_0(0)$. In addition, the pump-laser intensity and dye-molecule concentration are such that no dye-molecule ground-state depletion occurs during the pumping pulse, i.e., $n_0^0(z,t,\xi)\simeq N/4\pi \gg n_0^1(z,t,\xi)$. Then during pumping, from Eqs. (3.118), (3.124), and (3.125), the dye-molecule $S_1(0)$ excited-state density per unit solid angle n_0^1 is governed by

$$\partial_t n_0^1 = [3\sigma_a(\nu_p)NI_p/4\pi h\nu_p]\xi^2 + \gamma_R(\langle n_0^1\rangle - n_0^1)-\gamma_F n_0^1 \ . \tag{3.127}$$

Averaging this equation over ξ, using Eq. (3.126), yields an equation for the orientationally averaged dye-molecule $S_1(0)$ excited-state population density per unit solid angle $\langle n_0^1\rangle$, namely,

$$\partial_t\langle n_0^1\rangle = [\sigma_a(\nu_p)NI_p/4\pi h\nu_p]-\gamma_F\langle n_0^1\rangle \ . \tag{3.128}$$

The appropriate self-consistent solution of Eqs. (3.127) and (3.128) that satisfies the initial conditions set forth earlier gives the population densities at the end of the pump pulse:

$$\langle n_0^1(\tau_p)\rangle = (N_0^1/4\pi)(1-e^{-\gamma_F\tau_p}) \tag{3.129}$$

and

$$n_0^1(\tau_p,\xi) = (N_0^1/4\pi)\{[(3\gamma\xi^2+1)/(\gamma+1)] \times(1-e^{-(\gamma+1)\gamma_R\tau_p}) -(e^{-\gamma_F\tau_p}-e^{-(\gamma+1)\gamma_R\tau_p})\} \ , \tag{3.130}$$

where

$$N_0^1 = \sigma_a(\nu_p)NI_p/\gamma_F h\nu_p \tag{3.131}$$

is the total dye-molecule $S_1(0)$ excited-state density that would be produced if, during pumping, dye-molecule rotational relaxation was very fast, i.e., $\gamma \ll 1$ and $\gamma_R\tau_p \gg 1$. If the pump pulse duration is chosen such that $\exp(-\gamma_R\tau_p)\ll 1$ and γ is finite then the dye-molecule $S_1(0)$ excited-state density per unit solid angle approaches the steady-state value

$$n_0^1(\tau_p,\xi) = (N_0^1/4\pi)(3\gamma\xi^2+1)/(\gamma+1) \tag{3.132}$$

at the end of the pump pulse.

The polar angle α distribution of $n_0^1(\tau_p,\cos\alpha)$ given by Eq. (3.132) is plotted in Fig. 8 for several values of γ. Due to symmetry considerations only one quadrant is plotted. The angle α is measured from the vertical or x axis ($\alpha=0$). Also it should be noted that n_0^1 is rotationally symmetric about the x axis, i.e., independent of β.

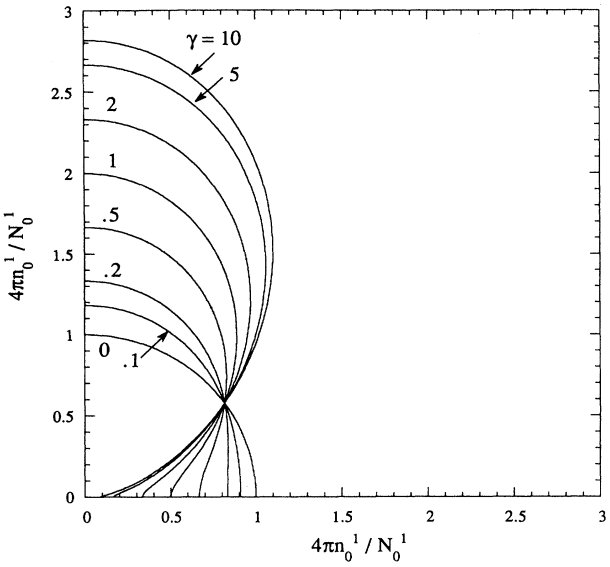

FIG. 8. Polar angle α dependence of the dye-molecule $S_1(0)$ excited-state density per unit solid angle n_0^1 produced by transverse laser pumping with constant-intensity x-polarized radiation, Eq. (3.132). The angle α is measured from the vertical x axis. The pumping duration τ_p is such that $\tau_p\gamma_R \gg 1$. The curves are parametric in $\gamma=\gamma_F/\gamma_R$.

This is because the pump and laser-light beams are polarized along the x axis. From Eq. (3.132) all the curves in Fig. 8 pass through the polar angle determined by $3\cos^2\alpha=1$. Figure 8 shows that when dye-molecule rotational relaxation is fast, $\gamma \ll 1$, the dye-molecule $S_1(0)$ excited-state density per unit solid angle n_0^1, is isotropically distributed; i.e., all excited dye-molecule orientations are equally probable. However, as γ is increased from 0.1 to 10 the dye-molecule $S_1(0)$ excited-state density per unit solid angle becomes more and more strongly peaked about the x axis. This asymmetric population distribution in polar angle α occurs when γ is finite because in this regime $S_1(0)$ excited dye molecules relax by fluorescence or nonradiative internal processes before rotating significantly.

Now suppose that immediately prior to short dye-laser-light pulse injection into the dye amplifier the $S_1(0)$ excited dye-molecule population density per unit solid angle is uniform along the length of the amplifier and given by the steady-state value, Eq. (3.132). If the duration τ_l of the x-polarized dye-laser pulse is such that $\gamma_F\tau_l \ll 1$ and $\gamma_R\tau_l \ll 1$, then amplification of the pulse is determined by a simplified version of Eqs. (3.118), (3.119), and (3.123)–(3.126), namely,

$$(n_s/c)\partial_t I_l(z,t)+\partial_z I_l(z,t) = 6\pi\sigma_s(\nu_l)I_l(z,t)\int_{-1}^{1} d\xi\,\xi^2 n_0^1(z,t,\xi) \quad (3.133)$$

and

$$\partial_t n_0^1(z,t,\xi) = -n_0^1(z,t,\xi)[3\sigma_s(\nu_l)I_l(z,t)/h\nu_l]\xi^2 \,. \quad (3.134)$$

Solution of these two coupled partial differential equations generally requires numerical integration. However, in many applications the dye-laser pulse energy fluence

$$\Gamma_l(z)=\int_{-\infty}^{\infty} dt\, I_l(z,t) \quad (3.135)$$

is of interest. In this case the treatment may be simplified. At the input to the amplifier the pulse energy fluence is known and given by

$$\Gamma_l(0)=\int_{-\infty}^{\infty} dt\, I_l(0,t) \,. \quad (3.136)$$

An equation governing the axial spatial evolution of Γ_l can be obtained by first formally integrating Eq. (3.134) to obtain

$$n_0^1(z,t,\xi)=n_0^1(\tau_p,\xi)\exp\left[-3\xi^2\int_{-\infty}^{t} dt' I_l(z,t')/\Gamma_s\right], \quad (3.137)$$

where $\Gamma_s=h\nu_l/\sigma_s(\nu_l)$ is the conventional[10,11,60] dye-laser pulse saturation fluence and $n_0^1(\tau_p,\xi)$ is given by Eq. (3.132). If Eq. (3.137) is substituted into the radiation transport Eq. (3.133) and the resulting equation is integrated over all time, it can be shown that

$$\partial_\zeta\Gamma(\zeta)=1-[2(\gamma+1)]^{-1} \times\int_{-1}^{1} d\xi(3\gamma\xi^2+1)\exp[-3\xi^2\Gamma(\zeta)] \,, \quad (3.138)$$

where $\zeta=g_0 z$ is the dimensionless amplifier gain length and $\Gamma=\Gamma_l/\Gamma_s$ is the normalized laser-pulse energy fluence. The quantity $g_0=\sigma_s(\nu_l)N_0^1$ is the small-signal gain coefficient when dye-molecule rotational relaxation is very fast during pumping, i.e., when $\gamma \ll 1$ and $\gamma_R\tau_p \gg 1$. Equation (3.138) together with the initial or boundary condition $\Gamma(0)=\Gamma_0=\Gamma_l(0)/\Gamma_s$ describes the amplification of short pulses. In general, the performance of a short-pulse dye-laser amplifier of length L, described by Eq. (3.138), depends on three dimensionless variables: γ, g_0L, and Γ_0. After the dye-laser pulse has passed a given axial location ζ in the amplifier, from Eq. (3.137), the dye-molecule $S_1(0)$ excited-state density per unit solid angle will be

$$n_0^1(\zeta,\xi)=n_0^1(\tau_p,\xi)\exp[-3\xi^2\Gamma(\zeta)] \,. \quad (3.139)$$

In Fig. 9, numerical solutions of Eq. (3.138) are presented for an amplifier with gain length $g_0L=4$. In this figure the light pulse energy gain $G=\Gamma/\Gamma_0 = G(\Gamma_0,\gamma,g_0L)$ and extraction efficiency $\epsilon_e=(\Gamma-\Gamma_0)/g_0L=\epsilon_e(\Gamma_0,\gamma,g_0L)$ are plotted as a function of normalized light pulse input energy fluence $\Gamma_0=\Gamma_l(0)/\Gamma_s$. In the figure, as noted, the curves are parametric in $\gamma=\gamma_F/\gamma_R$, which is the ratio of the dye molecule's fluorescence to rotational relaxation rates. In parts (a) and (b) of the figure the energy gain and efficiency for finite γ are normalized to the corresponding energy gain and efficiency for $\gamma=0$. In part (c) the energy gain and efficiency are plotted for the $\gamma=0$ case. This approach exhibits the importance of dye-molecule rotational relaxation for a wide range of Γ_0. Also, for comparison purposes the light pulse energy gain and extraction efficiency

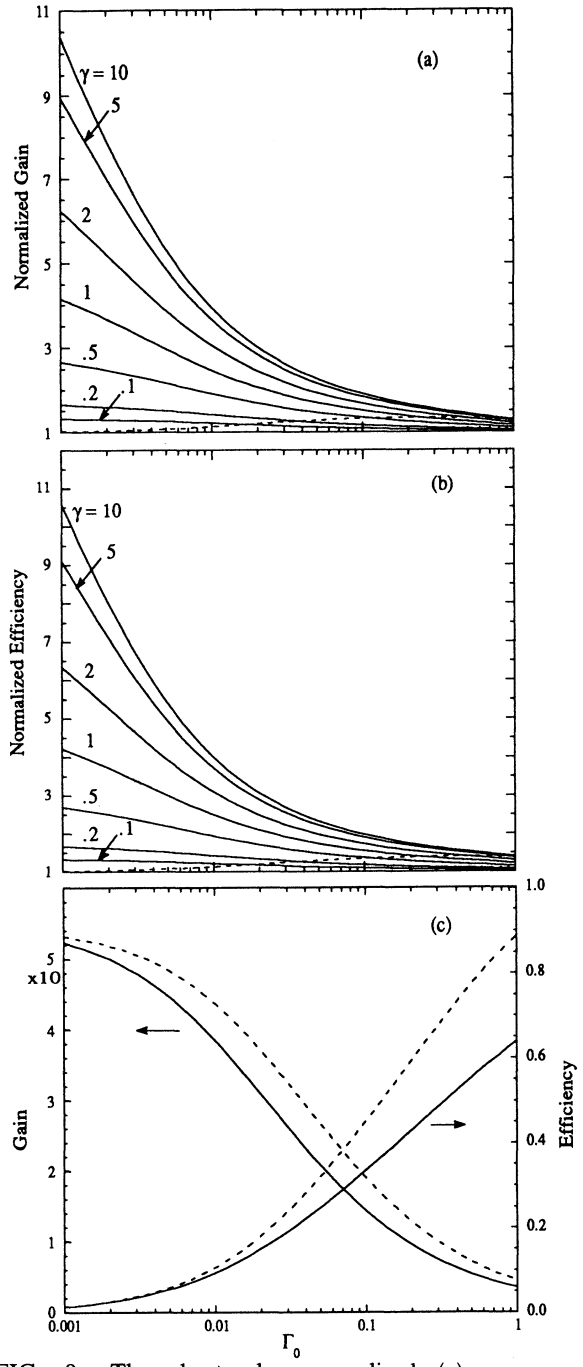

FIG. 9. The short-pulse normalized (a) energy gain $G(\Gamma_0,\gamma,g_0L)/G(\Gamma_0,0,g_0L)$ and (b) extraction efficiency $\epsilon_e(\Gamma_0,\gamma,g_0L)/\epsilon_e(\Gamma_0,0,g_0L)$ characteristics for a transverse-laser-pumped dye-laser amplifier of normalized gain length $g_0L=4$. Both the pump- and dye-laser-light beams are x polarized. Before passage of the dye-laser pulse the initial dye molecule $S_1(0)$ excited-state density per unit solid angle n_0^1 is given by Eq. (3.132) and plotted in Fig. 8. In (a) and (b) the curves are parametric in $\gamma=\gamma_F/\gamma_R$. In (c) the pulse energy gain $G(\Gamma_0,0,g_0L)$ and extraction efficiency $\epsilon_e(\Gamma_0,0,g_0L)$ of the amplifier are plotted for the normalization case $\gamma=0$. The dashed lines give the amplifier performance predicted by the Frantz and Nodvik (Ref. 60) theory of homogeneously broadened short-pulse amplifiers, Eq. (3.140).

obtained from the conventional solution

$$\Gamma=\ln[e^{g_0L}(e^{\Gamma_0}-1)+1] \tag{3.140}$$

derived by Frantz and Nodvik[60] are also plotted as dashed lines. Strictly speaking, this solution is valid for short-pulse dye-laser amplifiers only then $\gamma_F\tau_l \ll 1$ and $\tau_l\gamma_R \gg 1$. In this regime, negligible dye-molecule fluorescence relaxation but very fast dye-molecule rotational relaxation occurs during the light pulse. Consequently, during the pulse dye-molecule rotational relaxation maintains an isotropic $S_1(0)$ excited dye-molecule orientation distribution, i.e., $n_0^1 \neq n_0^1(\xi)$.

Figure 10 shows the $S_1(0)$ excited dye-molecule population density per unit solid angle n_0^1 after passage of the light pulse, Eq. (3.139), as a function of polar angle α for several values of γ. The curves are parametric in the normalized light pulse energy fluence $\Gamma=\Gamma_l/\Gamma_s$. Figure 9 shows a strong dependence of amplifier energy gain and extraction efficiency on γ. In general, dye-molecule rotational relaxation has the largest effect on amplifier performance when the light pulse normalized input energy fluence is in the small or intermediate signal regime, i.e., $\Gamma_0 \lesssim 1$. The enhanced amplifier energy gain and extraction efficiency for finite γ can be explained by the anisotropic dye-molecule $S_1(0)$ excited-state population density per unit solid angle distributions plotted in Figs. 8 and 10. As γ increases the initial dye-molecule orientation distribution, Fig. 8, becomes peaked about the x axis, producing greater light pulse energy gain and consequently larger extraction efficiency.

Equation (3.138) may be used to derive approximate analytic solutions for light pulse amplification in the small and large signal regimes. In the small-signal regime $\Gamma \ll 1$ and the exponential factor in the integrand may be expanded yielding an approximation to Eq. (3.138):

$$\partial_\xi\Gamma(\xi)=[(9\gamma/5+1)/(\gamma+1)]\Gamma(\xi) . \tag{3.141}$$

The solution of this equation is

$$\Gamma=\Gamma_0\exp[(9\gamma/5+1)g_0L/(\gamma+1)] . \tag{3.142}$$

Since $(9\gamma/5+1)/(\gamma+1)>1$, this result is consistent with results presented in Fig. 9 and discussed earlier. Equation (3.142) indicates that in the small-signal regime slow dye-molecule rotational relaxation yields a gain enhancement $G(\gamma)/G(0)=\exp[4\gamma g_0L/5(\gamma+1)]$, which can be large, i.e., $[G(\gamma)/G(0)]_{\max}=\exp(4g_0L/5)$. For example, if $g_0L=8$ then $[G(\gamma)/G(0)]_{\max}\simeq 600$. In the large signal regime $\Gamma \gg 1$. Due to the exponential factor in the integrand, in this case the principal contribution to the integral comes from the vicinity of $\xi=0$. Consequently, Eq. (3.138) may be approximated by

$$\partial_\xi\Gamma(\xi)=1-[2(\gamma+1)]^{-1}\int_{-\infty}^{\infty}d\xi(3\gamma\xi^2+1) \times\exp[-3\xi^2\Gamma(\xi)] \tag{3.143}$$

or

$$\partial_\xi\Gamma(\xi)=1-[2(\gamma+1)]^{-1}[\pi/3\Gamma(\xi)]^{1/2} \times\{1+[\gamma/2\Gamma(\xi)]\} . \tag{3.144}$$

Provided the second term on the right-hand side of Eq. (3.144) is small compared to 1, Eq. (3.144) may be integrated to obtain the transcendental equation

$$\Gamma=\Gamma_0+g_0L-(\gamma+1)^{-1}(\pi/3)^{1/2}\times[\Gamma^{1/2}-\Gamma_0^{1/2}-(\gamma/2)(\Gamma^{-1/2}-\Gamma_0^{-1/2})]\ . \tag{3.145}$$

The first iterative solution to this equation, namely,

$$\Gamma=\Gamma_0+g_0L-(\gamma+1)^{-1}(\pi/3)^{1/2}\times\{(\Gamma_0+g_0L)^{1/2}-\Gamma_0^{1/2}-(\gamma/2)[(\Gamma_0+g_0L)^{-1/2}-\Gamma_0^{-1/2}]\} \tag{3.146}$$

provides a good approximation to the large-signal solutions of Eq. (3.138) presented in Fig. 9.

(ii) Quasi-steady-state pulse amplification. Consider a dye-laser amplifier that is transversely laser pumped and operates in the quasi-steady-state regime. The pump- and dye-laser-pulse lengths are long compared to the dye-molecule fluorescence and rotational relaxation times, i.e., $\gamma_F\tau\gg1$ and $\gamma_R\tau\gg1$, where $\tau=(\tau_p,\tau_l)$. However, the ratio γ is finite. In addition, the pump- and dye-laser beams are polarized with their electric fields aligned along the x axis. Under these conditions the amplification of a dye-laser-light pulse is determined by a simplified version of Eqs. (3.118), (3.119), and (3.123), namely,

$$\partial_z I_l(z)=6\pi\sigma_s(\nu_l)I_l(z)\int_{-1}^{1}d\xi\,\xi^2 n_0^1(z,\xi)\ , \tag{3.147}$$

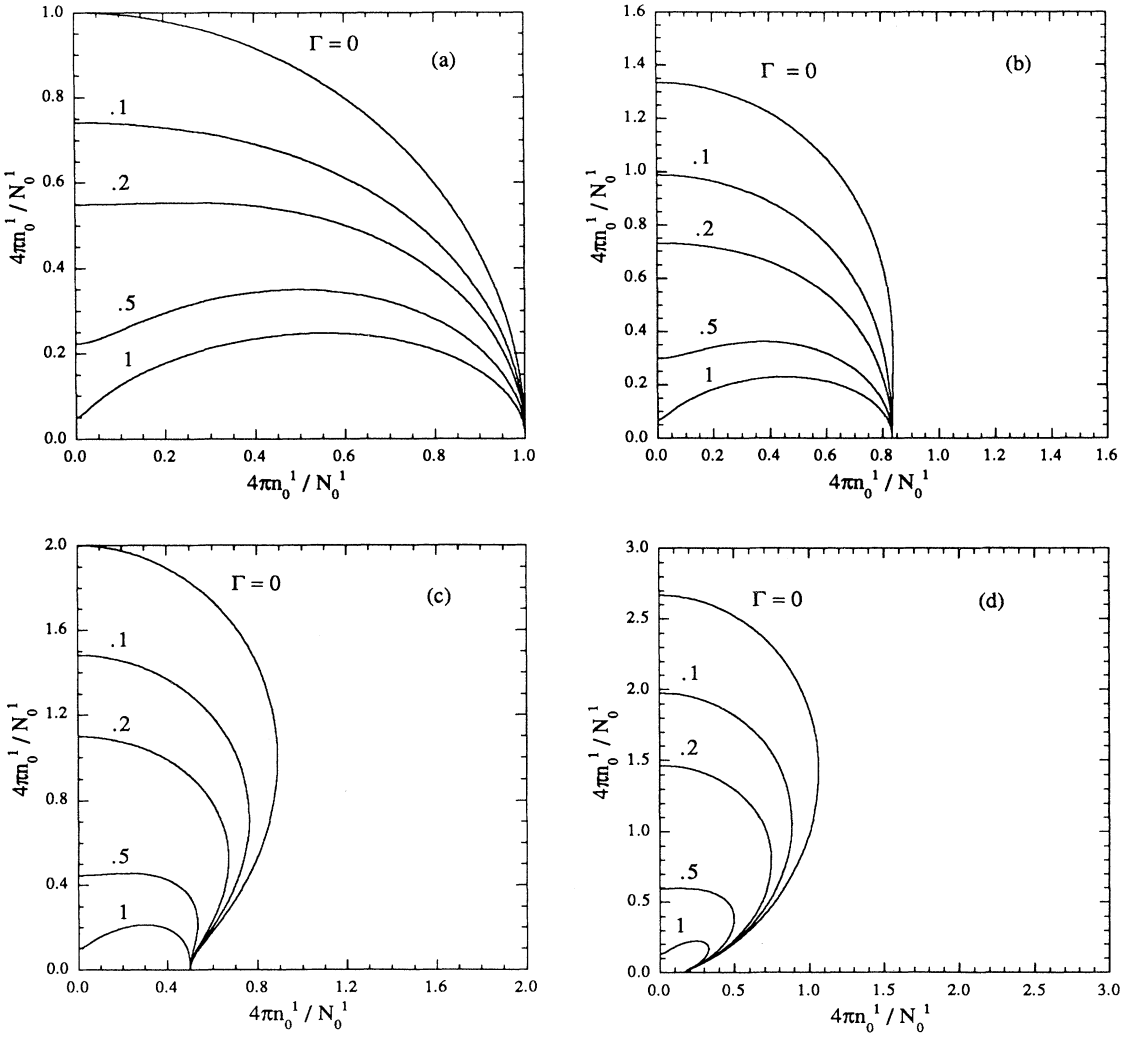

FIG. 10. Polar angle α dependence of the dye-molecule $S_1(0)$ excited-state density per unit solid angle n_0^1 after passage of a short dye-laser pulse of normalized fluence $\Gamma=\Gamma_l/\Gamma_s$ for several values of $\gamma=\gamma_F/\gamma_R$, namely (a) 0, (b) 0.2, (c) 1, and (d) 5. The normalization total number density N_0^1 is given by Eq. (3.131). The angle α is measured from the vertical x axis.

$$n_0^0\gamma_p+\gamma_R(\langle n_0^1\rangle-n_0^1)-\gamma_F n_0^1-n_0^1\gamma_e=0\ , \quad (3.148)$$

and

$$n_0^0+n_0^1=N/4\pi\ , \quad (3.149)$$

where the pump absorption γ_p and stimulated emission γ_e rates are given by Eqs. (3.124) and (3.125). Equation (3.149) is obtained by adding together the steady-state forms of Eqs. (3.118) and (3.119) and using Eqs. (3.97), (3.98), and (3.126) to simplify the result. The parametric time dependence of physical quantities is suppressed for simplicity. Orientationally averaging Eqs. (3.148) and (3.149) using Eq. (3.126) it can be shown that

$$\langle n_0^1\rangle=(N/4\pi)\eta(1+\gamma)F/[(\eta+I)(\gamma+F)] \quad (3.150)$$

where

$$F=F(\eta+I,\gamma)$$
$$=1-[(\gamma+1)/3\gamma(\eta+I)]^{1/2}$$
$$\times\tan^{-1}\{[3\gamma(\eta+I)/(\gamma+1)]^{1/2}\}\ . \quad (3.151)$$

The quantity $\eta=I_p/I_{ps}$ is the normalized pump intensity where I_{ps} is the conventional pump saturation intensity. The quantity $I=I_l/I_s$ is the normalized laser intensity where I_s is the conventional laser saturation intensity. In the limit of very rapid dye-molecule rotational relaxation, $\gamma\ll 1$, Eq. (3.150) for $\langle n_0^1\rangle$ reduces to the conventional form

$$4\pi\langle n_0^1\rangle=N_0^1=N\eta/(1+\eta+I)\ . \quad (3.152)$$

By substituting Eq. (3.150) into Eq. (3.148) and using Eq. (3.149) to eliminate n_0^0 it can be shown that

$$n_0^1=(N_0^1/4\pi)(1+\eta)$$
$$\times(3\gamma\xi^2+4\pi\langle n_0^1\rangle/N\eta)/[\gamma+1+3\gamma(\eta+I)\xi^2]\ , \quad (3.153)$$

where here and in the remainder of this section

$$N_0^1=N\eta/(1+\eta)\ , \quad (3.154)$$

which is the small-signal total dye-molecule $S_1(0)$ excited-state population density, including ground-state $S_0(0)$ depletion when dye-molecule rotational relaxation is very fast, i.e., $\gamma\ll 1$. By substituting Eq. (3.153) into Eq. (3.147) it can be shown that the normalized dye-laser-light intensity is governed by

$$\partial_\xi I(\xi)=\{(1+\eta)I(\xi)/[\eta+I(\xi)]\}$$
$$\times(1-\{(\gamma+1)F/[\eta+I(\xi)](\gamma+F)\})\ , \quad (3.155)$$

where the function F is given by Eq. (3.151) and $\xi=g_0z$ is the dimensionless amplifier gain length. Here the quantity $g_0=\sigma_s(\nu_l)N_0^1=\sigma_sN\eta/(1+\eta)$ is the small-signal gain coefficient when dye-molecule rotational relaxation is very fast, i.e., $\gamma\ll 1$. Equation (3.155) together with the initial or boundary condition $I(0)=I_0=I_l(0)/I_s$ determines the amplification of dye-laser-light pulses in the quasi-steady-state regime. In general, the performance of

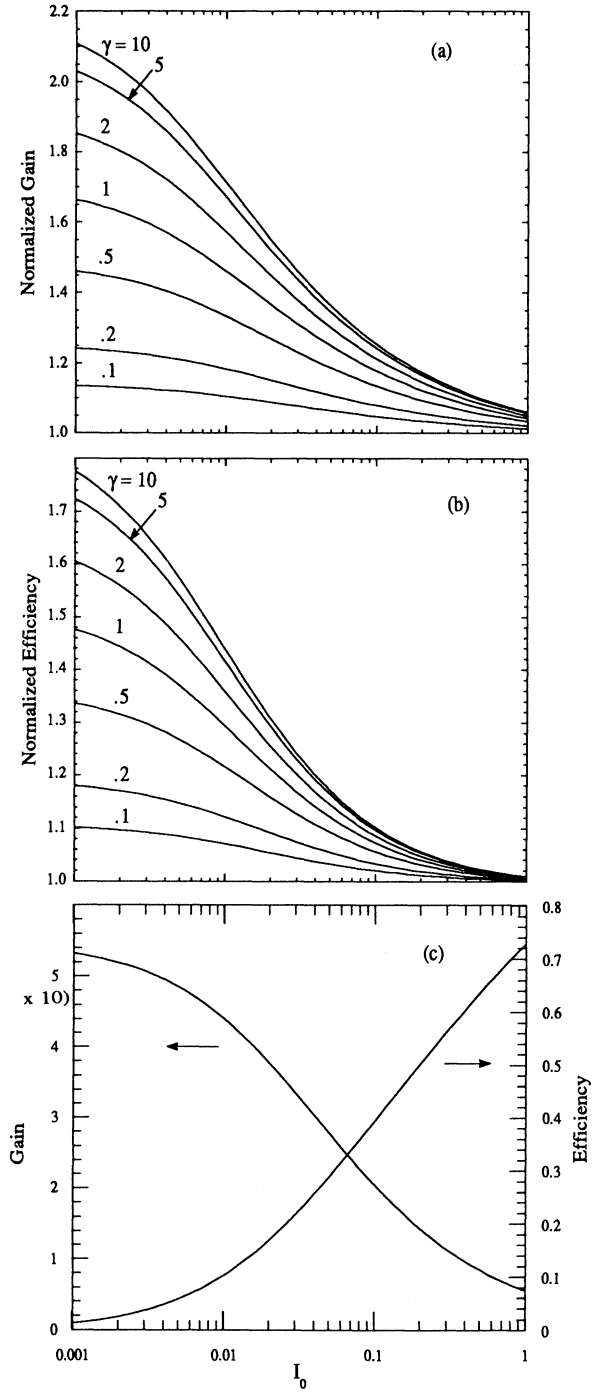

FIG. 11. The quasi-steady-state dye-laser-light pulse normalized (a) intensity gain $G(I_0,\gamma,\eta,g_0L)/G(I_0,0,\eta,g_0L)$ and (b) amplifier efficiency $\epsilon_a(I_0,\gamma,\eta,g_0L)/\epsilon_a(I_0,0,\eta,g_0L)$ for a transverse-laser-pumped dye-laser amplifier of normalized gain length $g_0L=4$. Both the pump- and dye-laser-light beams are x polarized. The normalized pump light intensity $\eta=I_p/I_{ps}=1$. The (a) and (b) curves are parametric in $\gamma=\gamma_F/\gamma_R$. In (c) the pulse intensity gain $G(I_0,0,\eta,g_0L)$ and amplifier efficiency $\epsilon_a(I_0,0,\eta,g_0L)$ of the amplifier are plotted for the normalization case $\gamma=0$. The $\gamma=0$ curves give the amplifier performance predicted by the conventional theory of homogeneously broadened steady-state amplifiers, Eq. (3.158).

a quasi-steady-state pulsed dye-laser amplifier of length L, described by Eq. (3.155), depends on four dimensionless variables: γ, η, g_0L, and I_0. In Fig. 11 numerical solutions of Eq. (3.155) are presented for an amplifier with gain length $g_0L=4$. In this figure the light pulse intensity gain $G=I/I_0=G(I_0,\gamma,\eta,g_0L)$ and amplifier efficiency $\epsilon_a=\epsilon_a(I_0,\gamma,\eta,g_0L)$ are plotted as a function of normalized input light intensity I_0. The regime of ground-state depletion often found in quasi steady-state dye amplifiers is treated by taking $\eta=1$. In the figure, as noted, the curves are parametric in $\gamma=\gamma_F/\gamma_R$. In parts (a) and (b) of the figure the intensity gain and amplifier efficiency for finite γ are normalized to the corresponding intensity gain and amplifier efficiency for $\gamma=0$. In part (c) the intensity gain and amplifier efficiency are plotted for the $\gamma=0$ case. This approach exhibits the importance of dye-molecule rotational relaxation for a wide range of I_0. The amplifier efficiency plotted in Fig. 11 is defined by

$$\epsilon_a=(\nu_p/\nu_l)[I_l(z)-I_l(0)]\Big/\sigma_a I_p\int_0^z dz\int_{4\pi}d\Omega\, n_0^0(z,\Omega)\ . \tag{3.156}$$

For generality, the linear dependence of amplifier efficiency on pumping quantum efficiency ν_l/ν_p has been removed by introducing the factor ν_p/ν_l into Eq. (3.156). After a considerable amount of analysis it can be shown that in normalized variables

$$\epsilon_a=[I(\zeta)-I_0]\left[(1+\eta)\zeta-\eta(1+\gamma)\int_{I_0}^{I(\zeta)}dI\{(\eta+I)F/I[(\eta+I)(\gamma+F)-(\gamma+1)F]\}\right]^{-1}\ . \tag{3.157}$$

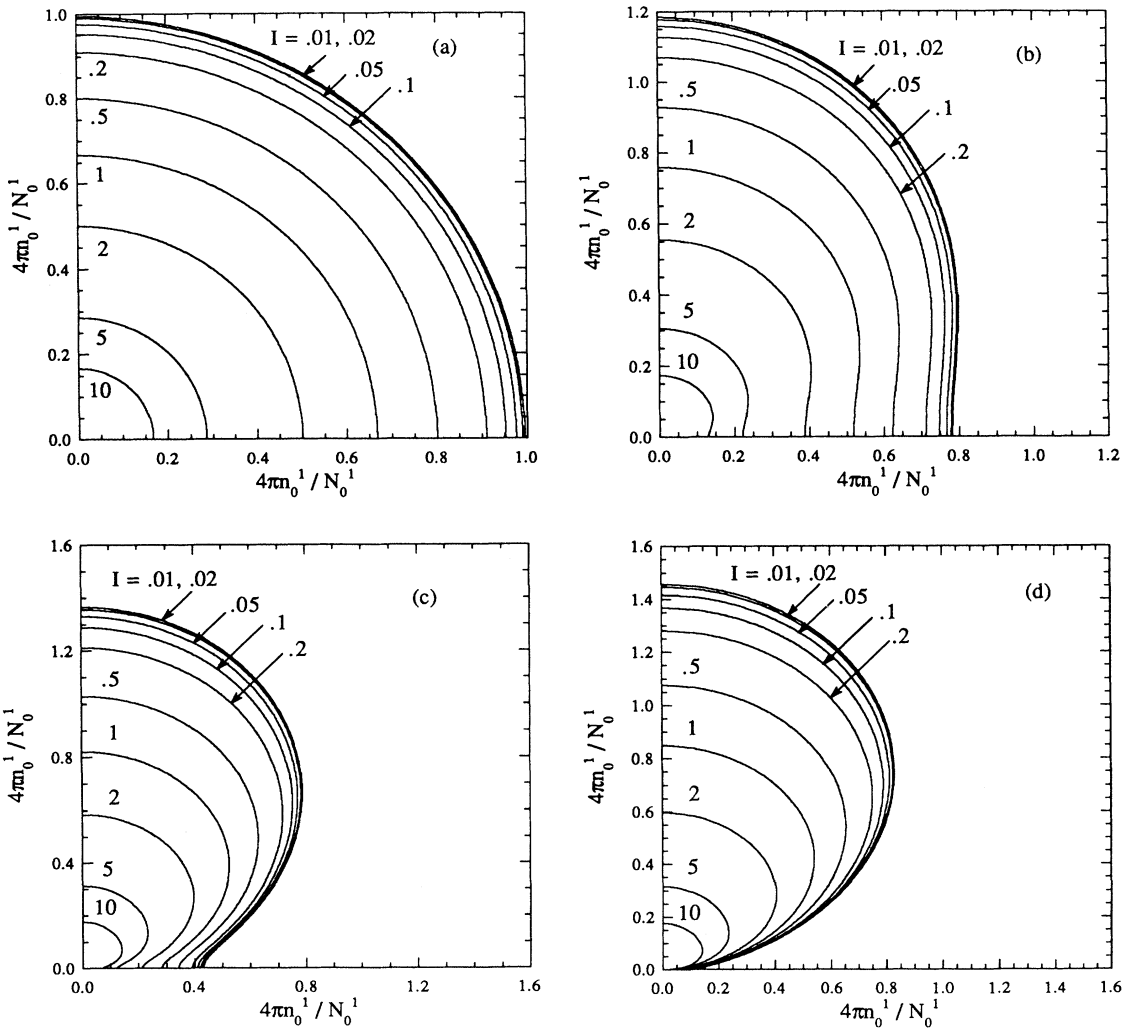

FIG. 12. Polar angle α dependence of the dye-molecule $S_1(0)$ excited-state density per unit solid angle n_0^1 during passage of a quasi-steady-state dye-laser pulse of normalized intensity $I=I_l/I_s$ for $\eta=1$ and for several values of $\gamma=\gamma_F/\gamma_R$, namely (a) 0, (b) 0.2, (c) 1, and (d) 5. The normalization total number density N_0^1 is given by Eq. (3.154). The angle α is measured from the vertical x axis.

In the limit of very rapid dye-molecule rotational relaxation $\gamma \ll 1$, Eq. (3.155) reduces to the conventional form

$$\partial_\xi I(\xi)=(1+\eta)I(\xi)/[1+\eta+I(\xi)] . \quad (3.158)$$

The solution of this equation yields the $\gamma=0$ curves displayed in Fig. 11. Integration of Eq. (3.158) yields the transcendental relation

$$(1+\eta)g_0L=(1+\eta)\ln G+I_0(G-1) . \quad (3.159)$$

In this limit the amplifier efficiency, Eq. (3.157) becomes

$$\epsilon_a=(I-I_0)/[(1+\eta)g_0L-\eta\ln G] . \quad (3.160)$$

Figure 12 shows the $S_1(0)$ excited dye-molecule population density per unit solid angle n_0^1 as a function of polar angle α for several values of γ. The curves are parametric in the normalized light intensity $I=I_l/I_s$ for $\eta=1$. Figure 11 shows a significant dependence of amplifier intensity gain and efficiency on γ. In general, dye-molecule rotational relaxation has the largest effect on amplifier performance when the light pulse normalized input intensity is in the small or intermediate signal regime, i.e., $I_0 \lesssim 1$. The enhanced amplifier intensity gain and efficiency for finite γ can be explained by the anisotropic dye-molecule $S_1(0)$ excited-state population density per unit solid angle distributions plotted in Fig. 12. As γ increases the dye-molecule $S_1(0)$ excited-state orientation distribution becomes peaked about the x axis, producing greater light pulse intensity gain and consequently larger amplifier efficiency.

Equation (3.155) may be used to derive approximate analytic solutions for quasi-steady-state dye-laser-light pulse amplification in the small- and large-signal regimes. In the small-signal regime $I \ll 1$ Eq. (3.155) may be approximated by

$$\partial_\xi I(\xi)=(1+\eta)I(\xi)\{1-[(\gamma+1)F/\eta(\gamma+F)]\}/\eta , \quad (3.161)$$

where

$$F(\eta,\gamma)=1-[(1+\gamma)/3\gamma\eta]^{1/2}\tan^{-1}\{[3\gamma\eta/(1+\gamma)]^{1/2}\} . \quad (3.162)$$

The appropriate solution to Eq. (3.161) for an amplifier of length L is

$$I=I_0\exp(Rg_0L) , \quad (3.163)$$

where

$$R=R(\eta,\gamma)=(1-\{(\gamma+1)F(\eta,\gamma)/\eta[\gamma+F(\eta,\gamma)]\})\times(1+\eta)/\eta . \quad (3.164)$$

Equation (3.163) holds in the small-signal regime for arbitrary γ and η. This result gives a good approximation to the numerical results in the small-signal regime. In Fig. 13 the function R is plotted as a function of η for several values of γ. Since R appears as a factor of g_0L in an exponential, its magnitude and functional dependence on η and γ leads to significant variations in amplifier behavior. For weak pumping $\eta \ll 1$, Eq. (3.163) reduces to

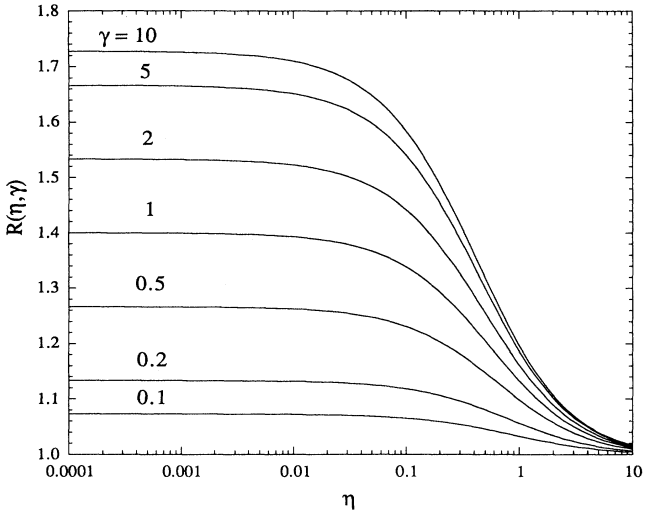

FIG. 13. Plot of the quasi-steady-state small-signal gain parameter R, Eq. (3.164), as a function of $\eta=I_p/I_{ps}$ for several values of $\gamma=\gamma_F/\gamma_R$.

$$I=I_0\exp[(9\gamma/5+1)g_0L/(1+\gamma)] , \quad (3.165)$$

in agreement with Eq. (3.111) when $J_{pxx}=I_p$. Equation (3.165) indicates that in the small-signal regime slow dye-molecule rotation relaxation yields a gain enhancement $G(\gamma)/G(0)=\exp[4\gamma g_0L/5(\gamma+1)]$ which can be large, i.e., $[G(\gamma)/G(0)]_{\max}=\exp[4g_0L/5]$. For example, if $g_0L=8$, then $[G(\gamma)/G(0)]_{\max}=600$. If ground-state depletion is included and $\eta=1$, then from Eqs. (3.163) and (3.164) $[G(\gamma)/G(0)]_{\max}=\exp(0.2g_0L)$ and the enhancement is much smaller. For example, if $g_0L=8$, then $[G(\gamma)/G(0)]_{\max}=5$. These results reveal the very sensitive dependence of amplifier performance on both η and γ. This behavior is explained as follows. Figure 14 shows the $S_1(0)$ excited dye-molecule population density per unit solid angle, n_0^1, as a function of polar angle α for $\eta=0.01$ and 1 and two values of γ, namely, 1 and 10. These plots indicate that for both values of γ as η is increased, corresponding to harder pumping, the dye-molecule $S_1(0)$ excited-state orientation distribution n_0^1 becomes less peaked about the x axis, producing smaller light pulse intensity gain. In the large-signal regime $I \gg 1$, Eq. (3.155) reduces essentially to Eq. (3.158), which is independent of γ. This is consistent with the numerical results displayed in Fig. 11.

In general, the previous results indicate that when the dye-molecule fluorescence rate γ_F becomes comparable to or greater than the dye-molecule rotational relaxation rate γ_R, i.e., $\gamma \gtrsim 1$, transversely pumped dye-laser light amplifier characteristics will depart significantly from the characteristics of conventional homogeneously broadened amplifiers. Also, under these circumstances amplifier measurements of stimulated emission cross sections must account for dye-molecule rotation relaxation or they may be significantly in error.

IV. TIME-DEPENDENT PHYSICAL SPECTRUM OF PULSED DYE-LASER-LIGHT COHERENCY MATRIX

In Sec. II a phenomenological semiclassical theory of laser-pumped, pulsed-dye-laser amplifiers including dye-molecule rotational relaxation was developed. In Sec. III this theory was used to study the amplification of partially polarized, quasimonochromatic light pulses. The polarization state of the light was treated using the coherency matrix formalism of Wiener[20] and Wolf.[21,22] The relationship between these theoretically calculated radiation field quantities and experimental measurements is established in this section by generalizing the theory of the time-dependent spectrum of light introduced by Eberly and Wodkiewicz.[30]

For plane polarized light, if $i(t,\nu;\Gamma)$ is the spectral intensity of the light detected by a Fabry-Perot interferometer-photodetector instrument, then[30]

$$i(t,\nu;\Gamma)=4c\epsilon_0\Gamma\int_{-\infty}^{t}dt_1\int_{-\infty}^{t}dt_2 e^{-(\Gamma-i\omega)(t-t_1)}\times e^{-(\Gamma+i\omega)(t-t_2)}\overline{\hat{V}^*(t_1)\hat{V}(t_2)} \tag{4.1}$$

if

$$E(t)=\hat{V}(t)+\hat{V}^*(t) \tag{4.2}$$

is the electric field of the light at the entrance to the interferometer. The quantities ν and Γ are the center frequency $\nu=\omega/2\pi$ and pass bandwidth, respectively, of the interferometer. The time-dependent spectrum of polarized light, Eq. (4.1), may also be written

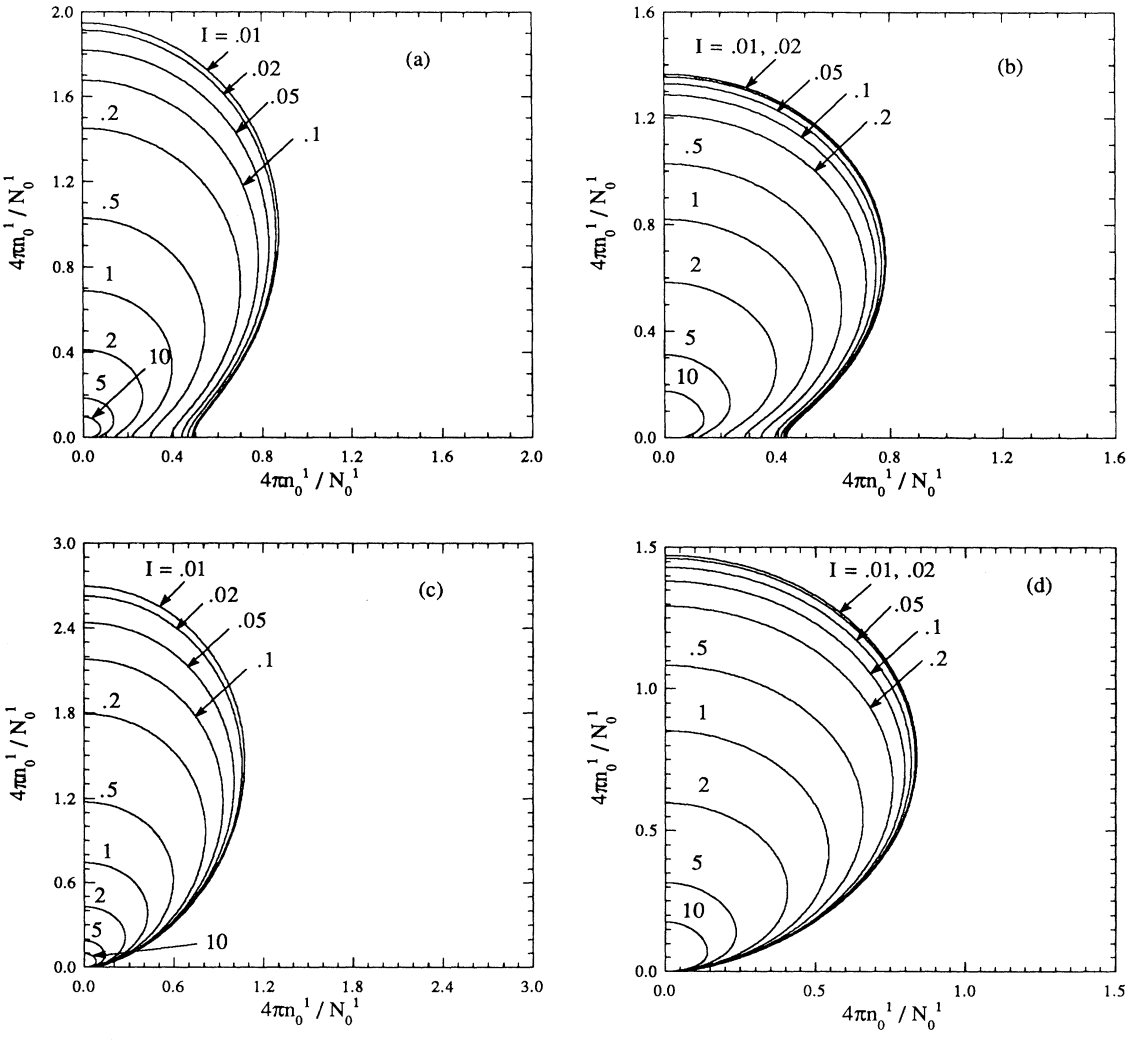

FIG. 14. Polar angle α dependence of the dye molecule $S_1(0)$ excited-state density per unit solid angle n_0^1 during passage of a quasi-steady-state dye-laser pulse of normalized intensity $I=I_l/I_s$ for several values of $\eta=I_p/I_{ps}$ and $\gamma=\gamma_F/\gamma_R$, namely for $\gamma=1$: (a) $\eta=0.01$ and (b) $\eta=1$, and for $\gamma=10$: (c) $\eta=0.01$ and (d) $\eta=1$.

$$i(t,\nu;\Gamma)=4c\epsilon_0\Gamma\overline{\tilde{V}(t,\nu;\Gamma)\tilde{V}^*(t,\nu;\Gamma)}\ , \tag{4.3}$$

where

$$\tilde{V}(t,\nu;\Gamma)=\int_{-\infty}^{t}dt'\hat{V}(t')e^{-(\Gamma+i\omega)(t-t')}\ . \tag{4.4}$$

In the following these results are generalized to the case of partially polarized quasimonochromatic light by using the measurement technique proposed by Wolf.[21,22]

Suppose the partially polarized light pulses emitted by the dye laser are examined with an optical detection system consisting of a compensator, polarizer, spectrometer, and a fast photodetector aligned in sequence.[21,30] The spectrometer-photodetector subsystem is a multichannel device in which each optical filter channel acts as a Fabry-Pérot interferometer-photodetector combination.[30] The optical detection system is oriented so that the entering laser light pulse is partially polarized in the x-y plane. Due to the compensator[21,22] the y component of the radiation electric field is retarded by an amount ϵ relative to the x component. It then passes through a polarizer,[21,22] which makes an angle θ with the positive x direction. If the radiation electric field at the entrance of the optical detection system is

$$\mathbf{E}(t)=\hat{\mathbf{V}}(t)+\hat{\mathbf{V}}^*(t)\ , \tag{4.5}$$

where $\hat{\mathbf{V}}(t)$ is the positive frequency part of the radiation electric field, then following the polarizer the component of the complex electric field vector $\hat{\mathbf{V}}(t)$ in the direction of θ is[21,22]

$$\hat{V}(t;\theta,\epsilon)=\hat{V}_x(t)\cos\theta+\hat{V}_y(t)e^{i\epsilon}\sin\theta\ , \tag{4.6}$$

where $\hat{V}_n(t)$ is the component of $\hat{\mathbf{V}}(t)$ in the n direction, $n=(x,y)$. The time-dependent physical spectrum or measured spectral intensity of this radiation, as determined by the spectrometer photodetector system, is given by

$$\begin{aligned}i(t,\nu;\Gamma,\theta,\epsilon)=&j_{xx}(t,\nu;\Gamma)\cos^2\theta+j_{yy}(t,\nu;\Gamma)\sin^2\theta\\&+j_{xy}(t,\nu;\Gamma)e^{-i\epsilon}\sin\theta\cos\theta\\&+j_{yx}(t,\nu;\Gamma)e^{i\epsilon}\sin\theta\cos\theta\ ,\end{aligned} \tag{4.7}$$

where $\overleftrightarrow{j}(t,\nu;\Gamma)$ is the time-dependent physical spectrum of the coherency matrix or simply the measured time-dependent spectral coherency matrix of the light pulse. Both the measured spectral intensity $i(t,\nu;\Gamma,\theta,\epsilon)$ and spectral coherency matrix $\overleftrightarrow{j}(t,\nu;\Gamma)$ have the units of intensity per unit frequency interval. Each of the measured spectral coherency matrix components are given by

$$j_{mn}(t,\nu;\Gamma)=4c\epsilon_0\Gamma\overline{\tilde{V}_m(t,\nu;\Gamma)\tilde{V}_n^*(t,\nu;\Gamma)}\ , \tag{4.8}$$

where

$$\tilde{V}_n(t,\nu;\Gamma)=\int_{-\infty}^{t}dt'\hat{V}_n(t')e^{-(\Gamma+i\omega)(t-t')} \tag{4.9}$$

and ν and Γ are the center frequency and pass bandwidth, respectively, of a given spectrometer channel. The overbar denotes ensemble average. The measured spectral coherency matrix is Hermitian. Its trace is the time-dependent physical spectrum[30] or measured spectral intensity, Eq. (4.3), of the light pulse if only the spectrometer-photodetector optical system is employed in the meausrements, i.e.,

$$i(t,\nu;\Gamma)=\mathrm{Tr}[\overleftrightarrow{j}(t,\nu;\Gamma)]\ . \tag{4.10}$$

The corresponding measured time-dependent coherency matrix $\overleftrightarrow{J}(t;\Gamma)$ of the partially polarized light pulse is given by

$$\overleftrightarrow{J}(t;\Gamma)=\int_{-\infty}^{\infty}d\nu\overleftrightarrow{j}(t,\nu;\Gamma)\ . \tag{4.11}$$

This coherency matrix is also Hermitian and its trace is the measured intensity of the light as determined by the spectrometer-photodetector system, i.e.,

$$I(t;\Gamma)=\mathrm{Tr}[\overleftrightarrow{J}(t;\Gamma)]\ . \tag{4.12}$$

Now the measured intensity of the partially polarized light examined by the complete optical detection system described earlier,

$$I(t;\Gamma,\theta,\epsilon)=\int_{-\infty}^{\infty}d\nu\, i(t,\nu;\Gamma,\theta,\epsilon)\ , \tag{4.13}$$

is obtained from Eq. (4.7):

$$\begin{aligned}I(t;\Gamma,\theta,\epsilon)=&J_{xx}(t;\Gamma)\cos^2\theta+J_{yy}(t;\Gamma)\sin^2\theta\\&+J_{xy}(t;\Gamma)e^{-i\epsilon}\sin\theta\cos\theta\\&+J_{yx}(t;\Gamma)e^{i\epsilon}\sin\theta\cos\theta\ .\end{aligned} \tag{4.14}$$

In general, these results may be used to relate laser-light pulse properties predicted by the pulsed-dye-laser model described in Sec. II to measured values. To illustrate how this may be done the case of nearly monochromatic light is now considered.

If the dye-laser-light pulses are quasimonochromatic as assumed in Sec. III, then from Eq. (3.1)

$$\hat{V}_n(t)=[\hat{E}_n(t)/2]e^{-i\omega_l t}\ . \tag{4.15}$$

Substituting Eq. (4.15) into Eq. (4.9) it can be shown that

$$\hat{V}_n(t,\nu;\Gamma)=(e^{-i\omega_l t}/2)\int_0^{\infty}d\tau\,\hat{E}_n(t-\tau)e^{-[\Gamma+i(\omega-\omega_l)]\tau}\ . \tag{4.16}$$

Suppose the dye-laser light is nearly monochromatic and the spectrometer parameters are such that

$$|\partial_t\hat{E}_n(t)/\hat{E}_n(t)|\ll\Gamma\ll\omega\ , \tag{4.17}$$

then the principal contribution to the integral in Eq. (4.16) comes from $\tau\lesssim O(\Gamma^{-1})$ and thus

$$\hat{V}_n(t,\nu;\Gamma)\simeq\hat{E}_n(t)e^{-i\omega_l t}/2[\Gamma+i(\omega-\omega_l)]\ . \tag{4.18}$$

For these circumstances the measured spectral coherency matrix of the radiation,

$$j_{nm}(t,\nu;\Gamma)=c\epsilon_0\overline{\hat{E}_n(t)\hat{E}_m^*(t)}\Gamma/[\Gamma^2+(\omega-\omega_l)^2]\ , \tag{4.19}$$

is obtained by substituting Eq. (4.18) into Eq. (4.8). Substituting Eq. (4.19) into Eq. (4.11) gives the measured coherency matrix of the light pulse:

$$J_{nm}(t)=c\epsilon_0\overline{\hat{E}_n(t)\hat{E}_m^*(t)}/2\ , \tag{4.20}$$

which is the ensemble average of the coherency matrix calculated in the theory developed in Sec. III. Equations (4.14) and (4.20) lead to the conventional measurement methodology[21,22] for the coherency matrix of quasimonochromatic light pulses.

V. SUMMARY AND CONCLUSIONS

In this paper a phenomenolgical semiclassical theory of pulsed-laser-pumped dye-laser amplifiers is presented. The theory accounts for the novel spectroscopic and relaxation properties of dye molecules in liquid solvents. It is applicable to pulse durations $\lesssim 10-100$ ns including the ultrashort pulse regime. Due to dye-molecule rotational relaxation the medium is optically anisotropic. This anisotropy is significant if the dye-laser medium has a fluorescence lifetime less than or comparable to the dye-molecule rotational relaxation time. Under this condition the amplification of dye-laser radiation depends on the directions of propagation and the polarization states of the pump- and dye-laser light beams and the dye-molecule fluorescence and rotational relaxation dynamics.

For light pulses of duration $\gtrsim 1$ ps, the optical anisotropy of the dye medium can be represented by dye-molecule electric susceptibility tensors. These susceptibility tensors characterize the polarization-dependent pump- and dye-laser radiation coupling to the dye molecules. Using Kramers-Kronig or Hilbert transform relations these tensors can be calculated from experimentally determined absorption and emission cross sections. In this regime, the coherency matrices of Wiener[20] and Wolf[21,22] conveniently characterize the time- and space-dependent polarization states of the pump- and dye-laser radiation. Rate equations describe the excited-state dynamics for dye molecules of a given orientation. Overall, the theory provides a self-consistent description that is applicable to both small- and large-signal regimes of amplification. All the physical parameters in the theory may be determined by conventional experimental techniques.

The theory presented here clarifies approaches used to date and provides a more complete description of previous experiments. In general, it should provide a significant improvement over conventional theories[1-11] of pulsed dye lasers which are based on a radiation transport-rate equation formalism that neglects dye-molecule rotational relaxation. In addition, it should be a useful point of departure for the analysis of dye-laser amplifiers that operate in the high-intensity and/or ultrashort-pulse length regimes. The purpose of using a phenomenological semiclassical approach was to develop a theory of pulsed dye lasers that accounts for the dye-molecule structure and its interaction with the radiation field and liquid solvent with physical parameters that are easily accessible to experimental measurement. Only a detailed comparison between the theory presented here with dye-laser experiments will determine if this objective has been successfully met. It seems clear that further progress will require better models of the dye-molecule structure and relaxation processes, particularly vibrational relaxation, and inclusion of nonlinear optical effects.

ACKNOWLEDGMENTS

This research was performed in part under the auspices of the U.S. Department of Energy by Lawrence Livermore National Laboratory under Contract No. W-7405-ENG-48.

APPENDIX

Consider the Cauchy-principal-value integrals Eqs. (3.77) and (3.78) when the absorption and stimulated emission cross sections are known at discrete radian frequency points $\omega=\omega_j$. For example, consider Eq. (3.77) and suppose that $\omega_j<\omega_p<\omega_{j+1}$. To evaluate Eq. (3.77) under this circumstance it is useful to express Eq. (3.77) as

$$\chi_p'(\omega_p)=2cn_s\left[\int_0^{\omega_j} d\omega\,\sigma_a(\omega)/\pi(\omega^2-\omega_p^2) + \int_{\omega_{j+1}}^{\infty} d\omega\,\sigma_a(\omega)/\pi(\omega^2-\omega_p^2) + \mathrm{P}\int_{\omega_j}^{\omega_{j+1}} d\omega\,\sigma_a(\omega)/\pi(\omega^2-\omega_p^2)\right] . \quad \text{(A1)}$$

The first two integrals may be computed by conventional numerical techniques.

Over the interval $\omega_j\le\omega\le\omega_{j+1}$ the absorption cross section can be approximately written

$$\sigma_a(\omega)=\sigma_a(\omega_j)+m_\sigma(\omega-\omega_j) , \quad \text{(A2)}$$

where

$$m_\sigma=[\sigma_a(\omega_{j+1})-\sigma_a(\omega_j)]/(\omega_{j+1}-\omega_j) . \quad \text{(A3)}$$

Using Eq. (A2) the Cauchy-principal-value integral in Eq. (A1) may be evaluated and the result is

$$\mathrm{P}\int_{\omega_j}^{\omega_{j+1}} d\omega\,\sigma_a(\omega)/\pi(\omega^2-\omega_p^2)=\{[\sigma_a(\omega_j)-m_\sigma\omega_j]/2\pi\omega_p\}\ln[(\omega_p+\omega_j)(\omega_{j+1}-\omega_p)/(\omega_p-\omega_j)(\omega_{j+1}+\omega_p)] + (m_\sigma/2\pi)\ln[(\omega_{j+1}^2-\omega_p^2)/(\omega_p^2-\omega_j^2)] . \quad \text{(A4)}$$

This approach to the numerical integration of Eqs. (3.77) and (3.78) is useful when the cross sections $\sigma_a(\omega)$ and $\sigma_s(\omega)$ are known from experimental measurements.

[1] *Dye Lasers*, 3rd ed., Vol. 1 of *Topics in Applied Physics*, edited by F. P. Schäfer (Springer, Berlin, 1990).
[2] L. G. Nair, Prog. Quantum Electron. 7, 153 (1975).
[3] M. Maeda, *Laser Dyes, Properties of Organic Compounds for Dye Lasers* (Academic, Orlando, 1984).
[4] U. Ganiel, A. Hardy, G. Neumann, and D. Treves, IEEE J. Quantum Electron. **QE-11**, 881 (1975).
[5] P. Juramy, P. Flamant, and Y. H. Meyer, IEEE J. Quantum

Electron. **QE-13**, 855 (1977).
[6]L. W. Casperson, J. Appl. Phys. **48**, 256 (1977).
[7]H. P. Grieneisen, R. E. Francke, and A. Lago, Appl. Phys. **15**, 281 (1978).
[8]G. Dujardin and P. Flamant, Opt. Commun. **24**, 243 (1978).
[9]C. Radzewicz, Z. W. Li, and M. G. Raymer, Phys. Rev. A **37**, 2039 (1988).
[10]A. Migus, J. L. Martin, R. Astier, and A. Orszag, in *Picosecond Phenomena II,* Vol. 14 of *Springer Series in Chemical Physics,* edited by R. Hochstrasser, W. Kaiser, and C. V. Shank (Springer, Berlin, 1980), pp. 59–63.
[11]A. Migus, C. V. Shank, E. P. Ippen, and R. L. Fork, IEEE J. Quantum Electron. **QE-18**, 101 (1982).
[12]D. W. Phillion, D. J. Kuizenga, and A. E. Siegman, J. Chem. Phys. **61**, 3828 (1974).
[13]O. I. Yaroshenko and K. I. Rudik, Sov. J. Quantum Electron. **11**, 354 (1981).
[14]G. Mourou and M. M. Denariez-Roberge, IEEE J. Quantum Electron. **QE-9**, 787 (1973).
[15]A. Lempicki, Acta Phys. Pol. A **50**, 179 (1976).
[16]P. R. Hammond, J. Appl. Phys. **57**, 4916 (1985).
[17]K. C. Reyzer and L. W. Casperson, J. Appl. Phys. **51**, 6075 (1980).
[18]K. C. Reyzer and L. W. Casperson, J. Appl. Phys. **51**, 6083 (1980).
[19]H. Fu, and H. Haken, Phys. Rev. A **36**, 4802 (1987).
[20]N. Wiener, J. Math. Phys. **7**, 109 (MIT, Cambridge, MA, 1928). Also, in *Selected Papers on Coherence and Fluctuations of Light,* edited by L. Mandel and E. Wolf (Dover, New York, 1970), Vol. 1, p. 83.
[21]E. Wolf, Nuovo Cimento **13**, 1165 (1959).
[22]M. Born and E. Wolf, *Principles of Optics,* 3rd ed. (Pergamon, New York, 1965).
[23]P. F. Moulton, in *Laser Handbook,* edited by M. Bass and M. L. Stitch (North-Holland, Amsterdam, 1985), Vol. 5, pp. 203–288.
[24]P. F. Moulton, J. Opt. Soc. Am. B **3**, 125 (1986).
[25]S. T. Lai, J. Opt. Soc. Am. B **4**, 1286 (1987).
[26]H. P. Jenssen and S. T. Lai, J. Opt. Soc. Am. B **3**, 115 (1986).
[27]*Tunable Solid State Lasers,* Vol. 47 of Springer Series in Optical Sciences, edited by P. Hammerling, A. B. Budgor, and A. Pinto (Springer-Verlag, Berlin, 1985).
[28]R. B. Schaefer and C. R. Willis, Phys. Rev. A **13**, 1874 (1976).
[29]J. C. Garrison, H. Nathel, and R. Y. Chiao, J. Opt. Soc. Am. B **5**, 1528 (1988).
[30]J. H. Eberly and K. Wodkiewicz, J. Opt. Soc. Am. **67**, 1252 (1977).
[31]P. R. Hammond, Opt. Commun. **29**, 331 (1979).
[32]P. R. Hammond, IEEE J. Quantum Electron. **QE-15**, 624 (1979).
[33]P. R. Hammond J. Chem. Phys. **70**, 3884 (1979).
[34]P. R. Hammond, IEEE J. Quantum Electron. **QE-16**, 1157 (1980).
[35]H. E. Lessing, and A. VonJena, in *Laser Handbook,* edited by M. L. Stitch (North-Holland, Amsterdam, 1985), Vol. 3, p. 753.
[36]J. P. Webb, W. C. McColgin, O. G. Peterson, D. L. Stockman, and J. H. Eberly, J. Chem. Phys. **53**, 4227 (1970).
[37]C. Lin and A. Dienes, Opt. Commun. **9**, 21 (1973).
[38]A. J. Taylor, D. J. Erskine, and C. L. Tang, Chem. Phys. Lett. **103**, 430 (1984).
[39]A. M. Weiner and E. P. Ippen, Chem. Phys. Lett. **114**, 456 (1985).
[40]C. H. Brito Cruz, R. L. Fork, W. H. Knox, and C. V. Shank, Chem. Phys. Lett. **132**, 341 (1986).
[41]J. Olmsted III, J. Phys. Chem. **83**, 2581 (1979).
[42]W.-K. Lee, A. Güngör. P. T. Ho, and C. C. Davis, Appl. Phys. Lett. **47**, 916 (1985).
[43]R. F. Kubin and A. N. Fletcher, J. Lumin. **27**, 455 (1982).
[44]W. Lahmann and H. J. Ludewig, Chem. Phys. Lett. **45**, 177 (1977).
[45]R. R. Alfano, S. L. Shapiro, and W. Yu, Opt. Commun. **7**, 191 (1973).
[46]*Handbook of Chemistry and Physics,* edited by R. C. Weast (CRC, Boca Raton, FL. 1982).
[47]P. P. Ho and R. R. Alfano, Phys. Rev. A **20**, 2170 (1979).
[48]Y. R. Shen and G. Z. Yang, in *The Supercontinuum Laser Source,* edited by R. R. Alfano (Springer-Verlag, Berlin, 1989), Chap. 1, pp. 1–32.
[49]F. Milanovich, in *Handbook of Laser Science and Technology,* edited by M. J. Weber (CRC, Boca Raton, FL, 1986), Vol. 3, p. 292.
[50]H. Haken, *Laser Theory,* Vol. XXV/2c, of *Encyclopedia of Physics,* 2nd corrected ed. (Springer-Verlag, Berlin, 1970), Chaps. VII and VIII.
[51]H. Haken, *Light* (North-Holland, Amsterdam, 1985), Vol. 2, Chap. 5.
[52]R. H. Pantell and H. E. Puthoff, *Fundamentals of Quantum Electronics* (Wiley, New York, 1969).
[53]Y. R. Shen, *The Principles of Nonlinear Optics* (Wiley, New York, 1984).
[54]A. Penzkofer, W. Falkenstein, and W. Kaiser, Chem. Phys. Lett. **44**, 82 (1976).
[55]D. W. Hall, R. A. Haas, W. F. Krupke, and M. J. Weber, IEEE J. Quantum Electron. **QE-19**, 1704 (1983).
[56]J. B. Birks, *Photophysics of Aromatic Molecules* (Wiley-Interscience, New York, 1970).
[57]S. J. Strickler and R. A. Berg, J. Chem. Phys. **37**, 814 (1963).
[58]J. B. Birks and D. J. Dyson, Proc. R. Soc. London Ser. A **275**, 135 (1963).
[59]P. G. Seybold, M. Gouterman, and J. Callis, Photochem. Photobiol. **9**, 229 (1969).
[60]L. M. Frantz and J. S. Nodvik, J. Appl. Phys. **34**, 2346 (1963).